



Norwegian University
of Life Sciences

Master's Thesis 2023 60 ECTS

Faculty of Chemistry, Biotechnology and Food Science

Discovery, production, and characterization of fucoidan-active enzymes from marine genomes

Victoria Jellestad Demmene

MSc. Biotechnology (Molecular Biology)

Acknowledgements

The present work was carried out at the Faculty of Chemistry, Biotechnology and Food Science at the Norwegian University of Life Sciences (NMBU) from August 2022 to May 2023, with Svein Jarle Horn, Nanna Rhein-Knudsen, and Diego Reyes-Weiss as supervisors. This project was a part of the Norwegian Seaweed Biorefinery Platform and was funded by The Research Council of Norway. The metagenomic dataset that set the groundwork for my thesis was provided by Runar Stokke (Department of Biological Sciences, Deep Sea Biology/Center for Deep Sea Research, University of Bergen).

I would first like to thank Svein for allowing me the opportunity to work on this subject and for inspiring me throughout this year. I am very grateful for all your constructive and insightful feedback. I would also like to express my immense gratitude to Nanna and Diego for all the time they have dedicated to guiding me in the lab and for feedback and advice during both the research and the writing process. I believe it is rare to have such inspiring, encouraging, knowledgeable, and incredibly patient supervisors. I can not find the words powerful enough to explain how much I have valued having you as my mentors.

A huge thanks to the entire BioRef group for being so welcoming, inclusive, and helpful. I feel very fortunate for having been surrounded by such a good environment the past year, and for having been part of this wonderful team. Thanks to Veronica for always listening to my lab stories and for going through the ups and downs of a master thesis alongside me. I appreciate the friendship we've created.

Lastly, a big thanks to family, friends, my volleyball teammates, and my supportive boyfriend. Thank you all for being so understanding and compassionate throughout this last year and at all other times as well. An extra special thanks to my big sister for being a great role model and someone I can always lean on. Having you as my sidekick and partner in crime is priceless.

Ås, May 2023

Victoria Jellestad Demmene

Abstract

Environmental challenges and decreasing amounts of fossil reserves make it challenging to meet the resource- and energy requirements of a growing world population. Biomass, with its organic material and carbon neutral qualities, can be used as a sustainable resource to substitute fossil resources. Until recently, terrestrial biomass has dominated sustainable biorefinery approaches, but marine biomass has several beneficial properties compared to terrestrial biomass. Seaweeds have a high carbohydrate content, and brown seaweeds particularly have great potential for sustainable marine biomass production where its polysaccharides can be utilized to produce fuels, chemicals, feed, food, and bioactive compounds. Extracting the different compounds in seaweed while preserving their structure is a big challenge, and the complete utilization of all the different compounds in seaweed is still not a reality. Fucoidan is a highly sulfated polysaccharide found in brown seaweeds that has recently gained much attention for being associated with biological and immunological properties, but the carbohydrate is highly unexplored and not well understood.

In this study, a marine metagenome was screened for protein sequences with the goal of identifying new fucoidan active enzymes that could be used to study and modify fucoidans. Through cloning, transformation, production, and activity testing of nine putative fucoidan active enzymes, the novel sulfatase AMOR_S25 was discovered. The sulfatase was active on fucoidans from *Macrocystis pyrifera* and enzymatic hydrolysates of fucoidan from *Fucus vesiculosus*, as well as on the artificial substrate p-nitrophenol sulfate (pNPS). Reactions with AMOR_S25 and pNPS allowed for quantitative analyses of sulfate release, which was used for enzyme characterization. AMOR_S25 was revealed to be very stable and has optimal activity at 40 °C and pH 6.5. Highest enzyme activity was achieved using 5 mM calcium and 150 mM sodium chloride. Kinetics analyses revealed a K_M value of 16.2 mM and V_{max} at 0.32 $\mu\text{M}/\text{min}$ on the pNPS substrate.

Putative fucoidan enzymes were also sourced from the *Lentimonas* sp. genome, where the enzyme FunA_50 was produced and shown to have activity on fucoidan from *F. vesiculosus*. Characterization of FunA_50 was done by quantifying reducing ends produced during degradation of the substrate, and the enzyme was found to be most active at 40 °C and pH 8.0. Further characterization of FunA_50 is ongoing.

Although further studies will be necessary to fully understand these novel enzymes in terms of structure, specificity and mode of action, the discovery and characterization of AMOR_S25 and FunA_50 will contribute to increase the understanding of fucoidans and fucoidan specific enzymes and possibly practical applications of fucoidan.

Sammendrag

Miljøutfordringer og minkende mengder fossile reserver gjør det utfordrende å dekke ressurs- og energibehovet til en voksende verdensbefolkning. Biomasse, med sitt organiske materiale og sine karbonnøytrale kvaliteter, kan brukes som en bærekraftig ressurs for å erstatte fossile ressurser. Inntil nylig har terrestrisk biomasse vært dominerende i bioraffineringsprosesser, men marin biomasse har flere fordelaktige egenskaper sammenlignet med landbaserte biomasse. Tare har et høyt karbohydratinnhold, og brun tare har spesielt stort potensial for bærekraftig marin biomasseproduksjon der polysakkaridene kan brukes til å produsere drivstoff, kjemikalier, fôr, mat og bioaktive forbindelser. Å ekstrahere de forskjellige stoffene i tang uten at deres kjemiske struktur blir endret er en stor utfordring, og fullstendig utnyttelse av alle de forskjellige stoffene i tare er fortsatt ikke en realitet. Fucoidan er et svært sulfatert polysakkarid som finnes i brun tare og som nylig har fått mye oppmerksomhet for å være assosiert med biologiske og immunologiske egenskaper, men karbohydratet er lite utforsket og ikke godt forstått.

I denne studien ble et marint metagenom screenet for proteinsekvenser med mål om å identifisere nye fucoidan-aktive enzymer som kan brukes til å studere og modifisere fucoidansukre. Gjennom kloning, transformasjon, produksjon og aktivitetstesting av ni antatte fucoidanaktive enzymer, ble den nye sulfatasen AMOR_S25 oppdaget. Sulfatasen var aktiv på fucoidan fra *Macrocystis pyrifera* og enzymatisk hydrolysert fucoidan fra *Fucus vesiculosus*, samt det kunstige substratet p-nitrofenolsulfat (pNPS). Reaksjoner med AMOR_S25 og pNPS muliggjorde kvantitative analyser for frigjøring av sulfat, som ble brukt til enzymkarakterisering. AMOR_S25 viste seg å være svært stabil og har optimal aktivitet ved 40 °C og pH 6,5. Det ble observert høyest aktivitet med 5 mM kalsium og 150 mM natriumklorid. Kinetikkanalyser viste en K_M -verdi på 16,2 mM og V_{max} ved 0,32 $\mu\text{M}/\text{min}$ på pNPS substratet.

Potensielle fucoidan-enzymmer ble også hentet fra *Lentimonas* sp. genomet, hvor enzymet FunA_50 ble produsert og vist å ha aktivitet på fucoidan fra *F. vesiculosus*. Karakterisering av FunA_50 ble gjort ved å kvantifisere reduserende ender produsert under nedbrytning av substratet, og enzymet har høyest aktivitet ved 40 °C og pH 8,0. Videre karakterisering av FunA_50 er pågående.

Selv om ytterligere tester vil kreves for å få økt innblikk i enzymenes struktur, spesifisitet, og virkemåte, vil oppdagelsen og karakteriseringen av AMOR_S25 og FunA_50 bidra til å øke

forståelsen av fucoidaner og fucoidan-spesifikke enzymer, samt muligens praktiske anvendelser av fucoidan.

Abbreviations

AMOR	Arctic Mid-Ocean Ridge
BLAST	The Basic Local Alignment Search Tool
CAZy	Carbohydrate-Active Enzymes
FCSP	Fucose-Containing Sulfated Polysaccharides
GH	Glycosidase Hydrolase
HPAEC-PAD	High-Performance Anion-Exchange Chromatography with Pulsed Amperometric Detection
HPIC	High Pressure Ion Chromatography
HPLC	High Performance Liquid Chromatography
ICS	Ion Chromatography System
IPTG	Isopropyl β -D-1-thiogalactopyranoside
LB	Lysogeny Broth
MALDI-ToF	Matrix Assisted Laser Deionization – Time of Flight
MSA	Multiple Sequence Alignment
OD	Optical Density
ON	Overnight
ORF	Open Reading Frames
PDB	Protein Data Bank
pNC	4-Nitrocatechol sulfate dipotassium
pNP	Potassium 4-nitrophneyl
SDS-PAGE	Sodium Dodecyl Sulfate - Polyacrylamide Gel Electrophoresis
SEC	Size exclusion chromatography
TB	Terrific Broth
TBS	Tris-Buffered Saline
TGS	Tris/Glycine/SDS

Table of Contents

Acknowledgements.....	ii
Abstract.....	iii
Sammendrag	v
Abbreviations.....	vii
1 Introduction.....	1
1.1 Transitioning to sustainable resources	1
1.2 Seaweed	2
1.3 Brown seaweed	3
1.4 Seaweed processing	5
1.5 Fucoidan.....	6
1.5.1 Structure.....	7
1.5.2 Fucoidan Extraction	9
1.5.3 Bioactivities	10
1.5.4 Fucoidan secretion	10
1.5.5 Exploring fucoidan.....	11
1.6 Fucoidan-acting enzymes.....	12
1.6.1 Fucoidanases	14
1.6.2 Sulfatases	16
1.7 Aim of study	18
2 Materials	19
2.1 Enzymes.....	19
2.2 Substrates	20
2.3 Cells and expression vectors	22
2.4 Culture media and buffers.....	22
2.5 Chemicals and compounds.....	23
2.6 Instruments and software programs	25
3 Methods.....	28
3.1 Bioinformatics.....	28
3.2 Cloning.....	28
3.3 Transformation of TOP10- and BL21 (DE3) <i>E. coli</i>	29
3.3.1 Storage of transformed cells	29
3.4 Small-scale protein expression tests	30
3.5 Enzyme production	31

3.6	Enzyme purification.....	31
3.7	Optimization of protein expression.....	32
3.8	Production of fucoidan oligomers.....	32
3.9	Enzyme activity assays	33
3.9.1	Oligomer detection using Size-Exclusion Chromatography.....	33
3.9.2	Monomer detection using High Performance Liquid Chromatography.....	33
3.9.3	Sulfate detection using High Pressure Ion Chromatography	34
3.9.4	MALDI-ToF-MS	34
3.10	Characterization of active fucoidan sulfatase	34
3.10.1	Determining optimal reaction conditions.....	35
3.10.2	Thermostability	35
3.10.3	Enzyme Kinetics	35
3.10.4	Time course.....	36
3.11	Characterization of active endo-fucoidanase from <i>Lentimonas</i>	36
4	Results & discussion.....	38
4.1	Bioinformatics.....	38
4.2	Cloning & transformation.....	41
4.3	Small-scale enzyme expression	41
4.4	Enzyme production & purification	42
4.5	Optimization of protein expression.....	44
4.6	Substrate production	46
4.6.1	SEC analysis of enzyme hydrolysates.....	46
4.6.2	MALDI-ToF-MS	47
4.7	Enzyme activity for AMOR and <i>Lentimonas</i> enzymes.....	48
4.7.1	Endo-fucoidanases	48
4.7.2	Exo-fucoidanases	50
4.7.3	Fucoidan sulfatases	53
4.8	Characterization of AMOR_S25.....	55
4.8.1	Effect of temperature on activity	56
4.8.2	Effect of pH on activity.....	57
4.8.3	Salinity and activity	58
4.8.4	Divalent metal ions and activity.....	59
4.8.5	Thermostability	61
4.8.6	Enzyme kinetics	63
4.8.7	Time course.....	65

4.9	Characterization of FunA_50.....	67
4.9.1	Effect of enzyme- and substrate concentrations on activity.....	67
4.9.2	Effect of temperature on activity	69
4.9.3	Effect of pH on activity.....	70
4.10	Conclusion and future perspectives	71
	References.....	73
	Appendix.....	81
	Appendix A: Expression vectors.....	81
	Appendix B: Bioinformatics	82
	Appendix C: His-tag purification chromatograms.....	83
	Appendix D: Chromatogram for monomer detection	84
	Appendix E: Calculations	85
	Appendix F: AMOR_S25 kinetics.....	87
	Appendix G: MALDI data	88

1 Introduction

1.1 Transitioning to sustainable resources

With a growing world population, currently constituting 8 billion people, it is becoming increasingly more challenging to meet resource- and energy demands. Due to environmental problems and decreasing amounts of fossil reserves, a transition from fossil to renewable resources is needed. Biomass represents a sustainable resource that could partly substitute fossil resources. Biomass is composed of organic material that originates from animals and plants and is gaining attention for being one of the most available renewable energy resources (Ani, 2016). Primary biomass is produced from CO₂ via photosynthesis in cyanobacteria, plants, and algae. These organisms capture about the same amount of carbon dioxide through photosynthesis as the amount released when the biomass is burned, making it a carbon-neutral energy source (EIA, 2022).

Industrial biorefining, which aims at converting biomass into added-value products such as biofuels and biochemicals, has traditionally been done using terrestrial biomass holding cellulose and lignin (Takkellapati et al., 2018). Marine biomass represents an alternative, as production of terrestrial biomass requires available land area and is potentially competing with food and feed plants, while marine biomass production does not. Growing in the sea, marine biomass requires neither freshwater nor additional nutrients or pesticides (Balina et al., 2017; Song et al., 2015). Compared to lignocellulosic biomass, seaweeds do not contain any lignin and therefore it does not require pretreatments prior processing (Song et al., 2015; Wi et al., 2009). Such advantages, and its vast geographical distribution (Sudhakar et al., 2018), point to the great potential of producing biomass in the sea for biorefining purposes.

Marine macroalgae, commonly known as seaweed, has traditionally been used for food, feed, and in fertilizers (Torres et al., 2019). In many Asian countries for example, seaweeds have been a critical part of the diet and has been used in traditional medicine for centuries (Ale & Meyer, 2013). Despite well-established industries for certain seaweed polymers like alginate, agar, and carrageenan, the possibility of utilizing the whole seaweed has not been fully explored. In addition to its traditional uses, seaweed is increasingly considered for use in production of biofuels, bioactive compounds, biochemicals, and other high value products. A lot of current research focuses on sustainable extraction and use of seaweed.

1.2 Seaweed

Seaweeds are plant-like organisms found in marine environments. They grow in coastal regions and are either free-floating or attached to rocks and other hard surfaces in areas where there is sufficient sunlight (Horn, 2000). Seaweeds are photosynthetic eukaryotes and are often thought to be the precursor of plants, but they lack plant structures such as roots, stems, and leaves (Sudhakar et al., 2018). There are over 10,000 species of seaweed globally (Torres et al., 2019) and they are classified into red (Rhodophyta), green (Chlorophyta), and brown (Phaeophyceae) seaweeds according to their photosynthetic pigments (Usov & Zelinsky, 2013)

Water makes up 71 % the Earth's surface, where over 96 % of it is seawater (USGS, 2019), providing an extensive area of habitats for seaweeds. Considering that seaweed also has a significantly higher photosynthetic efficiency than terrestrial plants (Song et al., 2015), they are – alongside microalgae and phytoplankton – essential primary producers for the planet. Kelps, which are large brown algae belonging to the order Laminariales, assimilate 1.8 kg carbon m⁻² year⁻¹, an amount up to ten times higher than marine phytoplankton (Wiencke & Bischof, 2012). This carbon assimilation efficiency is similar to the assimilation found in terrestrial forests with dense canopies. It is evident that the oceans and seaweed have essential roles in carbon sequestration, and there is in total approximately 60 times more CO₂ dissolved by seawater than by the Earth's atmosphere (Riebesell et al., 2009), making oceans work as buffer systems in relation to CO₂ emissions.

Generalizations about seaweed composition is near impossible, as seaweeds have a variable chemical composition depending on the life-stage, season and their geographical location and environments. Factors such as species and age will also affect seaweed composition. Still, seaweeds have a high moisture content of up to 94 %, are generally low on lipids but rich in minerals, and have a dry matter carbohydrate content of up to 50 % (El-Said & El-Sikaily, 2013; Fleurence, 1999; Holdt & Kraan, 2011). Marine macroalgae are generally considered to have a high amount of ash, despite that ash contents may vary considerably from 8 % to 40 % (dry weight) (Ito & Hori, 1989). Ash consists of the inorganic composites left after combustion, such as minerals and trace elements, and seaweeds have been shown to contain higher amounts of these types of compounds than land plants (Tabarsa et al., 2012). The polysaccharides in seaweeds are found as storage polysaccharides or structural polysaccharides in the cell wall.

Their composition and amount vary with taxonomy. Green seaweeds have sulfated polysaccharides (ulvans, xylans, mannans and sulfated galactans) for structural functions and starch as the main storage polysaccharide. Red seaweeds' structural sugars are agars, carrageenans, xylans, and porphyrins, and they use floridean starch as storage. Lastly, brown seaweeds have mainly alginic acids and fucoidan as structural polysaccharides and laminarins and mannitol as storage carbohydrates (Charoensiddhi et al., 2017; Horn, 2000).

There are biological activities, including antioxidant and antiviral properties, linked to seaweed components (e.g. polysaccharides, polyphenols, and minerals), and these activities give seaweeds a great potential for extraction of valuable compounds (Holdt & Kraan, 2011). Industrial extraction of polysaccharides from seaweeds is already established for compounds such as agar, alginates, and carrageenan. The gelling -, stabilizing -, and emulsifying properties of these compounds have made them useful in the pharmaceutical and cosmetics industry as well as in the hydrocolloid industry (Kılınç, 2013; Rhein-Knudsen et al., 2021). The compounds are utilized as gelling agents in food additives, as culture medium for diagnostic or laboratory purposes, a thickener or moisturizer in cosmetics, and as viscosity enhancers or as matrices in the pharmaceutical industry (Genicot et al., 2014; Ghanbarzadeh et al., 2018; Peteiro, 2018). In addition to desirable bioactivities, seaweed has efficient productivity with rapid growth rates and high biomass yields. Their short life cycles and multiple growth seasons makes them easy to breed, enabling an abundance in available biomass (Wang et al., 2008). The desirable high carbohydrate content with low amounts of lignin makes seaweed easier (compared to terrestrial plants) to utilize in bioconversion (Song et al., 2015; Wi et al., 2009).

1.3 Brown seaweed

Brown macroalgae can, due to efficient photon conversion, synthesize biomass faster than red and green macroalgae (Song et al., 2015). Photon conversion involves converting solar energy in the form of photons to chemical energy in the form of sugars, meaning that an organism with efficient photon conversion will produce a significant amount of carbohydrates. Brown seaweeds therefore have the highest areal productivity (average daily biomass production) (Widin et al., 2022) out of the three types of seaweeds and have gained extensive attention as a potential resource for sustainable biomass production.

Marine macroalgae is dependent on sunlight, and due to geographical variations in sunlight, the different groups and species of seaweeds have evolved to prefer different habitats. Brown algae absorb green light at medium wavelength and can live as deep as down to 50 meters, but most species will be found in the intertidal belt and upper sublittoral zone (Horn, 2000). Moreover, they normally live in colder water than red and green algae (Horn, 2000; Raven et al., 2002). Norway, with its long coastline of 100,915 km (Ministry of Climate and Environment, 2015) and cool water temperatures, makes an ideal habitat for brown seaweed species. The brown algae are the dominating type of seaweed, with members of the orders Laminariales and Fucales among those species most commonly found along the Norwegian coast (Horn, 2000).

Brown seaweed generally has a lower protein content than other seaweeds. The protein content may vary from 3-15 % of the dry weight, while red and green seaweeds have a protein content of 10-47 % of the dry weight (Fleurence, 1999). Carbohydrates, on the other hand, are abundant, constituting 51-55 % of dry weight (Seghetta et al., 2017). As previously mentioned, the carbohydrates for storage in brown seaweed are laminarin and mannitol. Laminarin is a β -(1 \rightarrow 3)-D-glucan with β -1,6 branches, while mannitol is the alcohol corresponding to the sugar mannose (Rhein-Knudsen et al., 2021).

Structural carbohydrates are located in the cell wall of the macroalgae. Most of the current cell wall knowledge is limited to land plants, but one model of the brown seaweed cell wall has been proposed by Deniaud-Bouet et al. (2014) (Figure 1). In this model, the brown seaweeds have a rigid cell wall that consists of cellulose, alginate, fucoidan, phenols, and proteins. Alginate and fucoidan are the main components, constituting up to 45 % of the algal dry weight, while cellulose, contrary to terrestrial plants, are only present in minor fractions (up to 10 %) (Deniaud-Bouët et al., 2017). Fucoidans are described as acting as cross-linkers between the cellulose microfibrils, and it has been hypothesized that short molecules of hemicellulose might act as intermediates between the fucoidan and the microfibrils (Deniaud-Bouët et al., 2017). The alginate found in the cell wall is a polymer consisting of β -D-mannuronic acid (M) and α -L-guluronic acid (G). Alginate form gels in the presence of calcium ions which contribute as structural elements (Manns et al., 2014). Alginate is the main skeletal component of the intercellular matrix, but the cell wall also contains fucoidan and protein in addition to the cellulose backbone. Additional components of the brown seaweed cell walls are polyphenols,

glycoproteins, phlorotannins, halide compounds such as iodide, and various ions (Deniaud-Bouët et al., 2017).

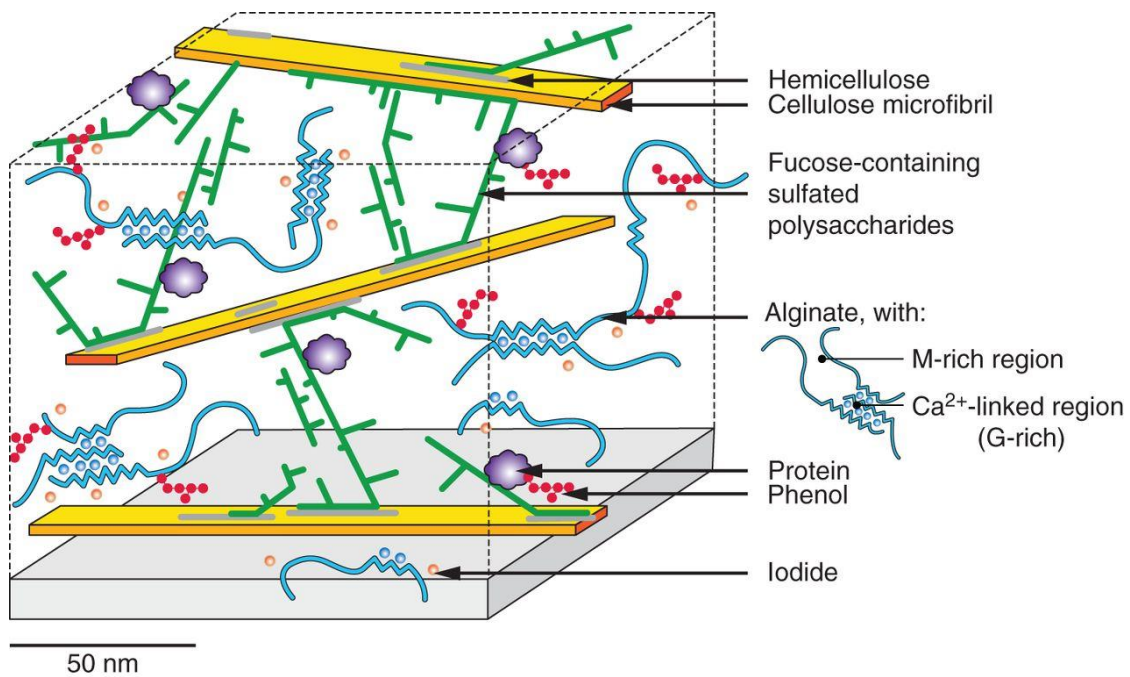


Figure 1: Proposed cell wall structure of brown seaweed from the order Fucales. Cellulose microfibrils are embedded in an alginate network. Hemicellulose links with cellulose and sulfated fucans, and the sulfated fucans will bind to proteins and phenols. Figure source (Deniaud-Bouët et al., 2014).

1.4 Seaweed processing

In the emerging bioeconomy, improved utilization of seaweed polysaccharides to produce fuels, food, feed, chemicals, and bioactive compounds is desired. Production of bioactive compounds requires that the polysaccharides are extracted from the algae. The process should give as high extraction yield as possible, keep the products intact, and with minimum co-extraction of other compounds. Seaweeds' complex- and varying composition and high moisture content can pose challenges for such extraction processes, and they may depend on several pretreatment steps. Pretreatment of seaweed biomass may include washing, filtering, and drying (Sudhakar et al., 2018), and there is a substantial amount of water that needs to be removed. Dewatering will often be unappealing from an energetic viewpoint, and implementing less energy-costly processes would positively impact both preservation of seaweed composition and downstream processing (Dussan et al., 2023). The complete utilization of all the different compounds in seaweed would require several different approaches. Still, brown seaweeds have a low cellulose content and lack

lignin completely, giving it an advantage over terrestrial plants when it comes to biological degradation, as no extensive pretreatments are needed (Rhein-Knudsen et al., 2021).

Producing energy from seaweed can be accomplished using several different methods, such as anaerobic digestion to methane (Sudhakar et al., 2018). Hydrolysis can be applied to generate fermentable sugars, and although some seaweeds can be hydrolyzed directly, extraction of the seaweed polysaccharides may be necessary prior to hydrolysis. Polysaccharide extraction can be done using hot water or chemicals, or by microwave-assisted, ultrasonic-assisted, or enzyme-assisted extraction (Xu et al., 2017). Once extracted, the sugars can be cleaved to fermentable mono- or oligosaccharides. Laminarin and mannitol, for example, can be fermented to ethanol by yeast such as *Saccharomyces cerevisiae* or bacteria such as *Zymobacter palmae* and *Escherichia coli*, respectively (Motone et al., 2016; Rhein-Knudsen et al., 2021). Cleaving sugars into monomers or oligomers is achieved either by acid-hydrolysis or enzymatic hydrolysis. Enzymatic treatments are milder than acid treatments and will have less effect on the yields, composition, and structure of the seaweed sugars (Ale & Meyer, 2013; Deniaud-Bouët et al., 2017).

Enzymatic degradation of seaweed is challenging due to the content of several different polysaccharides. Laminarin and cellulose from brown seaweed can be hydrolyzed to glucose using laminarases and cellulases, while alginate hydrolysis is conducted by alginate lyases (Rhein-Knudsen et al., 2021). Enzymes depolymerizing fucoidan are called fucoidanases. A strategy for producing fermentable sugars is to combine the different enzymes in an enzymatic cocktail. Due to variation in polysaccharide composition depending on species, season, and environment, creation of an enzyme cocktail requires thorough investigation of optimal enzymatic treatment for each specific seaweed species. Commercial enzymes for laminarin, cellulose and alginate, although rare and highly specialized, are currently accessible, but enzymes for fucoidan are yet to be commercially available.

1.5 Fucoidan

Seaweeds contain a number of different carbohydrates, and several of these compounds (e.g. alginates, agars, carrageenan) have established roles in the food, pharmaceutical, and biochemical industry. There is still ongoing research being conducted for these compounds, but less explored compounds are being increasingly more investigated as well. Fucoidan, being one

of these more unexplored compounds, has recently gained much attention for being associated with biological and immunological properties, such as having anti-tumor, antithrombotic, and immunomodulatory effects (Ale & Meyer, 2013; Kusaykin et al., 2016).

1.5.1 Structure

Fucoidan is considered a broad term used to describe fucose-containing sulfated polysaccharides (FCSPs) (Deniaud-Bouët et al., 2017). FCSPs with a backbone consisting of fucose units are classified as homofucans, while those that have a non-fucose backbone, e.g. β -1,6 linked D-galactose, are classified as heterofucans. As there is still much uncertainty about the different fucoidan structures and compositions from different seaweed sources, it is difficult to say what the exact compositions of different extracted fucoidans are. All the FCSP substrates used in this study are therefore simply termed “fucoidan”.

Fucoidans are water-soluble heteropolysaccharides that are composed of a backbone of either α -1,3-L-fucose units, or alternating α -1,3; α -1,4-L-fucose units. Some of them may contain β -1,6-linked D-galactose or β -1,3-linked D-glucuronic acid. The fucose units in the fucoidan, depicted in Figure 2, contain hydroxyl groups that are subject to various substitutions.

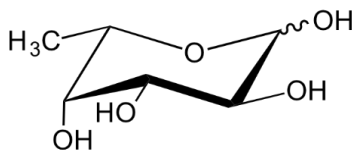


Figure 2: L-fucose, the monosaccharide unit in the polysaccharide fucoidan. The molecule commonly has substitutions of sulfate, acetate, or other monosaccharides. Figure source (Biosynth, 2023a).

The hydroxyl groups can be substituted with sulfate, acetate and/or side branches with glycosyl units. The fucoidan backbone with sulfate substitution is depicted in Figure 3. Monosaccharides such as glucose, galactose, mannose, and xylose may be substitutions as well, but observations of these compounds could also be due to contamination (Ale & Meyer, 2013; Fernando et al., 2019).

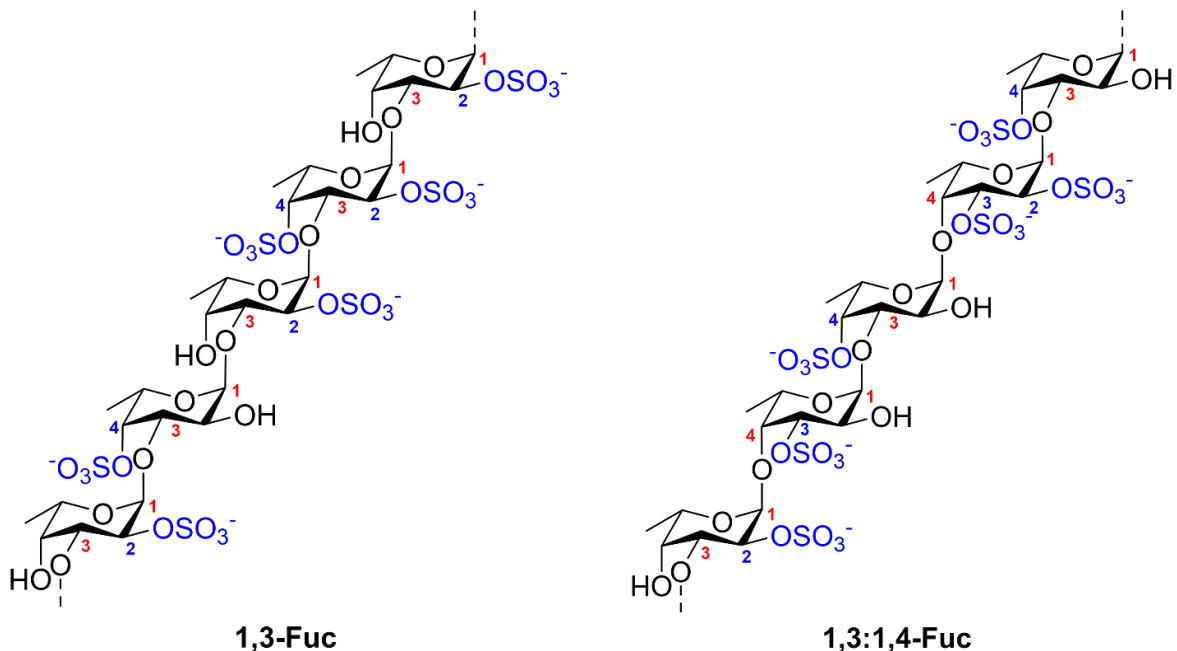


Figure 3: The backbone of the fucoidan molecule, which is composed of either α -1,3-L-fucose units (left), or alternating α -1,3; α -1,4-L-fucose (right). All fucoidans are sulfated, but there are large variations in amount and location of the sulfate groups. Figure source BioRef (ChemDraw v.21).

Illustrated on the left of Figure 3 are sulfate substitutions at C-2 and C-4 for some of the fucose units, which is common in brown seaweeds from the order Fucales. In Laminariales and Chordariales, sulfate ester groups are more common at C-4, while other sugar monomers can be side branches from C-2 (Zayed et al., 2020).

All fucoidans have a varying degree of sulfation, but acetylated fucose units are common occurrences as well. Acetyl substitutions will be localized randomly and occasionally throughout the fucoidan backbone, where residues linked at C-3 and C-4 are most common (Fernando et al., 2019). Mekabu, the sporophyll of brown algae *Undaria pinnatifida*, contains fucoidan which is highly O-acetylated. O-acetylation in fucoidan, which means that an oxygen atom in the fucoidan backbone is covalently bound to an acetyl group, may be involved in antiviral activity due to hydrogen bonding and hydrophobic interactions (Synytsya et al., 2014). Figure 4 illustrates acetylated fucoidan backbones, where the O-acetylation is shown in green.

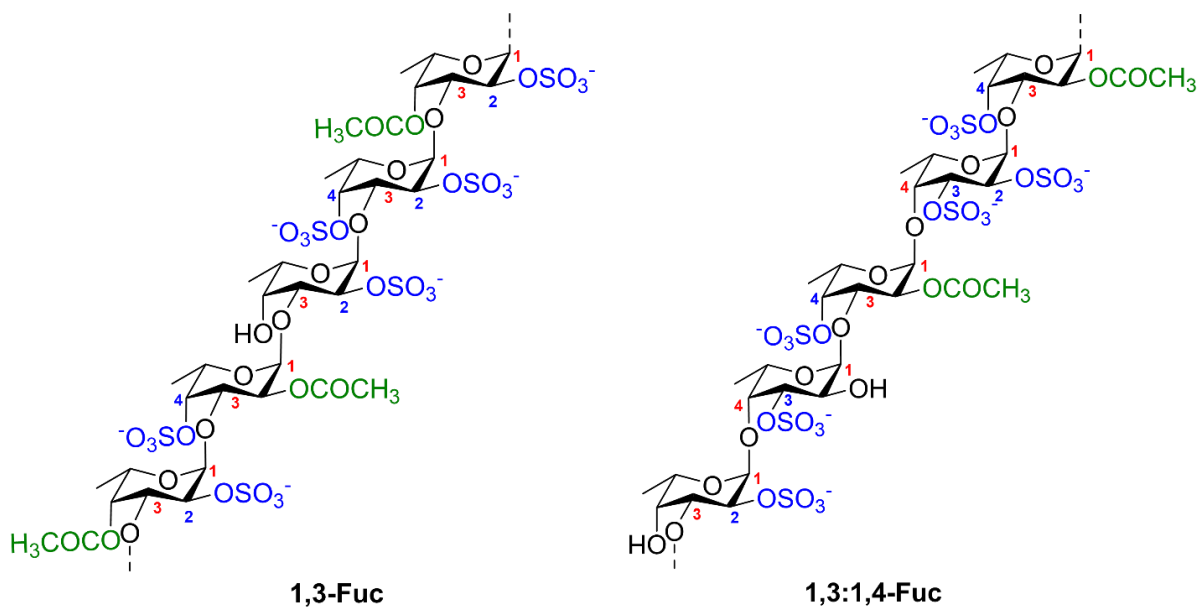


Figure 4: Sulfated and acetylated backbones of α -1,3-L-fucose (left) and alternating α -1,3; α -1,4-L-fucose (right) fucoidan.

FCSPs can also be found in other organisms than brown seaweeds. In such cases, the FCSPs have more regular and repetitive structures than seaweed fucoidan, and are only composed of L-fucose (Zayed et al., 2020). Some examples of the marine organisms containing FCSPs are echinoderms like sea urchins and cucumbers, and a few diatoms (Fonseca & Mourão, 2021; Silchenko et al., 2022).

1.5.2 Fucoidan Extraction

Fucoidan structure varies with seaweed species and seasonal and geographical variations, but it also varies with extraction technique. Because of that, the different extraction techniques will also influence the biological activities, as these are dependent on the fucoidan structure, even though it is still unclear which exact components are needed for bioactivity. Chemical- and hot water extraction, which are classical procedures for fucoidan extraction, give a low yield and degrade the fucoidan structure due to the harsh conditions, which may result in reduced biological activity. Microwave-assisted extraction can give a higher yield, but its effect on bioactivity is unknown. Enzyme-assisted extraction is believed to better conserve biological activity as no degradation of product is performed during extraction, but the technique requires a well-defined enzyme mixture with specific enzymes, since the cell wall of brown seaweeds have high complexity (Zhao et al., 2018). Recently, a new extraction protocol using the commercial cellulase mixture Cellic® CTec2 in combination with thermophilic alginate lyases has been

reported (Rhein-Knudsen et al., 2023). The new technique obtains higher yields of fucoidan and sulfate, and with less contamination of cellulose, laminarin, and alginate, than with traditional extraction techniques.

Besides affecting the chemical composition of fucoidan, the different extraction methods can also give different results regarding fucoidan size. Documented molecular weights of extracted fucoidan vary from 10 kDa to up to 950 kDa, the latter being the weight of fucoidan extracted from *Hizikia fusiforme* and *Sargassum fusiforme* (Holtkamp et al., 2009; Wang et al., 2019).

1.5.3 Bioactivities

Fucoidan has been shown to have an effect in inhibiting the growth of cancer cells and to have antioxidant, anti-coagulant, antiviral and immunoregulatory activities (Collic et al., 1991; Reys et al., 2021; Shi et al., 2017; Shiao et al., 2022), although the exact chemical components responsible for these activities are not known. More recently, fucoidan has been shown to contribute to alleviating metabolic syndrome, protecting the gastrointestinal tract, and improving bone health (Chen et al., 2023; Ohmes et al., 2022; Wang et al., 2019).

Due to all its therapeutic bioactivities and considering that it is non-toxic and rarely causes irritation, fucoidan has the potential to become highly valuable in medicine (Wang et al., 2019). Studies that are investigating administration of fucoidan drugs in term of tissue distribution and pharmacokinetics will be an important factor when applying fucoidan in clinical trials (Zayed et al., 2020). Modification of native fucoidans could alter, specify, or increase their biological activity. Particularly, modification of enzymatically derived oligomers, which is discussed more in detail later, could become highly relevant.

1.5.4 Fucoidan secretion

The carbon found in fucoidan originates from CO₂ fixated during photosynthesis. Recent findings actually suggest that fucoidan could have a role in carbon sequestration in the oceans. Brown seaweeds secrete up to 35 % of their net primary production, and fucoidan makes up about half of what's secreted (Buck-Wiese et al., 2023). A significant amount of the fucoidan of brown seaweed is consequently discharged into the ocean. Secretion is done without simultaneously removing nutrients (which would have led to a reduction in the primary productivity), resulting in secreted molecules that contribute to carbon dioxide removal. It has

indeed been shown that the secreted fucoidan sequester carbon at the same rate as the carbon stored in biomass (Buck-Wiese et al., 2023).

Fucoidans have shown to be more difficult to degrade than most other polysaccharides. The complex structure of the polymer is likely the reason, and the organisms degrading fucoidan are therefore required to be highly specialized with complex pathways and a repertoire of enzymes with different functions. Genomic and proteomic analyses of a *Lentimonas* strain revealed that it possessed 284 putative fucoidan-acting enzymes, where these proteins assemble into substrate-specific pathways with about 100 enzymes required per fucoidan (Sichert et al., 2020). The requirement of enzyme abundance and specificity makes it difficult for the microbial community to efficiently degrade FCSPs and the polysaccharides therefore have a very slow turnover and will accumulate in the ocean. Secreted fucoidan can accumulate in particles, and combined with its perseverance in the environment, it could sink into deeper water and partake in carbon sequestration in the sediment of the ocean (Silchenko et al., 2022). The research on the topic is still limited, but fucoidan has been found to endure whole centuries in deep sea sediments and is likely to contribute more to brown algae carbon dioxide removal than previously believed (Buck-Wiese et al., 2023).

1.5.5 Exploring fucoidan

The hydroxyl groups of fucoidans are prone to natural substitutions, and these hydroxyl groups, along with carboxyl, sulfate, and acetyl groups, can also be used for *artificial* modifications (Fernando et al., 2019). Such modifications are useful when tailoring the fucoidan in specific manners to alter the bioactivity. Another alteration that can be performed on the fucoidan polymers is cleavage by hydrolysis, which is necessary in order to obtain oligomers that can be modified (Fernando et al., 2019). Producing oligomeric elements from the full-length polymer is a promising way to overcome fucoidan's complexity, high molecular weight, high viscosity, and often poor dissolution rate, which all limit its pharmaceutical and industrial application (Suprunchuk, 2019; Wang et al., 2023).

The many bioactivities displayed by fucoidan are connected to the structural and molecular composition of the fucoidan molecule, where everything from its molecular weight to monosaccharide alignment and sulfate content will have an effect on the fucoidan properties (Ale & Meyer, 2013). One example of relationships between activity and molecular feature is

between high molecular weight and anticoagulant activity (Zayed et al., 2020). Still, as previously mentioned, extensive knowledge about which structural and chemical components are responsible for the different activities is lacking (Holtkamp et al., 2009; Vickers et al., 2018). There is furthermore an absence of standardized procedures regarding extraction, purification, and analytical procedures, making it difficult to properly correlate the chemical structures to the specific biological activities (Ale & Meyer, 2013; Usov & Zelinsky, 2013). Deficiency in fucoidan knowledge and standardized research methods can be explained by the heterogeneity of fucoidan with its varying degree of sulfation and acetylation, in addition to substitutions and possible contaminations. Both qualitative and quantitative assessments are necessary to increase compositional knowledge. Characterizing fucoidan polysaccharides is therefore considered a bottleneck for applying it industrially (Zayed et al., 2020).

One approach to study the chemical compositions and properties of fucoidans is by using enzymes. Enzymatic extraction and treatments are, as mentioned, methods to retrieve intact fucoidan from brown seaweed, but enzymatic hydrolysis of the fucoidan molecule itself is valuable to create a better understanding of the fucoidan structure and molecular activity. Enzymatic degradation into smaller units of a lower molecular weights is also thought to create more defined molecules that can be used for biomedical purposes (Jönsson et al., 2020). The method is used to obtain functional oligosaccharides, which are desirable to use in enzymatic and microbial conversions for creating added value derivatives (Arntzen et al., 2021; Jönsson et al., 2020; Usov & Zelinsky, 2013).

1.6 Fucoidan-acting enzymes

Fucoidan-acting enzymes are enzymes catalyzing modifications of fucoidan polysaccharides, and include glycohydrolases, sulfatases, and deacetylases. Enzymes used in hydrolysis of fucoidan can be found in marine invertebrates, bacteria, and some fungi (Kusaykin et al., 2016; Silchenko et al., 2022; Usov & Zelinsky, 2013), which is to be expected as fucoidan is a common marine polysaccharide. Still, the biological processing and metabolic utilization of fucoidan in these organisms is not well understood, as most of the fucoidan enzymes are found in highly specialized bacteria that produce a great number of different enzymes with various capabilities (Silchenko et al., 2022).

Investigating the enzyme system needed for processing different fucoidan polymers is therefore of great interest not only for fucoidan understanding and utilization, but also for insights into fucoidan utilization pathways in different organisms. Considering that the fucoidan polymer is heterogenous and highly complex, many different types of enzymes are needed for fucoidan degradation. Since the only compositional consistency in fucoidan molecules is its fucose backbone and sulfate substitutions, fucoidanases and fucoidan sulfatases have received most attention and will also be those in focus in this study.

Discovering fucoidan-acting enzymes that can be investigated will often involve investigating the genome of an organisms for genetic sequence similarities with genes encoding for known fucoidan-acting enzymes. Fucoidanases and fucoidan sulfatases have been confirmed to be expressed in some bacteria, such as *Lentimonas* sp., *Formosa algae*, and *Muricauda eckloniae* (Sichert et al., 2020; Silchenko et al., 2017; Tran et al., 2022), but an additional approach to discover these types of enzymes is by screening metagenomes. Metagenomic screening allows searching for enzymes in more than just one species at a time. It is conducted by searching the amino acid sequences obtained from the metagenome data against enzyme databases. Possible relevant activities are identified by sequence similarities between the obtained raw data and already characterized enzymes. Screening of a whole metagenome is also beneficial in terms of recovering the genetic material directly from the environment. As a result, there is no need to isolate or cultivate microorganisms in order to study their metabolic properties. Novel enzymes with desirable activities can be identified in even the most uncultivable microbes and from highly complex ecosystems (Madhavan et al., 2017).

Studies involving metagenomic samples from thermal vents in an Arctic Mid-Ocean Ridge (AMOR) have resulted in the discovery and characterization of several enzymes acting on seaweed polysaccharides. The AMOR metagenome can be valuable in screening for fucoidanases as the genetic material comes from marine organisms. The AMOR metagenome is also of particular interest because it is sampled from thermal vents. Enzymes discovered in thermal vents are likely to withstand high temperatures and have an increased likelihood of being thermophilic, which is useful for utilization alongside cellulases that have high temperature optima. Two enzymes discovered from the AMOR metagenome are alginate lyases AMOR_PL17A (Arntzen et al., 2021) and AMOR_PL7A (Vuoristo et al., 2019).

1.6.1 Fucoidanases

Fucoidanases are enzymes that hydrolyze fucoidan by catalyzing the cleavage of glycoside bonds in the fucoidan molecule (Kusaykin et al., 2016). Fucoidanases are therefore glycosidases (EC 3.2.1), and synonyms used for fucoidanases are fucosidases, fucanases, and fucoidan-hydrolases. Fucoidanases are classified in the Carbohydrate-Active Enzyme (CAZy) database (www.cazy.org) (Lombard et al., 2014), where they are grouped into different glycosyl hydrolase (GH) families depending on substrate specificity and mode of action. Each GH family includes enzymes having similar amino acid sequence and secondary structure, and some glycoside hydrolases are multifunctional enzymes because they have modules and catalytic domains that belong to several families (Kusaykin et al., 2016). Glycosyl hydrolase families associated with fucoidan activity, which are described more in detail below, are GH29, GH95, GH141, GH151, GH168, and GH107. Recently, a novel glycosyl hydrolase family, GH174, was also established (Liu et al., 2023).

The mode of action of fucoidanases can be understood by screening the fucoidan substrates and by determining the structure of the hydrolytic products. However, such an approach is challenged by the lack of a quantitative method for detecting enzyme specificity and rate of reaction. Reactions by fucoidanases are normally detected using Size Exclusion Chromatography (SEC), electrophoresis of the carbohydrates (C-PAGE), and High Performance Liquid Chromatography (HPLC). Some also use Fluorophore-Assisted Carbohydrate Electrophoresis (FACE), labeling fucooligosaccharides with a fluorophore or chromophore, and turbidimetry analyses (Kusaykin et al., 2016). These methods have some challenges in not being convenient, fast, or affordable enough for broad screening. For example, SEC is limiting in that it is slow and requires high substrate concentrations, while difficulties in C-PAGE are often associated with the lack of available oligomer standards. One conventional method has also been to use reducing sugar assays, though the method has been unsuccessful in some cases (Colin et al., 2006), probably due to interference from the structure as fucoidan is chemically and structurally complex (Kusaykin et al., 2016). Developing standardized procedures and tools for analysis is therefore still a big part of fucoidan and fucoidanase research.

Consequently, the knowledge of fucoidanase activity, specificity and mechanisms is limited. Nevertheless, it is clear that fucoidanases are, like other glycosidases, divided into two main

groups: endo- and exo acting enzymes (Figure 5). Endo-fucoidanases cleave glycosidic bonds *within* the fucoidan backbone and produce oligosaccharides, while exo-fucoidanases cleave the bonds from the end of the fucoidan molecule and produce fucose monosaccharides.

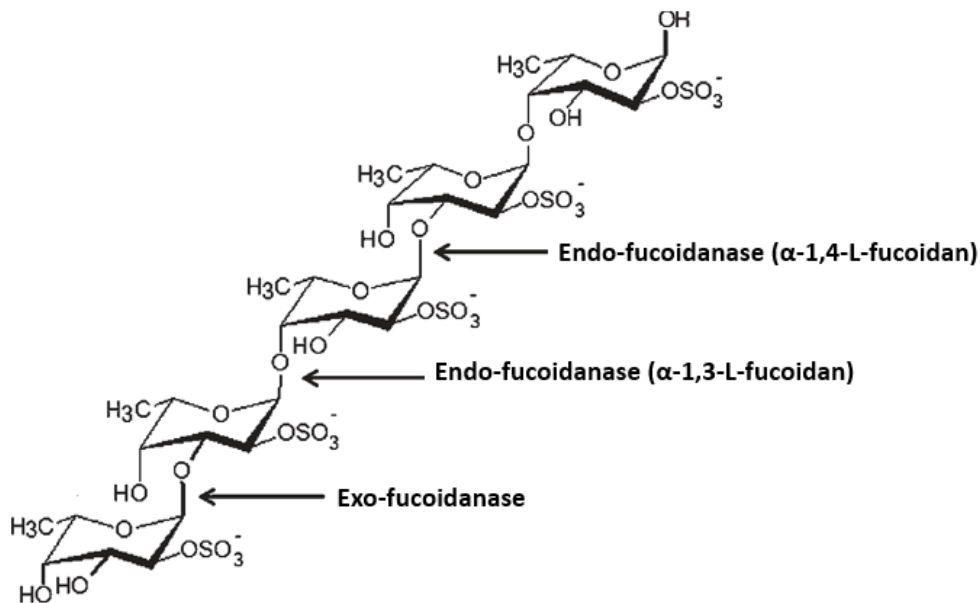


Figure 5: The sites of cleavage for fucoidanasases. Endo-fucoidanasases cleave glycosidic bonds *within* the fucoidan backbone with specificity towards either α -1,3- or α -1,4-bonds, while exo-fucoidanasases cleave the bonds from either the reducing end (not shown) or the non-reducing end. Figure adapted from Ale & Meyer (2013).

1.6.1.1 Endo-fucoidanasases

Endo-fucoidanasases cleave glycosidic bonds within the fucoidan molecule and the products are oligomers with various degree of polymerization. Endo-fucoidanasases have specificity towards either α -1,3- or α -1,4-bonds (Figure 5). The enzymes with specificity towards α -1,3-linkages are classified as enzyme family GH168, while those with specificity towards α -1,4-linkages are classified as GH107 (CAZy (Lombard et al., 2014)). A fucoidanasase with specificity towards α -1,3-linkages belonging to a novel glycoside hydrolase family GH174 has also been characterized (Liu et al., 2023). The first member of GH family 107 was a fucoidanasase active enzyme from the bacterium *Mariniflexile fucanivorans* named MfFcna (Colin et al., 2006), but there have been several new additions to this family which now contains 12 characterized enzymes. Along with MfFcna, only P5AFcna (from *Psychromonas* species SW5A) has had its structure elucidated (Vickers et al., 2018). Comparing the structure and mechanism of the two enzymes revealed that their catalytic mechanism seemed conserved, but variation in the architecture of the active sites

caused differences in substrate specificity. Additional endo-fucoïdanases that have been characterized are FunA of the GH168 family as well as Fp273 and FWf2 of the GH107 family (Silchenko et al., 2022).

1.6.1.2 Exo-fucoïdanases

Exo-fucoïdanases remove fucose units from the polysaccharide ends, where catalytic activity can be directed both towards the reducing- and the non-reducing ends. Exo-fucoïdanases are found in families GH29, GH95, GH141, and GH151, where GH29 has the most members and the biggest variety in catalytic activities. Families GH141 and GH151 are simply attributed with α -L-fucosidase activity, while GH95 enzymes have specified α -1,2-L-fucosidase and α -L-galactosidase activity. An enzyme in the GH29 family can be an α -1,3/1,4-L-fucosidase, α -1,2-L-fucosidase, α -1,6-fucosidase, or an α -L-glucosidase (CAZy (Lombard et al., 2014)). There are more characterized exo-fucoïdanases than endo-fucoïdanases, particularly in families GH29 and GH95. Some examples of characterized exo-fucoïdanases are from the marine bacterium *Wenyingshuangia fucanilytica*. These enzymes have been named FucWf1, FucWf2, FucWf3, and FucWf6 of the GH29 family and FucWf5 of the GH95 family (Silchenko et al., 2022). FucWf5 is suggested to take part in fucoidan debranching and is also shown to have higher activity on fucoidans than the GH29 enzymes. Exo-fucoïdanases have been identified in multiple other marine bacteria as well, including for example the BcFucA in *Bacillus cereus* (Li et al., 2021) or several exo- α -L-fucosidases in *Paraglaciicola* sp. (Schultz-Johansen et al., 2021).

1.6.2 Sulfatases

Sulfate ions are in abundance in the oceans, where they are widely distributed and often found as sulfated polysaccharides that have been assimilated by living organisms. In fact, sulfate ester groups are found on a huge number of marine polysaccharides compared to terrestrial polysaccharides and is potentially an adaptation to marine environments (Helbert, 2017). Part of the adaptation to marine life involved osmotic and ionic regulation corresponding with maritime waters, and sulfation has been shown to contribute to both these aspects (Aquino et al., 2004; Olsen et al., 2016).

Sulfatases are enzymes removing these sulfate ester groups by a hydrolytic mechanism, and the proteins are classified into currently four different families (S1-S4) in the SulfAtlas database (www.sulfatlas.sb-roscoff.fr) (Barbeyron et al., 2016; Stam et al., 2023). The majority of the

known sulfatases belong to the S1 family, and they have a conserved active site and adopt a similar fold comprising a large N-terminal domain and a smaller C-terminal domain. The S2 family comprises Fe(II) α -ketoglutarate-dependent arylsulfatases, while the S3 and S4 families both belong to the metallo-beta-lactamase superfamily and are separated into their respective families based on sequence similarities. Identified fucoidan sulfatases belong to the aryl sulfatase (S1) family, and are found in subfamilies S1_15, S1_16, S1_17, S1_22, and S1_25.

Like O-glycoside hydrolases, sulfatases can have either endo- or exo-activity. Endo-acting fucoidan sulfatases will cleave sulfate esters positioned within the fucoidan chain, while exo-acting will cleave sulfate esters positioned at the end. The S1_15 subfamily encompasses N-acetyl-D-galactosamine-6-sulfate exo-6-O-sulfohydrolases and D-galactose-6-sulfate 6-O-sulfohydrolases, while S1_16 encompasses D-Galactose-4-sulfate/N-acetyl-D-galactosamine-4-sulfate 4-O-sulfohydrolases. Known enzymatic activities for S1_17 include exo-Fucose-2-sulfate-2-O-sulfohydrolase for fucans and endo-3,6-anhydro-D-galactose-2-sulfate-2-O-sulfohydrolase for α -carrageenans. The subfamily S1_22 has unknown activity, and lastly S1_25 has exo-Fucose-3-sulfate-3-O-sulfohydrolase activity for fucans and exo-L-Rhamnose-3-sulfate-3-O-sulfohydrolase for ulvans. Some fucoidan-active sulfatases that have been characterized are SWF1, SWF4 (Silchenko et al., 2018), and PsFucS1 (Mikkelsen et al., 2021). SWF1 is classified as an exo-2O-sulfatase, while SWF4 is an exo-3O-sulfatase. PsFucS1 is presumably an exo-sulfatase.

Difficulties in purifying the sulfatases and producing them through heterologous expression are considered bottlenecks in researching fucoidan sulfatases (Helbert, 2017). Also, when investigating enzyme activity, there's frequently a small and possibly inaccurate amount of sulfate release observed. The reasons for the low number of sulfate release are likely that the sulfate groups are differentially located in the fucoidan molecule, and that there's frequently a lack of fucoidan degradation by fucoidanases prior sulfatase activity (Mikkelsen et al., 2021). Challenges such as these illustrate the need to further increase our knowledge of the enzymes themselves and how to work with them most efficiently.

The enzyme families of both fucoidanases and fucoidan sulfatases are summarized in Table 1.

Table 1: Families of enzymes acting on fucoidan polysaccharides that were of focus in this study. The enzyme families of shared functions in fucoidan are categorized according to the CAZy and SulfAtlas databases.

Enzyme family	Functions in fucoidan
GH168, GH107, GH174	Endo-fucoidanase
GH29, GH95, GH141 GH151	Exo-fucoidanase
S1_15, S1_16, S1_17, S1_22, S1_25	Sulfatase

1.7 Aim of study

Enzymatically converting seaweed carbohydrates to shorter-linked oligomers can create added-value products in the physiochemical, pharmaceutical, and agricultural industry. However, there are no commercial enzyme cocktails available to convert such sugars. Also, fucoidan with its huge number of significant bioactivities, along with fucoidan-acting enzymes, are not well understood. The main aim of this study was to contribute to increased knowledge of the fucoidan molecule as well as the enzymes acting on it by searching for and testing putative fucoidan active enzymes. The goal was to identify and characterize one or more novel fucoidanase(s) or fucoidan sulfatase(s) that can be used as part of an enzymatic toolbox to study and modify fucoidans. Ultimately, finding and characterizing a novel fucoidanase or sulfatase could contribute to the commercializing of fucoidan active enzymes. In this study, a metagenomic sample was obtained for the screening of putative fucoidan active enzymes, which were to be expressed and tested for activity. Additional in-house enzymes from the genome of *Lentimonas* sp. genome were to undergo activity testing as well. Any active enzymes were to be characterized by determining optimal conditions for activity with regards to factors such as temperature, salinity, and pH.

2 Materials

2.1 Enzymes

Table 2: Novel enzymes from the AMOR metagenome, collected from chamber CGB6.1. The sequences encoding for the enzymes were ordered as synthetic genes and cloned into their respective expression vectors by GenScript. Each gene underwent heterologous expression in *E. coli* before being purified.

Enzyme	Source	Enzyme family	Putative function
AMOR_639	AMOR_ CGB6.1	GH168	Endo-fucoidanase
AMOR_987	AMOR_ CGB6.1	GH168	
AMOR_151	AMOR_ CGB6.1	GH151	Exo-fucoidanase
AMOR_141	AMOR_ CGB6.1	GH141	
AMOR_95	AMOR_ CGB6.1	GH95	
AMOR_29	AMOR_ CGB6.1	GH29	
AMOR_S25	AMOR_ CGB6.1	S1_25	Sulfatase
AMOR_S16	AMOR_ CGB6.1	S1_16	
AMOR_S15	AMOR_ CGB6.1	S1_15	

Table 3: In-house putative fucoidan-active enzymes produced from glycerol stocks at BioRef, produced in the same manner as with the AMOR enzymes, described in 3.5.

Enzyme	Source	Enzyme family (CAZy)	Function/Putative function
Afc95A_28	<i>Lentimonas</i> sp.	GH29	Exo-fucoidanase
Fp277_23	<i>Lentimonas</i> sp.	GH107	Endo(1,4)-fucoidanase
Fp279_42	<i>Lentimonas</i> sp.	GH107	Endo(1,4)-fucoidanase
FunA_30	<i>Lentimonas</i> sp.	GH168	Endo(1,3)-fucoidanase
FunA_31	<i>Lentimonas</i> sp.	GH168	Endo(1,3)-fucoidanase
FunA_50	<i>Lentimonas</i> sp.	GH168	Endo(1,3)-fucoidanase
P5AFcnA	<i>Psychromonas</i> species SW5A	GH107	Endo-fucoidanase. Used as a benchmark enzyme and for production of fucoidan oligomers

2.2 Substrates

Table 4: Fucoidan sources for commercial and TFA hydrolyzed (oligomers) enzyme substrates.

Genus	Species	Supplier
<i>Macrocystis</i>	<i>pyrifera</i>	Sigma-Aldrich/Merck
<i>Alaria</i>	sp.	Sigma-Aldrich/Merck
<i>Undaria</i>	<i>pinnatifida</i>	Sigma-Aldrich/Merck
<i>Fucus</i>	<i>vesiculosus</i>	Sigma-Aldrich/Merck
<i>Saccharina</i>	<i>latissima</i>	Sigma-Aldrich/Merck
<i>Fucus</i>	<i>serratus</i>	Biosynth
<i>Laminaria</i>	<i>digitata</i>	Sigma-Aldrich/Merck
<i>Ascophyllum</i>	<i>nodosum</i>	Biosynth
<i>Laminaria</i>	<i>japonica</i>	Biosynth
<i>Lessonia</i>	<i>nigiscens</i>	Sigma-Aldrich/Merck
<i>Ecklonia</i>	sp.	Sigma-Aldrich/Merck
<i>Durivillea</i>	sp.	Sigma-Aldrich/Merck
<i>Cladosiphon</i>	sp.	Biosynth

Table 5: Carrageenan polysaccharides used for testing of sulfatase activity. The substrates include commercial carrageenans and TFA hydrolyzed (oligomers) enzyme substrates.

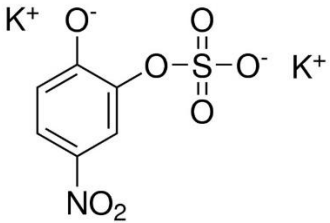
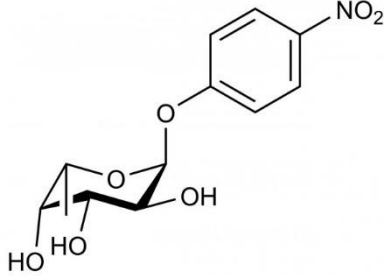
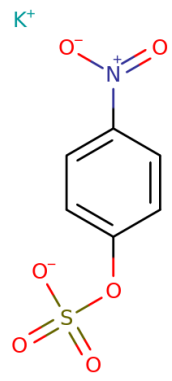
Type of carrageenan	Supplier
ι-carrageenan	TCI Chemicals
κ-carrageenan	TCI Chemicals
λ-carrageenan	TCI Chemicals

Table 6: Enzymatic hydrolysates (oligomers) produced during this project. The steps involved in producing the hydrolysates are described under methods (3.8).

Fucoidan source	Hydrolyzed by (enzyme)
<i>M. pyrifera</i>	P5AFcnA
<i>Alaria sp.</i>	P5AFcnA
<i>F. serratus</i>	P5AFcnA

<i>L. digitata</i>	P5AFcnA
<i>A. nodosum</i>	P5AFcnA
<i>Fucus vesiculosus</i>	FunA_50

Table 7: Artificial substrates used in activity assays and enzyme characterization experiments.

Substrate	Abbreviation	Structure
4-Nitrocatechol sulfate dipotassium salt	pNCS	 <p>(Sigma-Aldrich, 2023)</p>
p-Nitrophenyl- α -L-fucopyranoside	pNP-fuc	 <p>(Megazyme, 2023)</p>
Potassium 4-nitrophenyl sulfate	pNPS	 <p>(Biosynth, 2023b)</p>

2.3 Cells and expression vectors

Table 8: Cells used for transformation of *E.coli*, with supplier.

Cells	Supplier
One Shot™ BL21 (DE3) Chemically competent <i>E. coli</i>	Invitrogen
One Shot™ TOP10 Chemically competent <i>E. coli</i>	Invitrogen

Table 9: Expression vectors for expression in *E.coli*. The vectors are depicted in Figure 29 (Appendix A).

Vector	Supplier
pET-28a(+)	GenScript
pET-45b(+)	GenScript

2.4 Culture media and buffers

Table 10: Culture media and buffers.

Media/buffer	Contents	Area of use
Binding buffer	50 mM Tris pH 7.4 500 mM NaCl 20 mM Imidazole	Protein purification
Elution buffer	50 mM Tris pH 7.4 500 mM NaCl 500 mM Imidazole	Protein purification
Enzyme buffer 1	25 mM NaOAc pH 5.6 300 mM NaCl	Reactions with AMOR_ CGB6.1 endo- and exo- fucoidanases
Enzyme buffer 2	25 mM NaOAc pH 5.6 300 mM NaCl 10 mM CaCl ₂	Reactions with AMOR_ CGB6.1 sulfatases
Enzyme buffer 3	50 mM NaOAc pH 6.5	Reactions with AMOR_S25

	150 mM NaCl 5 mM CaCl ₂	
Enzyme buffer 4	20 mM Tris pH 7.4 200 mM NaCl	Reactions with <i>Lentimonas</i> enzymes
pH buffers Acetate	50 mM NaOAc 125 mM NaCl Varying pHs 3.6, 4.6, 5.6, and 6.0	Enzyme characterization
pH buffers Tris	50 mM Tris 125 mM NaCl Varying pHs 6.5, 7.0, 7.5, 8.0, and 9.0	Enzyme characterization
Lysogeny Broth (LB) media	10 g/L Tryptone 5 g/L Yeast extract 10 g/L NaCl	<i>E. coli</i> growth
Lysogeny Broth (LB) plates	10 g/L Tryptone 5 g/L Yeast extract 10 g/L NaCl 15 g/L Agar	<i>E. coli</i> growth
Terrific Broth (TB) media	20 g/L Tryptone 24 g/L Yeast extract 4 ml/L Glycerol TB salt (added after separate autoclaving)	<i>E. coli</i> growth
TB salt	2.31 g/L KH ₂ PO ₄ 12.54 g/L K ₂ HPO ₄	<i>E. coli</i> growth

2.5 Chemicals and compounds

Table 11: Chemicals and compounds with supplier.

Chemical/compound	Supplier
4-Hydroxybenzhydrazide (PAHBAH reagent)	Sigma-Aldrich/Merck

10X Tris/Glycine/SDS (TGS)	Bio-Rad
Agar powder	VWR
Any kD TM Mini-PROTEAN® TGX StainFree TM Protein Gels	Bio-Rad
Calcium chloride, CaCl ₂	VWR
D(+)-Glucose, C ₆ H ₁₂ O ₆ , anhydrous	Sigma-Aldrich/Merck
D-(+)-Fucose, C ₆ H ₁₂ O ₅	Sigma-Aldrich/Merck
D-(+)-Galactose, C ₆ H ₁₂ O ₆	Sigma-Aldrich/Merck
EDTA, C ₁₀ H ₁₆ N ₂ O ₈	Sigma-Aldrich/Merck
Ethanol absolute, C ₂ H ₆ O	VWR
Glycerol, C ₃ H ₈ O ₃ , 85 %	Sigma-Aldrich/Merck
Hydrochloric acid, HCl, 32 %	Sigma-Aldrich/Merck
Imidazole, C ₃ H ₄ N ₂ , ≥99 %	Sigma-Aldrich/Merck
Iron(II) chloride, FeCl ₂	Sigma-Aldrich/Merck
Isopropyl β-D-1-thiogalactopyranoside (IPTG), C ₉ H ₁₈ O ₅ S	Protein Ark
Kanamycin sulfate, C ₁₈ H ₃₆ N ₄ O ₁₁	Sigma-Aldrich/Merck
Magic Mark TM XP Western Standard	Invitrogen
Magnesium chloride, MgCl ₂	Sigma-Aldrich/Merck
Manganese(II) chloride, MnCl ₂	Sigma-Aldrich/Merck
Monoclonal mouse anti-polyhistidine- peroxidase antibody	Merck
Nickel(II) chloride, NiCl ₂	Sigma-Aldrich/Merck
<i>nor</i> -harmane (9 <i>H</i> -pyrido[3,4- <i>b</i>]indole)	Sigma-Aldrich/Merck
NuPAGE TM LDS Sample buffer (4X)	Invitrogen
NuPAGE TM Sample reducing agent (10X)	Invitrogen
Potassium hydroxide, KOH (HPLC)	Sigma-Aldrich/Merck
Potassium phosphate dibasic, K ₂ HPO ₄	Sigma-Aldrich/Merck
Potassium phosphate monobasic, KH ₂ PO ₄	Sigma-Aldrich/Merck
Precision Plus Protein TM Unstained Standards	Bio-Rad
S.O.C. medium	Invitrogen

Skim milk powder	Sigma-Aldrich/Merck
Sodium acetate, NaOAc	Sigma-Aldrich/Merck
Sodium chloride, NaCl	Sigma-Aldrich/Merck
Sodium hydroxide, NaOH	VWR
Sodium nitrate, NaNO ₃	Sigma-Aldrich/Merck
Sulfuric acid, H ₂ SO ₄ , 98 %	Sigma-Aldrich/Merck
SuperSignal™ West Pico PLUS chemiluminescent substrate	Thermo scientific
Trifluoroacetic acid, TFA (C ₂ HF ₃ O ₂)	Sigma-Aldrich/Merck
Tris	Sigma-Aldrich/Merck
Tryptone	Sigma-Aldrich/Merck
Tween® 20	Sigma-Aldrich/Merck
Yeast extract	Sigma-Aldrich/Merck
Zinc chloride, ZnCl ₂	Sigma-Aldrich/Merck

2.6 Instruments and software programs

Table 12: Instruments and software programs with supplier.

Instrument/software program	Supplier
110V 4000 rpm Laboratory Mini Professional Tabletop Centrifuge Lab Electric Centrifuge Machine	VWR
250 ml bottle top filter, 0.45 µm PES membrane	VWR
3510-DTH Ultrasonic Cleaner	Branson
AERS500 (2mm) column	Thermo Scientific
AS11-HC column	Thermo Scientific
Azure 400® Fluorescent Imager for Western Blots	Azure Biosystems
AzureSpot Analysis Software	Azure Biosystems
CarboPac™ PA210 guard (4 × 30 mm)	Thermo Fisher
ChemDraw/ChemOffice v21.0	PerkinElmer

Chemical Duty Pump (compressor), 220 V/ 50 Hz	Sigma-Aldrich/Merck
Chromleon™ 7 Chromatography Data System	Thermo Scientific
ChromLab Software	Bio-Rad
CLC Genomics Workbench 22.0.2	Qiagen
Dionex™ AERS™ 500 Carbonate Electrolytically Regenerated Suppressor	Thermo Scientific
Dionex™ UltiMate 3000 HPLC system	Thermo Scientific
Dionex™ ICS-6000 Capillary HPIC™ system	Thermo Scientific
Dionex™ IonPac™ AS11-HC IC Columns	Thermo Scientific
Ecotron incubator	Infors HT
Filtropur S 0.2 µM	Sarstedt
Filtropur S 0.45 µM	Sarstedt
flexAnalysis	Bruker
flexControl	Bruker
Gel Doc™ EZ Gel Imaging System	Bio-Rad
Gen5™ 2.0 Data Analysis Software	BioTek
Gradient thermal cycler, UNO96	VWR
HiPrep™ 26/10 Desalting column	Cytiva
His-Trap™ HP column, 5 mL	Bio-Rad
Implen™ OD600 DiluPhotometer™	Fisher scientific
MALDI target plate	Bruker
Mega Star 1.6R Centrifuge	VWR
Millipore Express® PLUS 0.22 µm PES, 500 ml	Sigma-Aldrich/Merck
Mini-PROTEAN Tetra Vertical Electrophoresis Cell	Bio-Rad
Multitron Standard Shaker	Infors HT
NGC™ Chromatography System with BioFrac Fraction Collector	Bio-Rad
Ni ²⁺ affinity HisTrap FF 5 mL column	GE HealthCare

Pico™ 21 Microcentrifuge	Thermo fisher
PowerPac™ Basic Power Supply	Bio-Rad
Programmable Rotator Multi RS-60	Biosan
Pullulan standard	Sigma-Aldrich/Merck
RefractoMax520	ERC
Rezex™ ROA-Organic Acid H + LC column (300 × 7.8 mm)	Dionex
SerialCloner 2.6.1	SerialBasics
Synergy™ H4 Hybrid Multi-Mode Microplate Reader	BioTek
Thermomixer™ C	Eppendorf
TSKgel®PW _{XL} guard column (6 mm × 4 cm, 12 μm particle size)	Tosoh
TSKgel®G4000PW _{XL} column (7.8 mm × 30 cm, 10 μm particle size)	Tosoh
TSKgel®G5000PW _{XL} column (7.8 mm × 30 cm, 10 μm particle size)	Tosoh
Trans-Blot Turbo Mini 0.2 μm PVDF Transfer Packs	Bio-Rad
Trans-Blot Turbo Transfer System	Bio-Rad
TX-400 Anti-friction rotor	Fisher Scientific
UltrafleXtreme™ MALDI-TOF/TOF	Bruker
Vibra-Cell™ VCX 750 Ultrasonic Liquid Processor	Sonics & Materials, Inc.
Vivaspin® 20, 10,000 MWCO PES	Sartorius

3 Methods

3.1 Bioinformatics

A metagenomic sample was obtained from the top chamber (CGB6.1) in the Arctic Mid-Ocean Ridge (AMOR) at 71° north in the Jan Mayen hydrothermal vent field, with depths of 550 to 700 m. The metagenome was computationally generated into protein sequences and screened for protein predictions using the databases dbCAN, CAZy and SulfAtlas. The presence of signal peptides was predicted using SignalP. The generation of protein sequences with predictions was conducted by Runar Stokke (Department of Biological Sciences, Deep Sea Biology/Center for Deep Sea Research, University of Bergen), and the work in this thesis thus began with the sequence selection described below once the data with protein predictions had been received.

Selection of target sequences for the described project was done by first selecting potential candidates based on their appointed enzyme families (Table 1). Next, only sequences that were neighboring genes (located on the same contig) and those with the prediction of a signal peptide were further evaluated. The online tools HMMER, BLAST, and RCSB PDB were used to narrow the selection down further. The HMMER software (HmmerWeb version 2.41.2.) allows for analysis of the biosequences by searching against protein family databases such as Pfam and by using profile hidden Markov Models (www.hmmer.org) (EMBL-EBI, 2022). The Basic Local Alignment Search Tool (BLAST) compares biological sequences to sequence databases and finds similar regions and estimates statistical significance (Altschul et al., 1990). The US data center RCSB PDB provides an archive for the 3D structure data of the Protein Data Bank (PDB) (www.RCSB.org) (Berman et al., 2000). The website selects, organizes, and annotates PDB data according to a set of standards. The final sequences were selected after a holistic evaluation that also included Multiple Sequence Alignments (MSAs) and phylogenetic trees constructed in CLC Workbench.

3.2 Cloning

Using the molecular biology software CLC Workbench and SerialCloner, the predicted signal peptides were digitally cut off and the sequences were cloned into their respective expression vectors. The sequences for the putative endo-fucoidanasases were cloned into plasmid vector pET-45b(+) with an N-terminal His-tag and restriction sites for restriction enzymes KpnI (5' end) and

PacI (3' end). The sequences for the putative exo-fucoidanases and sulfatases were cloned into vector pET-28a(+) with a C-terminal His-tag and restriction sites for NcoI (5' end) and XhoI (3' end). The choice of restriction sites was based on in-frame transcription with the His-tags, and some amino acids were added towards the end of the sequences for the same purpose. The constructs were codon optimized for expression in *E.coli* and produced by GenScript.

3.3 Transformation of TOP10- and BL21 (DE3) *E. coli*

The codon optimized and synthesized constructs holding the genes of interest were contained in vials of approximately 4 µg of lyophilized plasmid DNA. To prepare for transformation, each vial was centrifuged at 6000 x g for 1 minute before 20 µL sterilized water was added to dissolve the DNA. The vials were then vortexed for 1 minute each. Plasmids were transformed into two different *E.coli* strains; the TOP10 for storage and the BL21 (DE3) for protein expression. The TOP10 produce a large number of copies of the plasmids containing the inserts and do not carry the gene encoding T7 RNA polymerase, which make them ideal for storage cells (i.e. the strain where the construct is maintained). The BL21 (DE3) cells do carry the gene encoding T7 RNA polymerase and are therefore the cells used for expression. Once the BL21 (DE3) are transformed with the plasmid, the cells will require Isopropyl β-D-1-thiogalactopyranoside (IPTG) to induce expression of the T7 RNA polymerase from the lacUV5 promoter, and IPTG is therefore added to growing *E. coli* during enzyme production (3.5).

The plasmids were transformed into chemically competent TOP10 *E. coli* cells with 2 µL of plasmid DNA following the transformation protocol provided by Invitrogen (2013). After verification of the TOP10 transformants, chemically competent BL21 (DE3) *E. coli* cells were transformed following the protocol of Invitrogen (2010). Selection of all transformants were done by verifying growth on LB agar plates with Ampicillin for those genes cloned in vector pET-45b(+) and with Kanamycin for those genes cloned in vector pET-28a(+).

3.3.1 Storage of transformed cells

For preparation of glycerol stocks for storage, cell cultures for each plasmid were prepared from transformed TOP10- and BL21(DE3)-cells, giving a total of 18 cultures. By using sterile techniques, the verified transformants were transferred from their respective colonies on the agar plates to 5 mL antibiotic-containing (50 µg/mL Kanamycin or 100 µg/mL Ampicillin) LB-medium. The cells were incubated overnight at 37 °C with 180 rpm shaking. Glycerol stocks

were made by gently mixing 750 μ L of the cell culture with 500 μ L 50 % glycerol and then adding the solution to cryotubes for storage at -80 °C.

3.4 Small-scale protein expression tests

To evaluate if the transformed cells could produce the target enzymes, small-scale expressions trials of the proteins were performed. The clones were gently transferred from the glycerol stocks of BL21(DE3)-cells to LB agar plates with antibiotics. The plates were incubated overnight (ON) at 37 °C before one colony from each plate was selected and inoculated in LB + 50 μ g/mL antibiotic at 37 °C and 180 rpm. For expression, the ON culture was diluted 100 times in 50 mL TB media containing antibiotics. The cultures were incubated at 37 °C and 180 rpm until the optical density (OD), measured spectrophotometrically at 600 nm, was approximately 0.6-0.8. Gene expression was then induced ON at 18 °C with the addition of 1 mM IPTG.

Protein expression was analyzed with Sodium Dodecyl Sulfate-Poly Acrylamide Gel Electrophoresis (SDS-PAGE) and Western blotting to visualize successful protein expression. After inducing the small-scale cultures with IPTG and incubating overnight, a 30 μ L sample from each culture was mixed with 10 μ L 4X SDS sample buffer before being boiled for 5 minutes and applied to stain-free acrylamide gels. The proteins and protein ladder were separated by running the gel at 270 V for 20 minutes in a chamber containing Tris/Glycine/SDS (TGS) running buffer.

For western blot analysis, the proteins were transferred to a PVDF membrane for using the Bio-Rad Trans-Blot Turbo Transfer System. The membranes were blocked by incubating them in a Tris-buffered saline (TBS) solution containing 2 % Skim milk and 0.1 % Tween-20 (wash buffer) for 1 hour, shaking at room temperature. The membranes were incubated with a wash buffer containing 1:4000 dilution of Monoclonal mouse anti-polyhistidine-peroxidase antibody for 1 hour. Washing the membranes was done by incubating them with the wash buffer for 10 minutes in three rounds, followed by a rinse with milliQ water. The membranes were dyed with 4 mL SuperSignal™ West Pico Chemiluminescent Substrate to detect antibody-protein complexes prior to visualization by Azure 400® Fluorescent Imager and AzureSpot Analysis Software.

3.5 Enzyme production

For large scale enzyme production, clones were expressed as described in 3.4, but on a larger scale where the ON culture in LB + antibiotic was diluted 100 times in 500 mL TB media containing antibiotics. After inducing ON at 18 °C with the addition of 1 mM IPTG, the cells were harvested by centrifugation for 30 minutes at 4 °C and 4700 rpm. The supernatant was discarded and the cell pellets were stored at -20 °C until further processing.

3.6 Enzyme purification

Cell pellets were defrosted, resuspended in binding buffer, and sonicated for 5-10 minutes with a 30 % amplitude and at 15 second pulses with 15 second pauses. The sonicated solutions were centrifuged at 12,500 rpm and 4 °C for 30 minutes, and the supernatants, containing the bacterial proteins, were filtered before being loaded to the His-Trap™ HP column on the Bio-Rad purification system. The protein mixture was passed through a column containing a ligand with immobilized Ni²⁺ that selectively binds proteins containing the affinity polyhistidine tag (His-tag). The column was washed with binding buffer to remove contaminants and non-specific bounded proteins. Proteins were eluted with a gradient of imidazole from 0-500 mM (elution buffer). The eluting solution was collected in fractions of 1 mL using a fraction collector connected to the purification system.

Fractions collected from the protein purification that had high absorbance values (280 nm) were analyzed with SDS-PAGE to confirm presence of correct protein. A 30 µL sample from each protein-containing fraction was run on acrylamide gels as described in 3.4. The Precision Plus Protein™ Unstained Standards was used for estimation of molecular weights. Following confirmation by SDS-PAGE analysis, the fractions containing the target protein were collected and loaded to a HiPrep™ 26/10 Desalting column to remove imidazole while simultaneously changing the buffer (the buffer was different for each enzyme; Table 10). The eluting solutions were again collected in fractions of 1 mL each using a fraction collector connected to the purification system.

Following buffer exchange, the fractions with confirmed enzymes from SDS-PAGE were collected in a Vivaspin 20, 10 000 MWCO filter (selected based on protein size) tube to concentrate the protein solutions. Concentration was done by centrifugation at 4 °C and 4000

rpm for intervals of 15 minutes, where molecules smaller than 10 kDa would be filtered out as the pore size of the membrane is 10 000 Da. Absorbance measurements (280nm) were taken in between intervals to assess the progress, and the concentration was concluded either when a protein concentration approached or exceeded 20 μ M. To ensure that absorption values were within the instrument's standard curve, the samples were diluted before measurement to not exceed an absorption value of 1. The protein concentrations were calculated based on the proteins' respective theoretical extinction coefficients (<https://web.expasy.org/protparam/>) (Gasteiger et al., 2005) using Beer's law (Appendix E).

3.7 Optimization of protein expression

Improving protein expression for enzymes not expressing at the initial small-scale expression tests was conducted by setting up experiments with varying expression conditions. Expressions were induced with different concentrations of IPTG (0.2 μ M; 0.5 μ M; 1 μ M) and at different times in the growth curve of *E. coli* (optical densities 0.6, 0.8, and 1.0). All expressions were done overnight at 18 °C and 180 rpm. The following day, 300 μ L of each culture was sampled out and spun down at 14,000 rpm for 3 minutes. The supernatants were discarded, and the pellets were resuspended in 10 μ L 4X SDS loading buffer, boiled for 5 minutes, and analyzed by Western blot analysis as described in 3.4.

3.8 Production of fucoidan oligomers

Fucoidan oligosaccharides were used as substrates for testing putative exo-fucoidanases and sulfatases and were prepared by partially hydrolyzing the commercial fucoidan substrates. 100 mg fucoidan was solubilized in 10 ml 1 M TFA and incubated at 60 °C for 1 hour. After cooling down to room temperature, the samples were neutralized with 6 mL 5 % NH_4OH .

Fucoidan oligomers were also produced enzymatically using the GH107 endo-fucoidanase P5AFcnA. The P5AFcnA has activity on fucoidans *M. pyrifera*, *L. digitata*, *Alaria* sp., *F. serratus*, and *A. nodosum* (Vickers et al., 2018; unpublished results from the BioRef lab). 10 mg/mL fucoidan solutions were prepared in 20 mM Tris pH 7.4, 200 mM NaCl before solubilizing overnight at 25 °C shaking. Enzyme was added to a final concentration of 0.5 μ M and the solution was incubated at 25 °C for 24 hours before enzymes were inactivated by boiling for 5-10 minutes. Control samples were included as well and were made using the buffer. The

enzymatic products from the five reactions were evaluated by Size Exclusion Chromatography (SEC), as described in 3.9.1, and the substrates were stored at -20 °C.

Any confirmed activity of endo-fucoidanases during the project would be followed with production of fucoidan oligomers with those respective enzymes and their substrates as well.

3.9 Enzyme activity assays

Enzymatic reactions were set up with 1 μ M enzyme and substrate concentration 10 mg/ml fucoidan for testing putative endo-fucoidanases, and substrate concentration 1-2 mg/ml fucoidan for testing putative exo-fucoidanases and sulfatases. The fucoidan substrates were derived from various sources (Table 4). The reactions ran overnight in 25 mM NaOAc pH 5.6 and 300 mM NaCl at 32 °C. Reactions with putative sulfatases had 10 mM CaCl₂ added. Enzymatic products were analyzed by SEC (3.9.1), HPLC, (3.9.2 - 3.9.3), and Matrix-Assisted Laser Desorption/Ionization Time-of-Flight Mass Spectrometry (MALDI-ToF) (3.9.4). Results generated by SEC and HPLC were analyzed using the Chromeleon 7.0 software.

Enzyme activity was also assayed by investigating reactivity with artificial substrates. Reaction mixtures of 1 μ M enzyme and 0-100 mM of either 4-Nitrocatechol fucose (pNP-fucose) (putative fucoidanases) or 4-Nitrocatechol sulfate (pNPS) and 4-Nitrocatechol sulfate (pNCS) (putative sulfatases) were incubated at 32 °C for approximately 1 hour before being visually evaluated and measured spectrophotometrically (410 nm) for color development.

3.9.1 Oligomer detection using Size-Exclusion Chromatography

Endo-fucoidanase activity was assayed by detecting reduction in fucoidan size with SEC using an Ultimate3000 system connected to RI-detector. 5–10 mg/mL sample was injected into a set-up with guard column TSKgel®PWXL connected to a TSKgel®G4000PWXL- and a TSKgel®G5000PWXL column. Elution was done at flowrate 0.5 mL/min with 0.15 M NaNO₃, 0.01 M EDTA at pH 6. Pullulan samples of 1.3-800 kDa were used as standards.

3.9.2 Monomer detection using High Performance Liquid Chromatography

Fucose release from exo-fucoidanase activity was quantified by HPLC using two different systems depending on the availability of the apparatuses. One system used was the ICS-6000 Capillary HPLC™ performing Anion-Exchange Chromatography with pulsed Amperometric Detection (HPAEC-PAD). The other system used was the UltiMate 3000 HPLC connected to an

RI-detector. For the UltiMate 3000 system, sugars were separated on a Rezex™ ROA-Organic Acid H + LC column and elution was done isocratically with 5 mM Sulfuric acid at 65 °C and flowrate 0.6 mL/min. For the ICS-6000 system, samples were passed through a 0.22 µM filter and the sugars were separated on a CarboPac™ PA210 guard column an analytical column. Isocratic elution was done with 1 mM KOH for 13 minutes. For both methods, fucose, glucose, and galactose were used as sugar standards.

3.9.3 Sulfate detection using High Pressure Ion Chromatography

To determine total sulfate release from reactions with an active sulfatase, the sulfate content of the fucoidan had to be quantified. The fucoidans were weighed out and solubilized in 2 M TFA to a total concentration of 10 mg/ml fucoidan. The samples were incubated at 100 °C for 8 hours before being measured.

The sulfate content of the fucoidan substrates and the sulfate release following sulfatase reactions were quantified with High Pressure Ion Chromatography (HPIC) with suppressed conductivity using the ICS-6000 system with column the AS11-HC and suppressor Dionex AERS500. Isocratic elution was done with 5 mM KOH for 10 minutes, with a flowrate of 0.38 mL/min. K₂SO₄ was used as calibration standards.

3.9.4 MALDI-ToF-MS

Formation of sulfated fucose and sulfated fuco-oligosaccharides up to 2000 Da were detected using MALDI-ToF-MS. The enzyme hydrolysates were mixed with 2.5 mg/mL *nor*-harmane matrix in a 1:1 volume ratio and 1 µL was applied to a stainless steel MALDI target plate and dried by evaporation at room temperature. The samples were analyzed using an ultrafleXtreme™ mass spectrometer in the negative-ion mode. The matrix applied was 9*H*-pyrido[3,4-*b*]indole (*nor*-harmane) and had been prepared in the BioRef group as described by Antonopoulos et al. (2005).

3.10 Characterization of active fucoidan sulfatase

To determine the optimal reaction conditions for the active AMOR enzyme, enzyme reactions with 1.5 µM and 10 µM enzyme and varying artificial substrate concentration of 0-100 mM was incubated for 45 min at 32 °C. The reactions were stopped by adding 300 µl of 1 M NaOH. After evaluating enzyme activity on the artificial substrate (Figure 35; Appendix F), 30 mM pNPS was

used to conduct characterization of the active enzyme. Characterization of the sulfatase involved finding its optimal reaction condition in terms of temperature, pH, salinity, presence of ions, and determining its kinetics. An assessment of its thermal stability was also performed. All reactions, as well as control samples, with artificial substrates were measured spectrophotometrically at 410 nm.

3.10.1 Determining optimal reaction conditions

For all samples, 1.5 μ M enzyme was mixed with 30 mM pNPS to a total volume of 75 μ L and incubated for 90 minutes. The reactions were run in triplicates, and they were stopped by adding 1 M NaOH to a sample dilution of 5X or 10X. The reactions for finding optimal temperature were done in enzyme buffer 2 (25 mM NaOAc pH 5.6; 300 mM NaCl; 10 mM CaCl₂) by setting up reactions at 10 °C, 20 °C, 25 °C, 30 °C, 35 °C, 40 °C, 45 °C, 50 °C, 60 °C, 75 °C, and 90 °C. The pH was tested in the same buffer but at optimal temperature and pH values 3.6, 4.6, 5.6, 6.0, 6.5, 7.0, 7.5, 8.0, and 9.0. Salinity was investigated at optimal temperature and pH at NaCl concentrations 18, 150, 300, 450, 600, 800, 1000, 1300, 1600, and 2000 mM. Lastly the effect of ions on activity was investigated under optimal conditions in a buffer free of ions, where 10 mM of NiCl₂, CuCl₂, MnCl₂, FeCl₂, ZnCl₂, MgCl₂ and CaCl₂ were added to its respective reaction. Once the ion with the most positive effect on enzyme activity was identified, its optimal concentration was determined by measuring activity at 0, 5 and 10 mM additions of the ion.

3.10.2 Thermostability

The sulfatase was pre-incubated at optimal conditions before 1.5 μ M was taken out and added to 30 mM pNPS at time points 0 min, 15 min, 30 min, 45 min, 60 min, 90 min, 2 h, 3 h, 4.5 h, and 24 h. The reactions were stopped by adding 300 μ L 1 M NaOH after the enzyme had been incubated with pNPS for 90 minutes.

3.10.3 Enzyme Kinetics

Mixtures of 1 μ M enzyme and varying substrate concentrations 0-60 mM pNPS were incubated at optimal conditions and absorbance (410 nm) measurements were taken every 2 minutes using the SynergyTM H4 Hybrid Multi-Mode Microplate Reader. The absorbance of p-nitrophenol measured during the enzymatic reaction when sulfate was cleaved of the pNPS molecule, was used to calculate the amount of sulfate released. By using Beer's law $c = A/(L\epsilon)$ (described in

3.6) with molar absorption coefficient for p-nitrophenol at $18,000 \text{ M}^{-1}\text{cm}^{-1}$, the concentration of released sulfate was calculated.

Values for K_m and V_{max} of the active AMOR enzyme were calculated according to Michaelis–Menten kinetics (Cornish-Bowden, 1981). Initial velocity v_0 of the enzymatic reaction was plotted against substrate concentration [S] to give a Michaelis-Menten curve, and the reciprocals, $1/v_0$ and $1/[S]$, were plotted against each other to give a Lineweaver-Burk plot. The slope and Y-intercept of the Lineweaver-Burk plot was used to calculate K_m and V_{max} (Appendix E).

3.10.4 Time course

The sulfatase was further examined through time courses on both the substrates it exhibited activity on and at two different enzyme concentrations. Mixtures of 5 mg/mL substrate and either 1 μM or 0.1 μM enzyme were incubated at optimal conditions for time points 0, 0.5, 1, 2, 3, 5, 10, 22, 24, and 30 hours. The reactions were then stopped by boiling and sulfate release was quantified using HPLC according to 3.9.3.

3.11 Characterization of active endo-fucoidanase from *Lentimonas*

To determine the optimal reaction conditions for the active *Lentimonas* endo-fucoidanase, the p-hydroxybenzoic acid hydrazide/4-Hydroxybenzhydrazide (PAHBAH) reagent was used to assess formation of reducing ends during the reaction with its suitable fucoidan substrate. Reducing ends of carbohydrates will in alkaline solutions react with acid hydrazides and give yellow anions. Setting up reactions with the enzymatic products and with PAHBAH can therefore be used in a simple calorimetric method that will detect less than 1 μg reducing ends (Lever, 1972).

The buffer used in all the experiments were 20 mM Tris pH 7.4 and 200 mM NaCl, and the reactions were run in triplicates for 45 minutes prior to being stopped by either boiling for 10 minutes or by addition of 90 mL NaOH. The reactions then had PAHBAH reagent, made according to Lever (1972) added in 1:1 ratio and were incubated at 100 °C for 10 minutes, followed by a cooldown and then absorbance measurements at 410 nm. Determining the enzyme concentration resulting in the highest yield was done by setting up reactions of 6 mg/ml fucoidan with either 1 μM , 0.1 μM , or 0.01 μM enzyme. For determining the substrate concentration providing the highest yield, 1mg/mL, 2 mg/mL, 4 mg/mL, and 8 mg/mL fucoidan were mixed with 1 μM and 0.1 μM enzyme, respectively. For finding optimal temperatures, 6 mg/ml

fucoïdan were incubated with 1 µM enzyme at 5 °C, 10 °C, 15 °C, 20 °C, 25 °C, 30 °C, 35 °C, 40 °C, 50 °C, 60 °C and 75 °C. Different pH values were tested by incubating 1 µM enzyme and 8 mg/mL fucoïdan at pH 3.6, 4.6, 5.6, 6.0, 6.5, 7.0, 7.5, 8.0, and 9.0.

4 Results & discussion

4.1 Bioinformatics

The total amount of predicted proteins from the AMOR CBG6.1 dataset was 476275, where 16179 Open Reading Frames (ORFs) had significant hits to dbCAN, CAZy, and SulfAtlas (or multiple hits to each). Altogether, in these different enzyme families, a total of 451 putative endo-fucoidanasases, exo-fucoidanasases, and sulfatases were identified. The putative enzymes were from the families GH168, GH29, GH95, GH141, GH151, S1_15, S1_16, S1_17, S1_22, and S1_25. Out of these, 43 possible targets for enzyme production were selected based on the presence of a signal peptide (predicted by SignalP) and for being neighboring genes located on the same contig. The presence of a signal peptide is desirable because it suggests that the protein is secreted, a necessary feature for bacterial degradation of a biopolymer like fucoidan, making it more likely that the protein has fucoidan activity. A contig is described as a contiguous length of genomic sequence that can be seen as a collection of overlapping DNA segments (Green, 2023). Sequences located on the same contig could indicate that their encoded proteins act together for fucoidan degradation and/or modification. Perhaps they even act synergistically, meaning their simultaneous activity is greater than the summation of each individual activity. The DNA segments can also be found as Polysaccharide Utilization Loci (PULs), which are co-localized clusters of genes which encode proteins involved in the same pathways (Helbert, 2017).

Using the online tools HMMER, BLAST, and RCSB PDB, the 43 candidates were narrowed down to 9. HMMER was used to search for outputs that revealed potential shared attributes between the sequences and enzymes of the families encompassing fucoidanasases and sulfatases. BLAST was used to compare sequence identities, and those sequences having either too low (below 20 %) or too high (above 95 %) identities with sequences in the databases used by BLAST were excluded. The RCSB PDB website was used to look further into the enzymes of at least 20 % sequence similarity and evaluate the likelihood of the novel sequence having the desired activities. Enzymes found in the human gut, for example, are likely not active on fucoidan, and were therefore omitted. Construction of MSAs and phylogenetic trees by CLC Workbench was used for further investigation of sequence similarity and possible evolutionary history. Examples of HMMER, BLAST and RCSB PDB outputs for one of the putative fucoidan

sulfatases (Figure 30), as well as a MSA (Figure 31), are provided in Appendix B. Figure 6 depicts the phylogenetic tree constructed for the initial 43 selections.

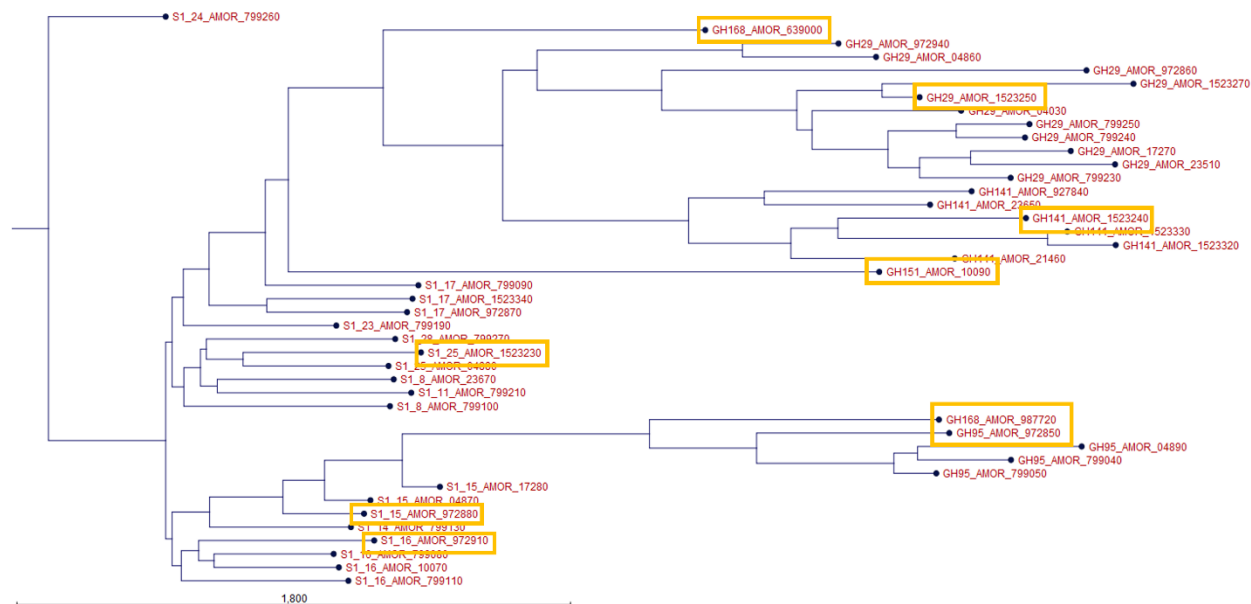


Figure 6: Phylogenetic tree of the 43 initially selected sequences. The tree was constructed by CLC Workbench. The selected sequences are marked with yellow boxes. In order to enhance the chance of a positive hit, it was attempted to select candidates from different clusters

By taking a holistic approach in evaluating the outputs from the online tools and bioinformatic software, nine sequences were selected (Figure 6; Table 13) and appointed new names for simplicity.

Table 13: Appointed protein names of the nine selected sequences, enzyme family and important criteria for selection.

Appointed name	Enzyme family	Selection criteria
AMOR_29	GH29	Annotated as α -L-fucosidase on HMMER 64-76 % on BLAST Relevant RSCB PDB hits, almost exclusively hits of around 35 % identity with α -L-fucosidases. Located on the same contig as AMOR_S25 and AMOR_141
AMOR_95	GH95	55-60 % on BLAST Relevant RSCB PDB hits, with α -L-fucosidase hits of

		<p>around 25 %</p> <p>Located on the same contig as AMOR_S15 and AMOR_S16</p>
AMOR_141	GH141	<p>Annotated as having a beta-helix on HMMER</p> <p>58-79 % on BLAST</p> <p>Located on the same contig as AMOR_29 and AMOR_S25</p>
AMOR_151	GH151	<p>Annotated as a glycosyl hydrolase on HMMER</p> <p>Only one hit in the metagenome, and has high novelty</p> <p>55-66 % on BLAST</p>
AMOR_369	GH168	<p>Annotated as glycohydrolases on HMMER</p>
AMOR_987		<p>Low percentages on BLAST (although above 20 %) and no hits on RSCB, but they are putative endo-fucoidanase, which were desired</p>
AMOR_S15	S1_15	<p>Annotated as a sulfatase on HMMER</p> <p>60-71 % on BLAST</p> <p>Relevant RSCB PDB hits, such as 33 % identity with a putative secreted sulfatase</p> <p>Located on the same contig as AMOR_S16 and AMOR_95</p>
AMOR_S16	S1_16	<p>Annotated as a sulfatase on HMMER</p> <p>68-75 % on BLAST</p> <p>Relevant RSCB PDB hits with sulfatases and located on the same contig as AMOR_S15 and AMOR_95</p>
AMOR_S25	S1_25	<p>Annotated as a sulfatase on HMMER</p> <p>69-83 % on BLAST</p> <p>Relevant RSCB PDB hits, such as 34 % identity with marine bacterium <i>Formosa agariphila</i></p> <p>Located on the same contig as AMOR_29 and AMOR_141</p>

4.2 Cloning & transformation

The amino acid sequences obtained from the AMOR metagenome that were codon optimized for expression in *E. coli* were cloned with a His-tag either on the N-terminal or C-terminal of the sequence to facilitate binding to a His-tag column during affinity chromatography for purification of the proteins. The choice of terminal for the His-tag was based on cloning previously conducted for AMOR enzymes (unpublished data; Nanna Rhein-Knudsen).

Transformation of TOP10 and BL21 (DE3) *E. coli* with the cloned vectors were successful, as confirmed by colony formation on antibiotic resistant (Kanamycin or Ampicillin) LB agar plates (data not shown).

4.3 Small-scale enzyme expression

To test if the transformed cells were expressing the selected genes, a small-scale expression of each AMOR enzyme was conducted and analyzed by SDS-PAGE analysis and Western blot, as depicted in Figure 7.

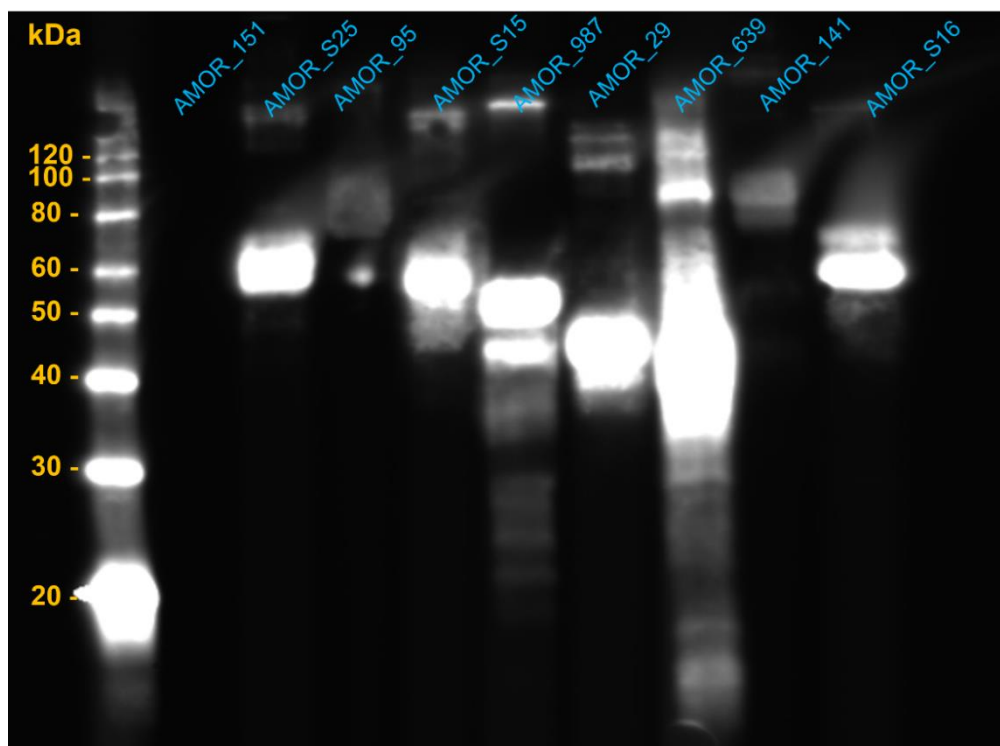


Figure 7: Verification of expressed AMOR genes by Western blotting. 10 μ L sample was applied to each well, with the Magic MarkTM XP Western Standard marking the molecular weights. With the exception of AMOR_151, all genes were expressed.

Strong bands at the expected molecular weights appeared for 8 of the 9 AMOR enzymes (Figure 7). All the putative fucoidanases and fucoidan sulfatases expressed in *E. coli*, with the exception of the putative exo-fucoidanase AMOR_151. Lack of successful AMOR_151 production could be a result of expression conditions, improper folding of protein, i.e. formation of inclusion bodies, a not optimal expression vector or *E. coli* not being a suitable host for this protein.

Expression of AMOR_151 could be possible by changing expression conditions. One could try to achieve expression by altering the IPTG concentration, by changing the incubation temperature and time, growth media, or by using another expression host or expression vector. The new host could either be a different species, such as *Pichia pastoris* or *Bacillus* or a different strain of *E. coli*.

Analysis of AMOR_151 after sonication was also done, to check if the enzyme actually did express but was simply not properly folded. The folding of proteins is to some extent unpredictable and can result from several factors such as expression happening too fast or disulfide bridges that cannot be formed and will impact the added His-tag. If the protein is present as inclusion bodies, a possible solution could be to attempt refolding or changing expression conditions as mentioned above. Additionally, the location of the His-tag could also be changed and/or the His-tag could be cleaved off by restriction enzymes if needed. But as the Western Blot showed no sign of AMOR_151 expression, this was not tried. AMOR_151 was also a candidate for optimization, which is discussed in more detail below (4.5). However, it was not feasible to conduct this experiment within the time scheduled for this study.

4.4 Enzyme production & purification

The AMOR enzymes were produced from *E. coli* BL21 (DE3) cells that were transformed during this study (as described above), while the *Lentimonas* enzymes FunA_30, FunA_31, and FunA_50 were produced from in-house *E. coli* glycerol stocks originating from a different project. All enzymes were purified with the BioRad purification system. Appendix C shows two examples of obtained affinity chromatograms, from the putative exo-fucoidanase AMOR_29 and the putative sulfatase AMOR_S25 (Figure 32).

SDS-PAGE analyses of the eluted fractions were used to verify the production and purity of the enzymes. Strong bands at the expected molecular weights were observed for each enzyme purified, as exemplified in Figure 8.

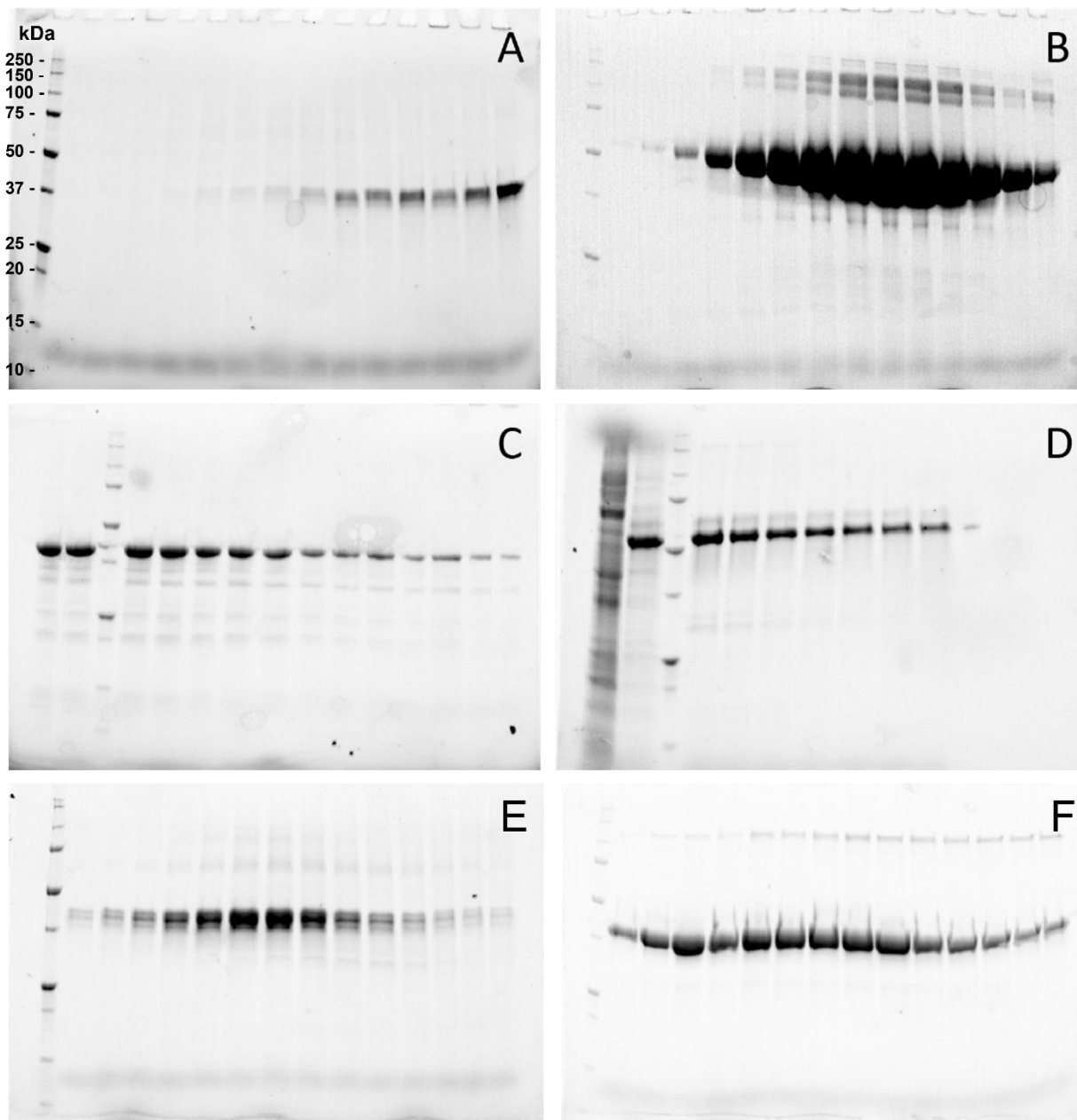


Figure 8: Examples of SDS-PAGE gels following protein purification, showing putative AMOR enzymes AMOR_639 (A), AMOR_S15 (B), AMOR_29 (C) and AMOR_S16 (D), as well as the *Lentimonas* enzymes FunA_50 (E) and FunA_31 (F). 10 μ L sample was applied to each well, with the Precision Plus Protein™ Unstained Standards marking the molecular weights (shown in A).

The putative AMOR enzymes had expected bands at approximately 46 kDa (AMOR_639), 42 kDa (AMOR_29), and 59 kDa (AMOR_S16), without visible contamination from other proteins.

The *Lentimonas* proteins were also pure, with expected bands at approximately 43 kDa (FunA_31) and 45 kDa (FunA_50). AMOR_S15 had thick bands at the expected 57.4 kDa, but there were indications of contamination between 100 and 150 kDa. Still, the large amount of protein at the correct size overruled the small amount of contamination and was still sufficient for testing enzymatic activity. The contamination was likely due to proteins binding to the column with weak affinity, as the column wash was conducted with low amounts of imidazole, and some contaminants might still have been bound to the column. For most of the AMOR proteins, samples from the column washes did also have visible bands at the respective sizes, as exemplified in Figure 8D. One potential explanation could be that the protein was only partly bound to the His-tag column and that some of the protein would be un-bound from the column during the wash step. Weak binding to the column could be due to a semi-internal His-tag, as described above, or due to saturation of the column where the volume of protein solution applied to the column would be higher than its capacity, making some of the protein unable to bind strongly. The *Lentimonas* enzymes had been successfully purified prior to this study, so it was known that the target protein would bind to the His-tag column. Thus, there were no samples from the column washes of *Lentimonas* purifications that were tested on SDS-PAGE.

Buffer exchange of the proteins was conducted after verification through SDS-PAGE analysis to transfer the protein into a buffer system suitable for downstream applications. The buffer exchange chromatograms for AMOR_29 and AMOR_S25 are shown in Figure 32 (Appendix C) example calculation of final protein concentration using Beer's law is included in Appendix E.

4.5 Optimization of protein expression

Enzymes encoded in an *E. coli* plasmid that do not express successfully can undergo optimization. Endo-fucoidanases Afc95A_28, Fp277_23, and Fp279_42 from the *Lentimonas* genome that had not been expressed prior to this study were tried optimized. Assessing various media and temperatures had previously been investigated but had not resulted in successful expression. In this study, varying IPTG concentrations and different optical densities (*E. coli* growth) used for induction were tested for their effects on expression for the enzymes and evaluated through Western blotting. The results are shown in Figure 9.

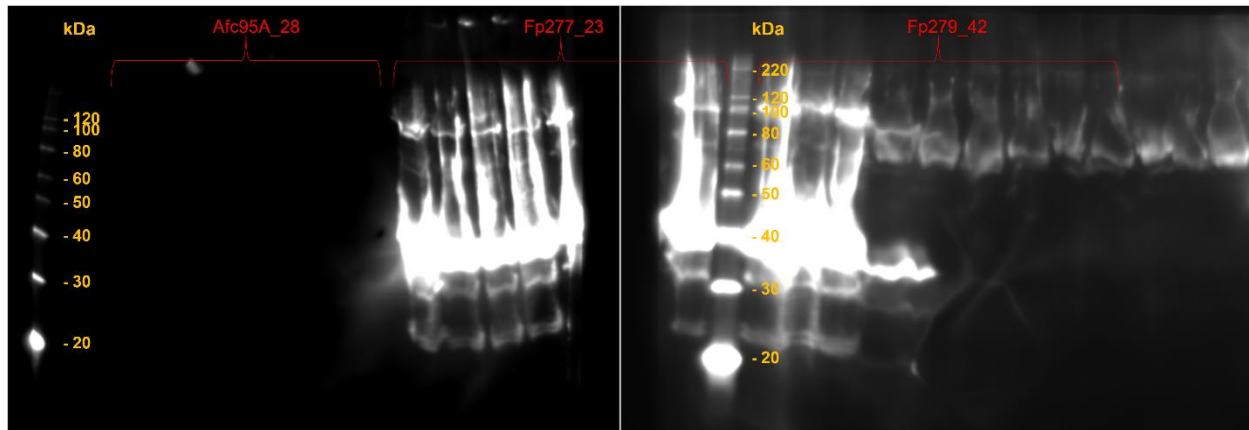


Figure 9: Western blot of optimization trials for *Lentimonas* proteins Afc95A_28, Fp277_23, and Fp279_42. 10 μ L sample was applied to each well, with the Magic Mark™ XP Western Standard marking the molecular weights.

The protein Afc95A_28 did not express in any of the varying ODs or IPTG concentrations. Fp277_23 had significant expression in all conditions as visible by bands at the expected size of 38 kDa, while Fp279_42 expressed in all conditions as well (bands at expected 78 kDa), but with a lower yield than Fp277_23. It was unexpected that these enzymes would express in all the tested conditions, as they had not previously been expressed successfully with different media and at different temperatures. Investigating previously tested expression conditions as well as further testing could have been conducted had there been more time, and such tests can potentially be run in the future.

As previously mentioned, the putative exo-fucoidanase AMOR_151 had not been expressing successfully either and optimizing AMOR_151 by testing different expression conditions similar to those tested on Afc95A_28, Fp277_23, and Fp279_42, is certainly of interest in the near future.

If obtaining a high yield of protein is desired, optimizing protein expression can also be done for enzymes already successfully expressing. Such optimization would involve similar experiments as those mentioned above with testing different media, temperatures, IPTG concentrations, or optical density at induction. An alternative to optimization that would also yield more protein would be to produce a larger batch and/or purify the protein in several rounds to avoid overloading the column. Protein productions in this project was performed in flask containing 500 mL media. Protein production could be tried out in fermenters that hold higher volumes and ensure high airflow and controlled reaction conditions, which normally enhance protein yield.

4.6 Substrate production

Most likely, exo-fucoïdanases and sulfatases act on oligomers rather than polymers, although that is not fully elucidated. The putative AMOR exo-fucoïdanases and sulfatases were therefore tested on both fucoïdan polymers and fucoïdan oligomers. Oligomeric fucoïdan substrates were obtained either by enzymatic hydrolysis using the P5AFcnA endo-fucoïdanase or by partial acid hydrolysis as described in 3.8. Fucoïdan is normally fully degraded using 2 M TFA for 8 hours. For the production of oligomers, a partial hydrolysis was performed using less harsh reaction conditions. The exact structures and compositions of the fucoïdan substrates are thus not known as the reaction is not controlled. MALDI analyses on the TFA reaction products have been run in the BioRef lab to confirm the presence of oligomers of different degree of polymerization, but that was beyond the scope of this thesis.

4.6.1 SEC analysis of enzyme hydrolysates

Reactions with the in-house endo-fucoïdanase P5AFcnA were set up with different commercial fucoïdan substrates to produce fucoïdan oligomers. Enzyme activity on fucoïdans would be observed as a change from high to low molecular weights in the SEC as chromatograms. P5AFcnA successfully hydrolyzed fucoïdans from *M. pyrifera* and *L. digitata* (Figure 10) as well as *Alaria* sp., *F. serratus*, and *A. nodosum* (data not shown).

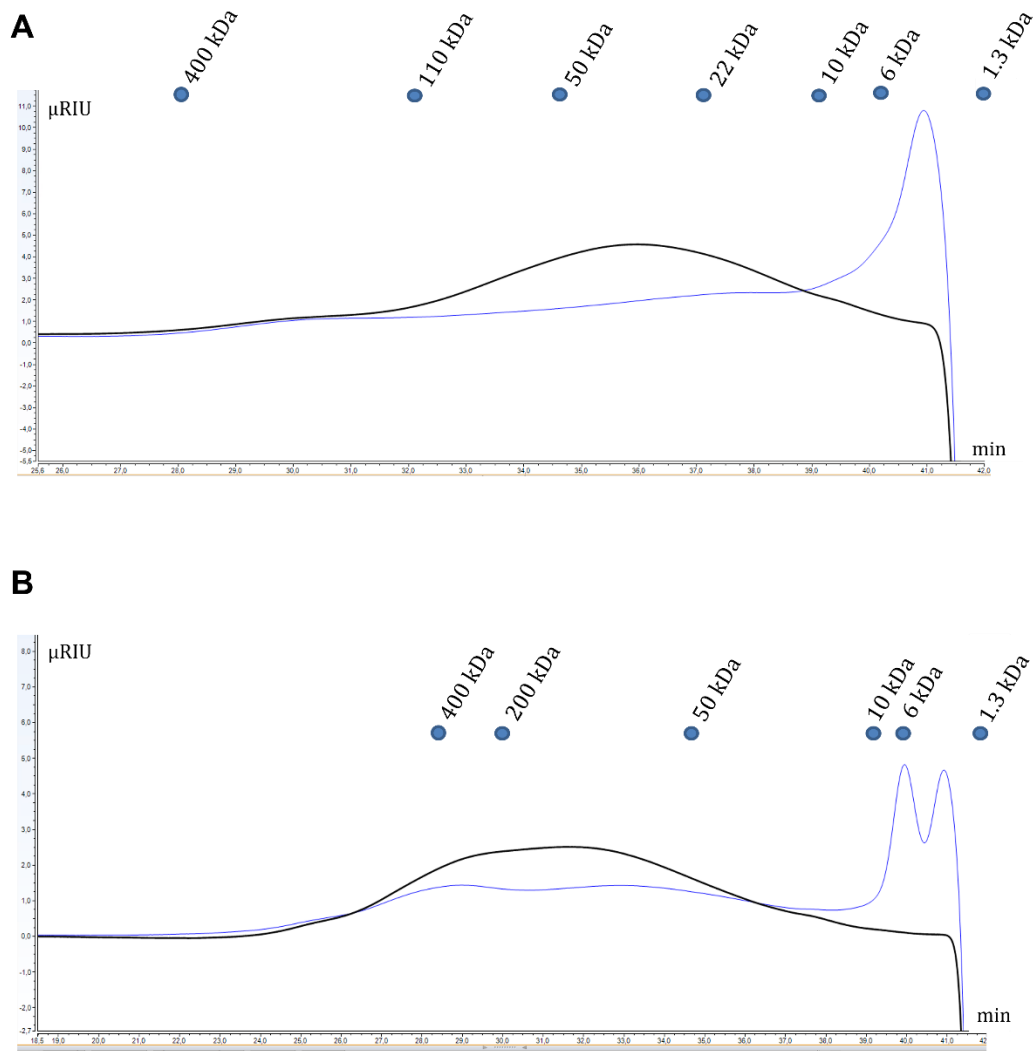


Figure 10: Size exclusion chromatograms of enzymatic products from endo-fucoidanase P5AFcnA reacting with fucoidan from *M. pyrifera* (A) and *L. digitata* (B) with Pullulan standards to determine size, as indicated by blue circles. The black lines represent the substrate (fucoidan) controls, while the blue lines represent the samples.

4.6.2 MALDI-ToF-MS

MALDI-ToF-MS was used to analyze the products from the enzymatically hydrolyzed substrates. Figure 11 shows the MALDI-ToF-MS spectra of the enzymatic products created when *M. pyrifera* fucoidan was degraded by P5AFcnA. The signals and their intensities for all the fucoidans hydrolyzed by P5AFcnA are summarized in Table 15 (Appendix G).

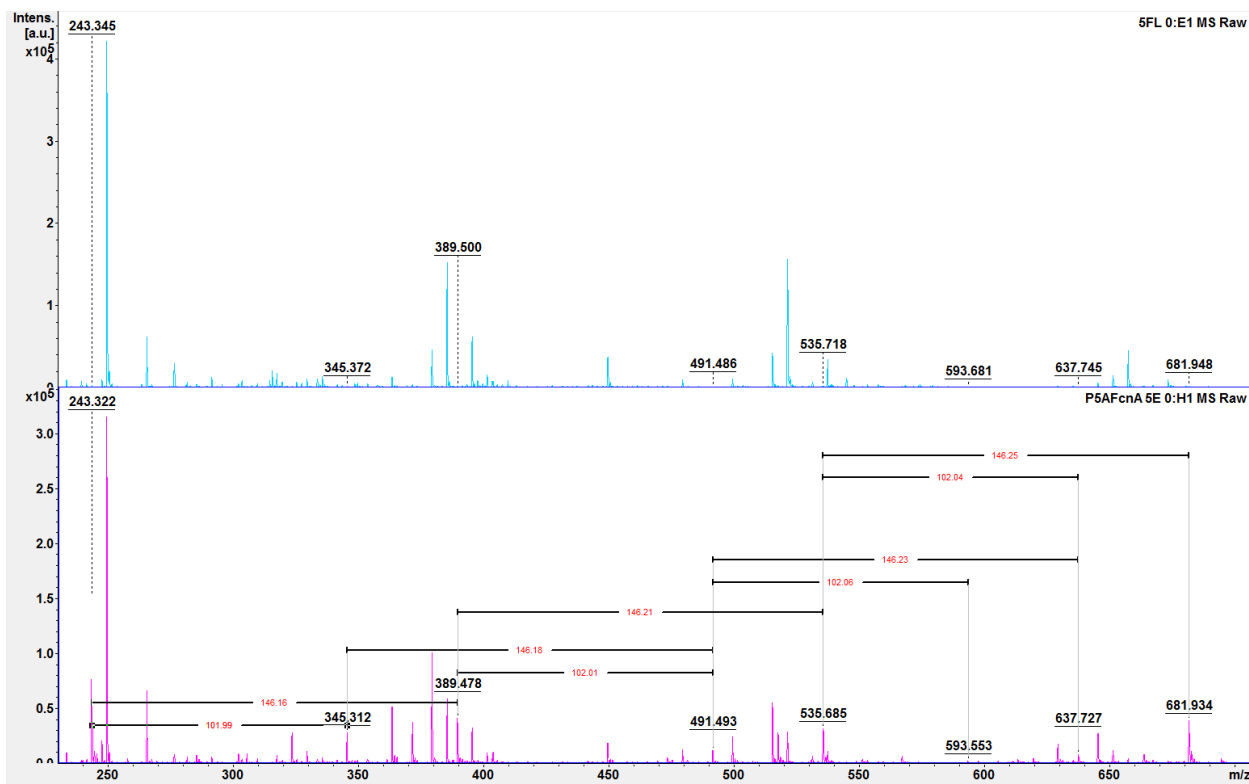


Figure 11: MALDI-ToF MS spectra of substrate controls (top) compared with enzymatic products generated by endo-fucoidanase P5AFcnA reacting with fucoidan from *M. pyrifera* (bottom). Note mass differences of 102 and 146 kDa in the enzymatic hydrolysate.

Signals were detected at $m/z = 243, 345, 389, 491, 535, 593, 637,$ and 681 . The presence of fucose oligosaccharides became evident upon measurement of the signals distances between each other. A (dehydrated) fucose unit in a fucoidan oligosaccharide has a molecular weight of approximately 146 Da, while the sodium-sulfate group attached to the fucose weighs around 102 Da. As the MALDI spectra reveals (Figure 11), signals with distances from each other of approximately 146 kDa and 102 kDa were found. Thus, MALDI-ToF analyses confirmed the SEC data that P5AFcnA hydrolysis of fucoidan was successful.

4.7 Enzyme activity for AMOR and *Lentimonas* enzymes

4.7.1 Endo-fucoidanases

Enzyme activity of the putative endo-fucoidanases AMOR_639, AMOR_987, as well as the *Lentimonas* FunA_30, FunA_31, and FunA_50, were tested on a range of fucoidan substrates (Table 4) and analyzed by SEC and MALDI. Active enzymes would cleave the fucoidan substrates into oligomers of various sizes which would be observed as reduction of molecular

weights of the SEC chromatograms. However, as exemplified in Figure 12, none of the AMOR proteins resulted in chromatograms that differed from their respective substrate controls, indicating no hydrolytic activity on any of the tested substrates. Analyses by MALDI showed no significant peaks on the spectra, confirming that none of the enzymes were active on these substrates.

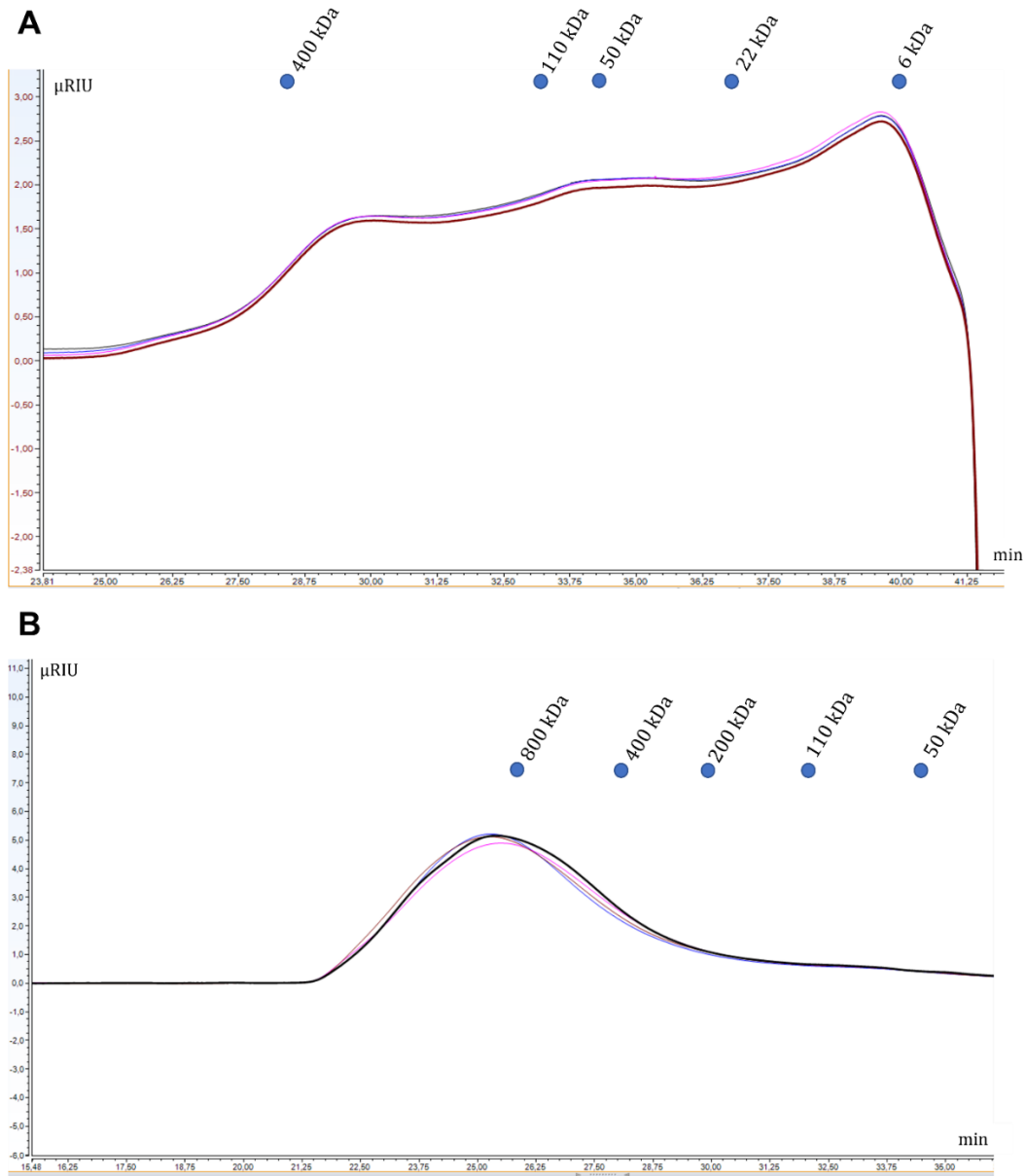


Figure 12: Size exclusion chromatograms from samples of AMOR_987 reacting with fucoidan from *L. digitata* (A) and AMOR_639 reacting with fucoidan *L. japonica* (B) with Pullulan standard to determine size, as indicated by blue circles. The light brown lines represent the substrate (fucoidan) controls, while the blue, pink, and black lines represent the samples (triplicates).

There were no significant peaks detected in the MALDI spectra of the fucoidans treated by the *Lentimonas* enzymes, but SEC analyses indicated activity by FunA_50 on fucoidan from *F. vesiculosus*, as shown in Figure 13. MALDI detects low molecular weight compounds, from sulphated monomers to short oligosaccharides. Discovering endo-activity by SEC analysis but not by MALDI indicates that FunA_50 degrades fucoidan into larger fragments than can be detected by MALDI. The fact that FunA_50 was only active on fucoidan from *F. vesiculosus* fucoidan, and that it produced large fragments, indicates that the enzyme is highly specific (e.g., requires a specific combinations of substitutions to carry out hydrolysis). It could also be an exo-fucoidanase releasing fucose or sulfated fucose monomers, or a debranching enzyme cutting off the branches at the fucoidans. Studies to look into these possibilities are currently going on in the lab. Once established that FunA_50 was active on fucoidan from *F. vesiculosus*, fucoidan oligomers were prepared by this enzyme as well and used as substrates for the other enzymes.

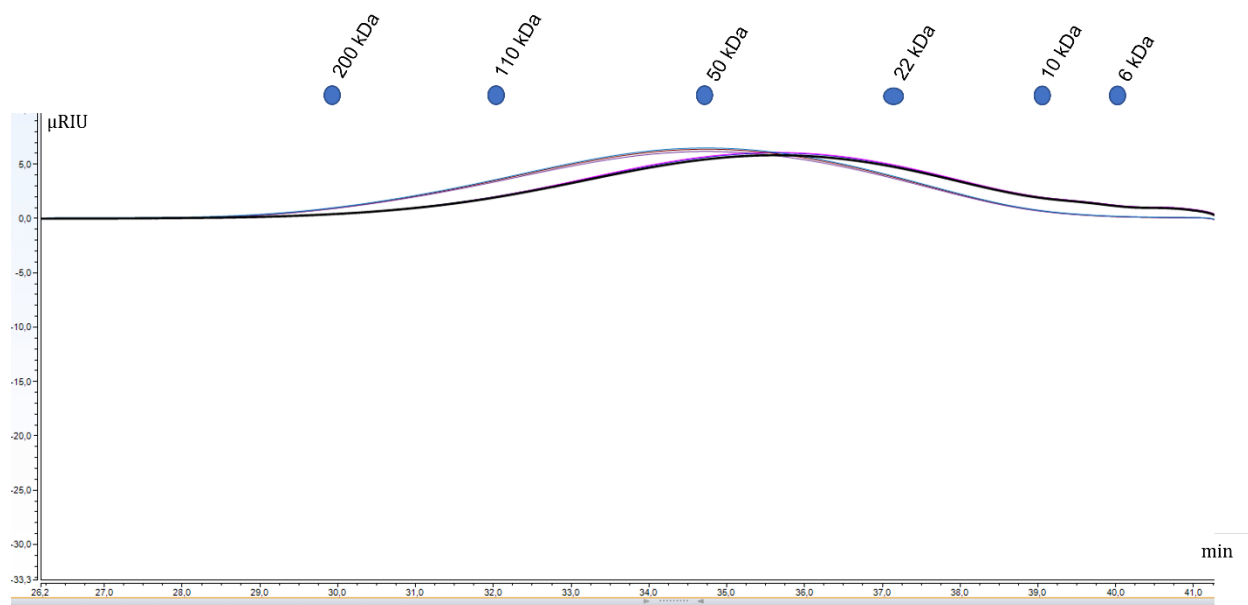


Figure 13: Size exclusion chromatograms from samples of FunA_50 reacting with *F. vesiculosus* with Pullulan standard to determine size, as indicated by blue circles. The lightly colored lines represent the substrate (fucoidan) controls, while the black line represents the samples (triplicates).

4.7.2 Exo-fucoidanases

The uncertainty regarding substrate composition as well as the mode of action for fucoidan active enzymes makes it challenging to limit what types of substrates to test activity on. It is not confirmed whether exo-fucoidanases act on oligomers, polymers, or both. Therefore, in addition to the commercial fucoidan polymers, putative exo-fucoidanases AMOR_29, AMOR_95, and

AMOR_141 were tested on fucoidan oligomers from partial TFA hydrolysis and hydrolysates made from in-house enzymes (3.8).

Screening for exo-fucoidanase activity was carried out by quantifying possible sugar monomer release by HPLC. The peaks in the HPLC chromatogram were aligned with fucose standards to identify possible fucose peaks in the samples. Evaluation of the chromatograms (Figure 14) indicated that no fucose was released upon incubation of substrate and enzyme, and it was concluded that no exo-fucoidanase activity was detected for the putative enzymes on the tested substrates. There were fucose monomers detected in the samples, but the difference from the substrate controls were not significant. The finding of fucose in the controls is likely due to some fucose monomers being present in the substrate, which is definitely the case for the TFA hydrolysates as these substrates are partially hydrolyzed.

Since the putative exo-fucoidanases are expected to release either fucose or modified fucose, and the exact structures of the fucoidan substrates were unidentified, additional peaks other than fucose could appear on the chromatograms. Analyzing such additional peaks in the chromatograms would aid in detecting release of compounds that did not have standards, such as sulfated- or acetylated fucose. However, the additional peaks that were detected did not differ from the control samples, as exemplified in Figure 33 (Appendix D), indicating no activity.

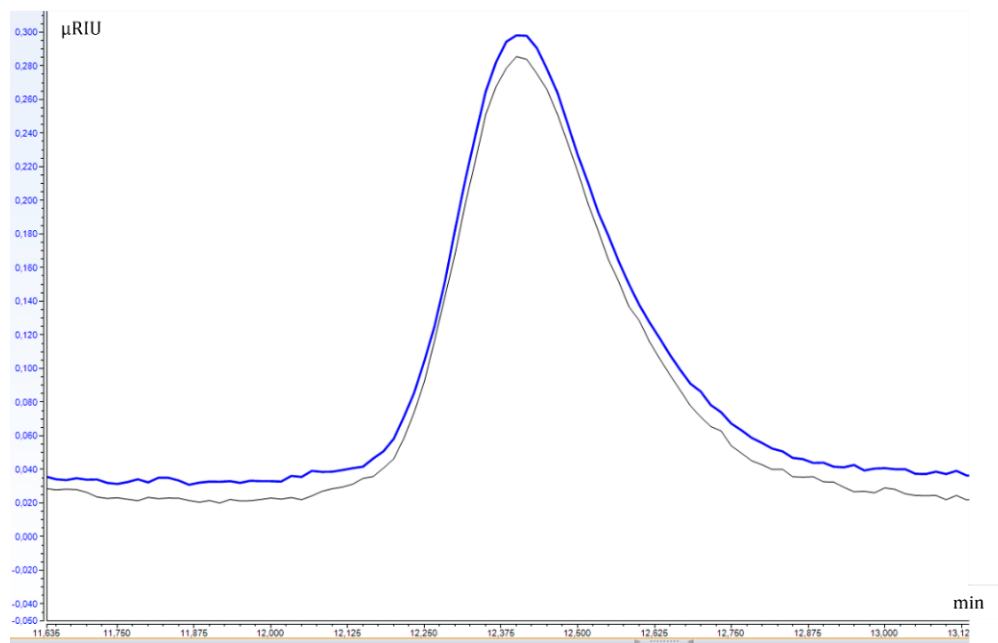


Figure 14: HPAEC-PAD chromatograms from samples of AMOR_29 reacting with TFA hydrolyzed *F. vesiculosus*. Fucose standards were used to detect fucose peaks. The black line represents the substrate (fucoidan) control, while the blue line represents the samples (triplicates).

As already stated, two different HPLC systems, the UltiMate 3000 HPLC system and the ICS-6000 Capillary HPICTM system, were used for detection of fucose in this study. The systems have different sensitivities, with the ICS-6000 being the more sensitive one. Since monomers are small in size and have low molecular weights, quantifying them exclusively by the ICS-6000 would perhaps have been desirable as the system might have detected monomer release that the less sensitive system could not. However, the possibility is slim, as none of the samples analyzed by the ICS-6000 indicated any activity either. Moreover, there was high demand and limited availability of the ICS-6000, as well as there being other active enzymes that exhibited activity and were to be characterized. Therefore, further troubleshooting with monomer detection for the putative exo-fucoidanases was not prioritized in this study.

The putative exo-fucoidanases were also tested on the artificial substrate pNP-fucose to assess whether any of the enzymes would cleave off fucose from the pNP molecule. pNP-fucose is colorless, but if the fucose group is cleaved off, in this case by an exo-fucoidanase, the product p-nitrophenol will emit a yellow color measurable at 410 nm. The experiments showed no significant color development with either AMOR_29, AMOR_95, or AMOR_141. Thus, none of the proteins exhibited activity on pNP-fucose.

No noticeable activity does not have to mean that the enzymes do not have enzymatic activity. Reasons for apparent inactivity could be due to the reaction conditions, substrate specificity, that the enzyme is active on carbohydrates other than fucoidan or other fucoidans than tested in this study, or that it is only active when working synergistically with additional enzymes. The complex structure of fucoidans can lead to steric hindrance which shields glycosidic linkages from being cleaved by fucoidanases (Sichert et al., 2020). It might be that activity of the fucoidanase depends on other enzymes, such as sulfatases, to cleave off substitutions on the fucoidan first. There was in fact conducted a small test in this study where the putative AMOR exo-fucoidanases were tested for activity on the enzymatic products of AMOR_S25 with *M. pyrifera* and enzymatically hydrolyzed *F. vesiculosus*. The reaction set up followed that of the previous activity assays, but there was still no activity detected (data not shown).

The reactions conditions for the putative AMOR enzymes were based on already identified enzymes from the AMOR metagenome (Arntzen et al., 2021). Therefore, testing out different reaction conditions such as temperature and pH, as well as setting up reactions with additional substrates and perhaps also additional enzymes, is something to consider looking into for future experiments with these proteins.

4.7.3 Fucoidan sulfatases

With the same reasoning as for the exo-fucoidanases, putative fucoidan sulfatases AMOR_S15, AMOR_S16, and AMOR_S25 were also tested on fucoidan polymers, acid fucoidan hydrolysates, and the enzymatic hydrolysates produced in-house. For the reactions with these enzymes the release of sulfate was measured, as sulfatases do not participate in cleavage of glycosidic bonds but catalyze the removal of sulfate ester groups attached to the fucose molecules. Likewise, as with presence of oligosaccharides in the batch of fucoidan polymers and presence of fucose monomers in the batch of fucoidan oligomers, sulfate molecules are typically also detected in the control samples. Some sulfate may be released during the TFA hydrolysis carried out to make the oligomeric substrates. Comparing with the controls, the chromatograms indicated no activity for AMOR_S15 and AMOR_S16 which was supported by no significant peaks in the MALDI spectra. Significant peaks in the spectra would be those signifying a mass reduction of 102 kDa, which is the molecular weight of sulfate, as discussed in 4.6.2. MALDI-analysis did not suggest activity for AMOR_S25, but the HPLC analyses revealed activity for

AMOR_S25 on fucoidan polymers from *M. pyrifera* and the enzymatic hydrolysate from *F. vesiculosus*, as shown in Figure 15.

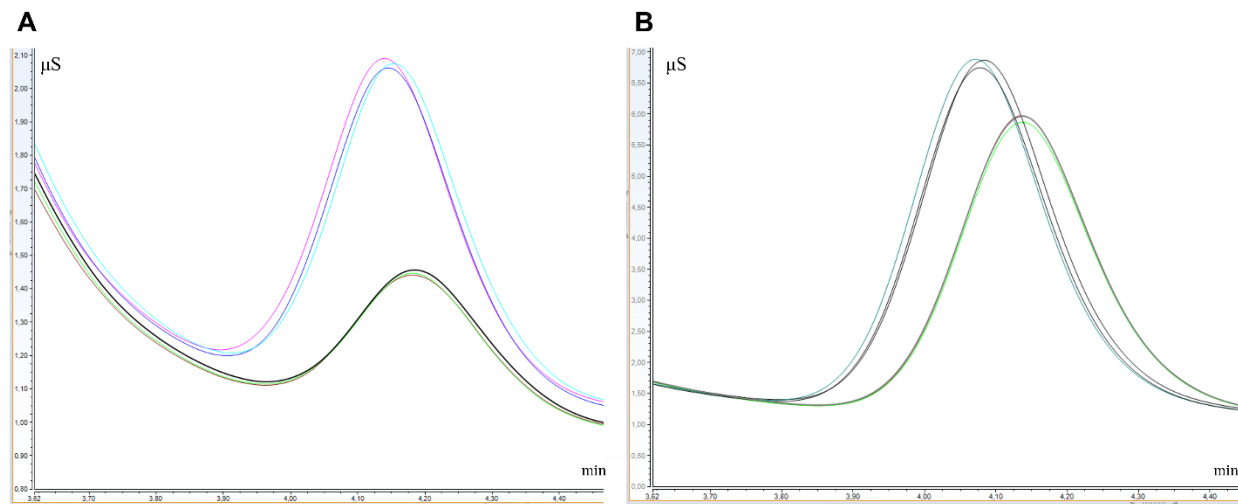


Figure 15: HPIC chromatograms from samples of AMOR_S25 reacting with fucoidan from *M. pyrifera* (A) and enzymatically hydrolyzed fucoidan from *F. vesiculosus* (B). Standards of K_2SO_4 were used to detect sulfate peaks. The black, light brown, and neon green lines represent the substrate (fucoidan) controls, while the remaining lines represent the samples (triplicates).

The reason why activity was not detected by MALDI-analyses could be that the oligomers it exhibits activity on are too large to be detected, which would be difficult to confirm or dismiss, as the exact substrate composition is unknown. Noticing differences between the control and the reaction sample can also be difficult if background noise is prohibiting it.

The putative sulfatases were also tested on the artificial substrates pNPS and pNCS to assess whether any of the proteins would cleave off sulfate from the pNP or pNC molecule. While activity on pNPS is measured the same way as pNP-fucose, pNCS already has a yellow color prior to cleavage but will undergo a color change to a darker yellow/orange if the sulfate group is cleaved off. Color development, similar as to that observed in Figure 35, was observed visually and spectrophotometrically for AMOR_S15 and AMOR_S25 on pNPS, but not for AMOR_S16. The color change associated with activity on pNCS was observed for AMOR_S16 only (data not shown).

Activity on artificial substrate(s) but not on fucoidan could mean that they are active on fucoidan types that haven't been tested, or that the sulfatases are active on other sulphate-containing substrates than fucoidan. There are polysaccharides other than fucoidan, especially marine ones, that are highly sulfated. Carrageenan, for example, is a highly sulfated polysaccharide found in

red seaweeds. The putative sulfatases were therefore also tested for activity on carrageenan (Table 5). No indications of activity were observed for AMOR_S15 or AMOR_S25, but AMOR_S16 did have activity on *k*-carrageenan (data not shown). As the focus of this study was on fucoidan and fucoidan active enzymes, investigating carrageenan active enzymes would have been beyond the scope of this thesis, and was therefore not investigated further. Still, investigations of AMOR_S16 activity on κ -carrageenan can certainly be of interest in a different project.

The key findings of the sulfatase activity assays are summarized in Table 14.

Table 14: Summary of enzyme activity for putative fucoidan sulfatases of the AMOR metagenome.

Putative sulfatase	Activity on fucoidan	Activity on pNPS	Activity on pNCS
AMOR_S15	No	Yes	No
AMOR_S16	No	No	Yes
AMOR_S25	<i>M. pyrifera</i> & enzymatic hydrolysate of <i>F. vesiculosus</i>	Yes	No

4.8 Characterization of AMOR_S25

AMOR_S25 was the most interesting sulfatase since it showed activity on fucoidan substrates. Additionally, its ability to release sulfate from the artificial substrate pNPS allowed for convenient quantitative characterization of the enzyme. In addition to the challenge of obtaining quantitative measurements, characterizing the sulfatase by using the actual fucoidan substrates can also be difficult because the exact structure and concentration of the substrates are unknown. The activity of AMOR_S25 was thus characterized at different temperatures, salinities (NaCl), and pHs. The influence of different ions on activity was also investigated. After obtaining the data from these experiments of various reaction conditions, thermostability and enzyme kinetics were investigated, followed by a time course using the fucoidan from *M. pyrifera* and enzymatically hydrolyzed *F. vesiculosus*.

4.8.1 Effect of temperature on activity

The effect of temperature on AMOR_S25 activity was tested in 90-minute reactions at 10 °C, 20 °C, 25 °C, 30 °C, 35 °C, 40 °C, 45 °C, 50 °C, 60 °C, 75 °C, and 90 °C. The results are presented in Figure 16.

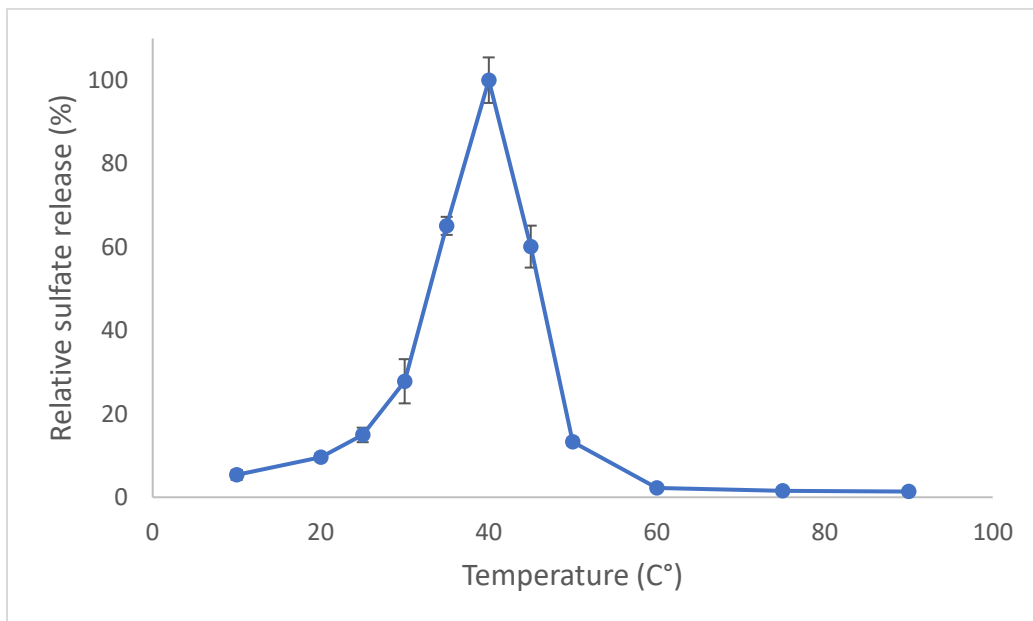


Figure 16: AMOR_S25 activity with increasing temperature 10-90 °C. The relative sulfate release (%) was measured after 1.5 μ M enzyme reacted with 20 mM pNPS for 90 minutes in 25 mM NaOAc pH 5.6, 300 mM NaCl. Each data point represents the average value of three triplicates, with the control values subtracted.

The data shows that temperature had a strong effect on enzyme activity, with a clear peak in activity at 40 °C. An optimal temperature of 40 °C for the AMOR_S25 aligns nicely with the source of this enzyme, since the sequence was obtained from a marine genome collected in a chamber with temperature 30-40 °C. The enzyme still had activity, although only 5 % of maximal activity, down to 10 °C, and had less than 2 % of maximal activity retained when surpassing 60 °C. At 30 °C, 28 % of the activity was retained, while 13 % was retained at 50 °C. In comparison, the alginate lyases AMOR_PL7 and AMOR_PL17 are collected from chambers located deeper in the ocean at a higher temperature, and enzyme characterizations showed their optimal temperatures to be of 65 °C and 90 °C, respectively (Arntzen et al., 2021; Vuoristo et al., 2019). The fucoidan active sulfatase PsFucS1 also has a high optimal temperature, which was surprising as its origin was that of a mesophilic marine bacterium (Mikkelsen et al., 2021). Other previously characterized fucoidan sulfatases have optimal temperatures closer to that of AMOR_S25, with 40-45 °C for SWF1 and 30-35 °C for SWF4 (Silchenko et al., 2018), as well

as around 40 °C for fucoidan sulfatases characterized decades ago (Furukawa et al., 1992). Optimal temperatures for some carrageenan sulfatases are documented to be 34 °C, 40 ± 5 °C as well (Genicot et al., 2014; Préchoux et al., 2013).

4.8.2 Effect of pH on activity

The effect of pH on AMOR_S25 activity was tested for 90-minute reactions at pH values 3.6, 4.6, 5.6, 6.0, 6.5, 7.0, 7.5, 8.0, and 9.0 at 40 °C. The results are presented in Figure 17.

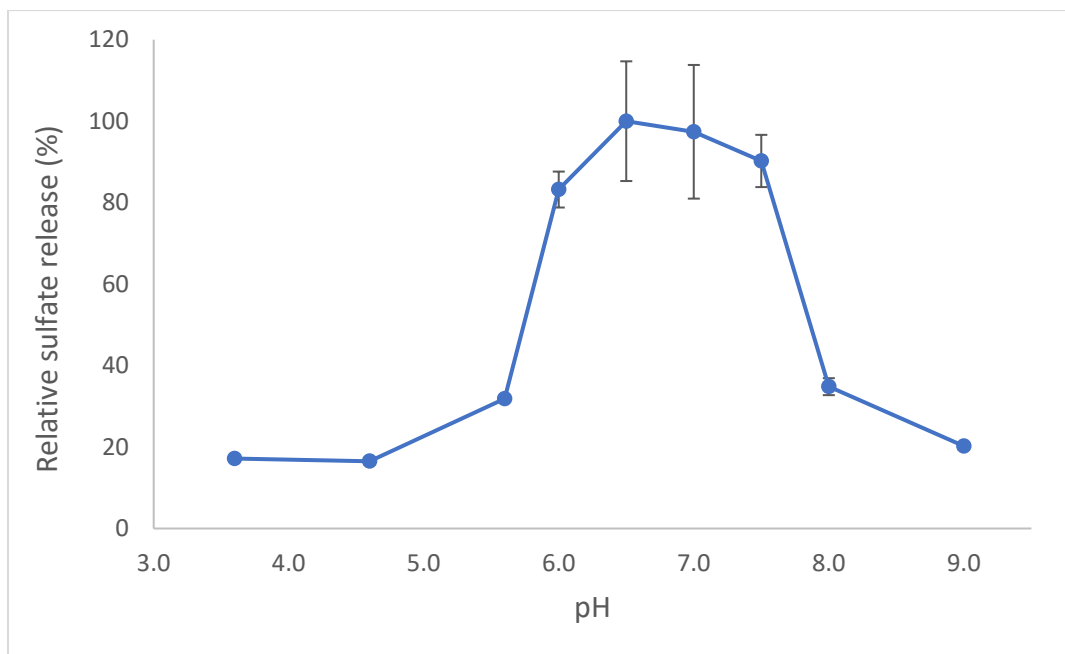


Figure 17: AMOR_S25 activity with increasing pH 3.6-9.0. The relative sulfate release (%) was measured after 1.5 µM enzyme reacted with 20 mM pNPS for 90 minutes at 40 °C in 125 mM NaCl. Each data point represents the average value of three triplicates, with the control values subtracted.

The highest AMOR_S25 activity is observed at pH 6.5. The data at pH 6.5 and 7.0 have rather high standard deviations, but optimal enzyme activity is clearly found in the pH-range 6.0-7.5, which is identical to the optimal pH range for fucoidan sulfatases from *Vibrio* sp. N-5 (Furukawa et al., 1992). The optimal pH range is furthermore similar to that of the previously characterized fucoidan sulfatase PsFucS1 (Mikkelsen et al., 2021) as well as fucoidan sulfatases SWF1 and SWF4 (Silchenko et al., 2018). The sulfatase's ideal pH is also in the same range as other AMOR enzymes, where the alginate lyases have optimal pH values in the range 5-7 (Arntzen et al., 2021; Vuoristo et al., 2019). The optimal pH is also close to that of a sulfatase from a

different AMOR chamber, which has the optimal pH of 5.6 (unpublished data; Nanna Rhein-Knudsen).

4.8.3 Salinity and activity

The effect of salinity on AMOR_S25 activity was tested in 90-minute reactions at NaCl concentrations 18, 150, 300, 450, 600, 800, 1000, 1300, 1600, and 2000 mM at 40 °C, pH 6.5. The results are presented in Figure 18.

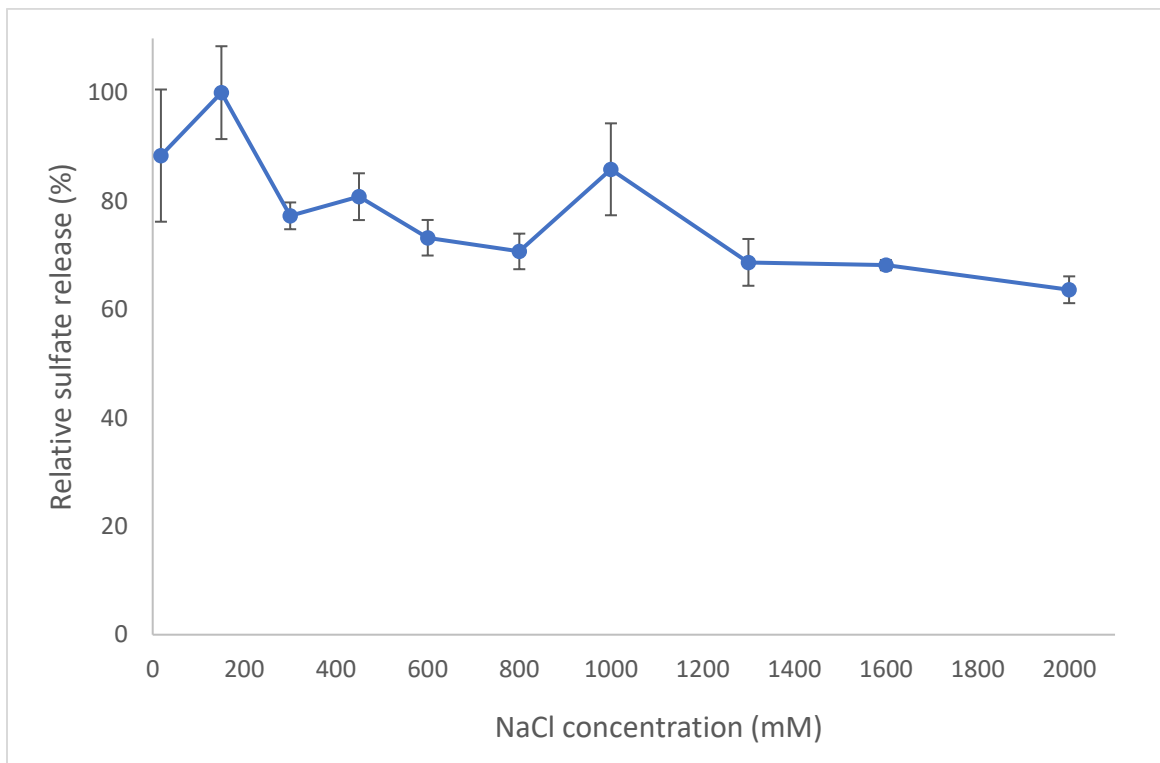


Figure 18: AMOR_S25 activity with increasing salt concentration 18-2000 mM. The relative sulfate release (%) was measured after 1.5 μ M enzyme reacted with 20 mM pNPS for 90 minutes at 40 °C in 50 mM NaOAc pH 6.5. Each data point represents the average value of three triplicates, with the control values subtracted.

The impact of salinity concentration on AMOR_S25 activity was small, and the enzyme showed high activity for all tested salinities. Both AMOR_PL17A and AMOR_PL7A (Arntzen et al., 2021; Vuoristo et al., 2019) share the AMOR_S25 attribute of being active in a broad salinity range. Regardless of the small differences between salinity concentrations, presence of salt was still necessary for optimal activity of AMOR_S25, with a concentration of 150 mM resulting in highest sulfate release.

AMOR_S25 is a marine enzyme, and it was therefore expected that the optimal salt concentration for AMOR_S25 would be quite high, and that there would be less activity at the

lowest (18 mM) NaCl concentration than what was observed. With the enzyme buffer containing 300 mM NaCl, it could have potentially affected the results as the sulfatase would have had time to stabilize and would hardly need additional salt to be active. Still, enzymes require salt to avoid denaturing, and keeping the enzyme in a buffer without salt would lead to precipitation and would render the enzyme inactive for any sort of testing. In the characterization of the AMOR-derived alginate lyase AMOR_PL17A, reactions were run for only 5 minutes to decrease the effects of stability on observed activity (Arntzen et al., 2021), and perhaps decreasing the reaction time for AMOR_S25 would reveal less activity at lower salt levels. Another strategy could be to purify the enzyme in a buffer without salt and perform salinity experiments immediately after purification. Nonetheless, characterizations of other marine sulfatases show large variations in optimal NaCl concentrations, from 25 to 500 mM (Genicot et al., 2014), signifying that the optimal salinity of AMOR_S25 was as expected for a marine sulfatase. Still, had there been more time in this study, it would have been interesting to run additional salinity tests to investigate how salt affects the stability of this particular sulfatase, and how that consequently affects its activity.

4.8.4 Divalent metal ions and activity

The effects of ions on AMOR_S25 activity were tested for 90-minute reactions with various 10 mM ionic solutions. The ions tested were Ni^{2+} , Cu^{2+} , Mn^{2+} , Fe^{2+} , Zn^{2+} , Mg^{2+} and Ca^{2+} . The results are presented in Figure 19.

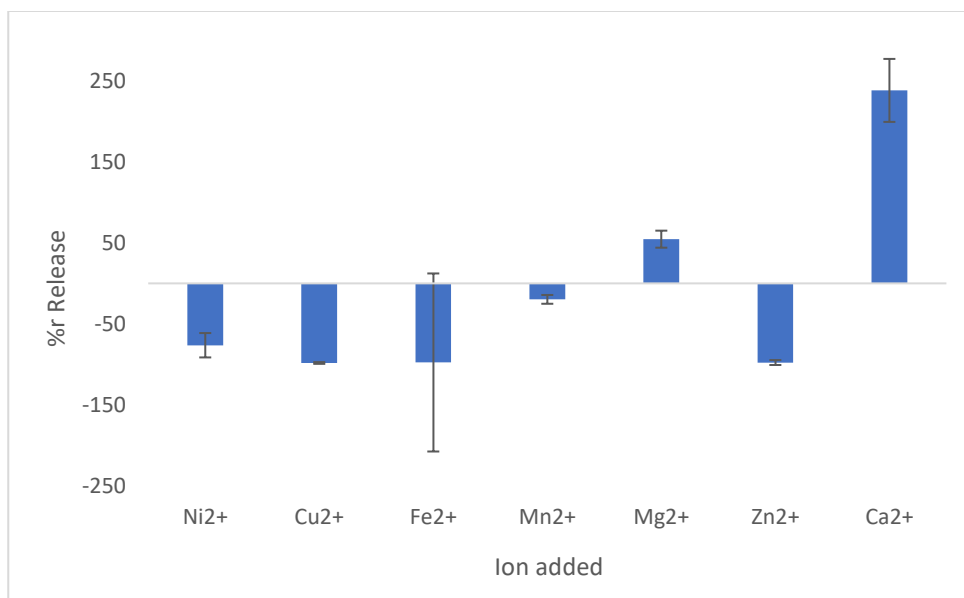


Figure 19: AMOR_S25 activity with addition of various divalent metal ions. The sulfate release (μM) was measured after $1.5 \mu\text{M}$ enzyme reacted with 20 mM pNPS for 90 minutes at $40 \text{ }^\circ\text{C}$ in 50 mM NaOAc pH 6.5. Each data point represents the average value of three triplicates, with the control values subtracted.

Both magnesium and calcium had a positive impact on AMOR_S25 activity, with the presence of calcium ions clearly resulting in the highest enzyme activity at 238 % higher than without calcium. All other ions inhibited enzyme activity. The high standard deviation detected for the reactions with addition of iron is likely due to interference from color in the FeCl_2 solution.

Once established that calcium ions had the most significant effect on enzyme activity out of all tested ions, the effect of specific calcium concentrations on AMOR_S25 activity was tested for 90-minute reactions at $40 \text{ }^\circ\text{C}$. The results are shown in Figure 20.

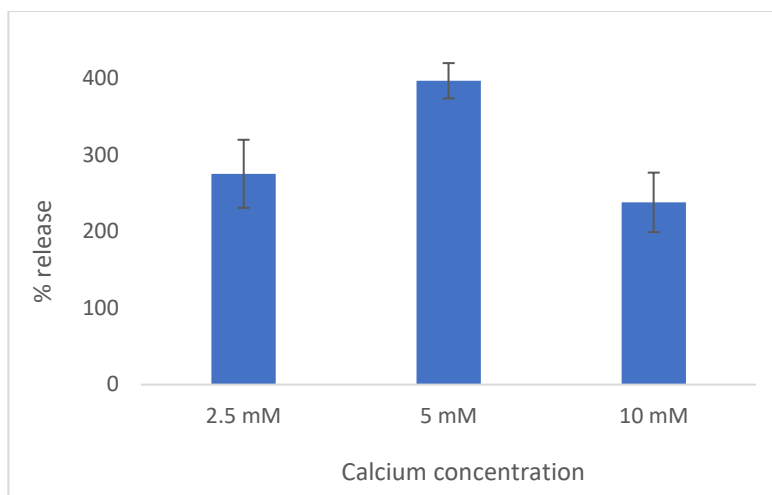


Figure 20: AMOR_S25 activity with addition of increasing calcium concentration 2.5-10 mM. The sulfate release (μM) was measured after 1.5 μM enzyme reacted with 20 mM pNPS for 90 minutes at 40 °C in 50 mM NaOAc pH 6.5. Each data point represents the average value of three triplicates, with the control values subtracted.

AMOR_S25 activity was highest at 5 mM calcium, where the activity increased with 397 % compared to reactions with no calcium. Calcium dependence for AMOR_S25 was expected, as calcium has proven necessary for sulfatase activity in the past (Mikkelsen et al., 2021; Silchenko et al., 2018) and since the catalytic site for S1 sulfatases is conserved with a coordinated metal (commonly calcium) ion present near the cleft (Hanson et al., 2004; Hettle et al., 2018), acting as a co-factor. The calcium concentration in seawater is approximately 400 ppm and marine organisms consequently tend to have significant calcium contents (Lenntech, 2023). Seaweeds' calcium content can be as high as 7 % of dry weight (El-Said & El-Sikaily, 2013), which means seaweed sulfatases have calcium readily available.

In this study, magnesium ions also had a positive impact on AMOR_S25 activity, although not as significant as with calcium, which are traits seen for other marine sulfatases as well (Chao et al., 2015; Mikkelsen et al., 2021). All other ions had an inhibitory effect on activity, which are similar effects as with PsFucS1, where all tested ions except Mg^{2+} , Mn^{2+} and Ca^{2+} hindered activity (Mikkelsen et al., 2021). Sulfatases SWF1 and SWF4 were likewise inhibited by Cu^{2+} , Mn^{2+} , Ni^{2+} , and Co^{2+} (Silchenko et al., 2018).

4.8.5 Thermostability

Thermal stability was assessed by pre-incubating AMOR_S25 in 50 mM NaOAc pH 6.5, 300 mM NaCl at optimal temperature 40 °C for different durations up to 24 hours. At each time

interval, 1.5 μM enzyme was mixed with 20 mM pNPS for 90 minutes at 40 °C. The results are shown in Figure 21.

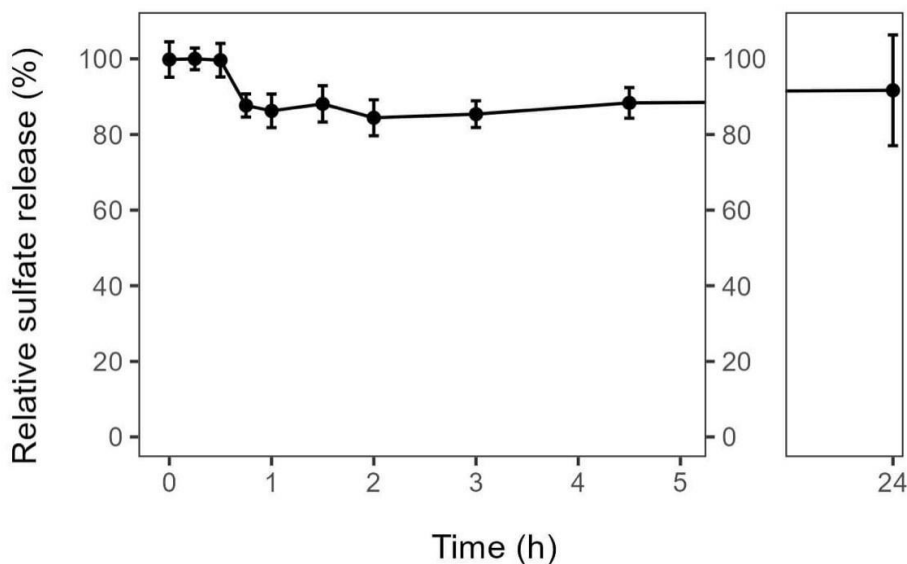


Figure 21: Thermal stability of AMOR_S25 after being incubated for 15 min to 4.5 h and up to 24 h. The relative sulfate release (%) was measured after 1.5 μM enzyme reacted with 20 mM pNPS for 90 minutes at 40 °C in 50 mM NaOAc pH 6.5, 300 mM NaCl. Each data point represents the average value of three triplicates, with the control values subtracted.

The enzyme proved to have high thermal stability, although a small loss of activity was observed after 45 minutes of incubation. The activity was stable from 45 minutes and until 24 hours, with approximately 90 % retained enzyme activity. Marine sulfatase PsFuc1, as well as Ary423 from *Flammeovirga pacifica*, shares the high thermostability, although as both optimal temperatures were higher than for AMOR_S25, their thermal stabilities were also tested at higher temperatures. PsFucS1 retained almost 60 % enzyme activity after 12 hours at 68 °C, while Ary423 retained more than 70 % after 12 hours at 50 °C (Chao et al., 2015; Mikkelsen et al., 2021).

To gain even further insights to the stability of the enzyme, one could conduct an experiment for a longer duration than 24 hours or test the thermal stability at a higher temperature. The stability might decrease significantly over time at even a slightly increased temperature, as seen for AMOR_PL17A, where the enzyme was stable for 24 hours at 60 °C but the activity declined at 65 °C (Arntzen et al., 2021).

4.8.6 Enzyme kinetics

The kinetics experiment and the testing for optimal enzyme conditions were conducted by spectrophotometrically measuring the absorbance emitted from enzymatic products. When using the artificial substrate pNPS it is the absorbance of the p-nitrophenol that is measured, but the absorbance value corresponds to the amount of sulfate released as the color emitted from pNP appears after sulfate is released from the pNP molecule. The intensity of the color therefore determines the amount of sulfate released in the reaction and the exact amount of sulfate released can consequently be calculated by Beer's law as mentioned in 3.6. The sulfate release of various substrate concentrations is illustrated in Figure 36 (Appendix F).

The kinetic analysis of AMOR_S25 on pNPS involved testing activity at different substrate concentrations and the plotting of a Michaelis-Menten curve (Figure 22) as well as a Lineweaver-Burk plot (Figure 23). The Michaelis-Menten curve is made by plotting the substrate concentration on the x-axis against the reaction velocity on the y-axis, and the graph will be of similar shape for most enzymes. The Lineweaver-Burke plot is made by plotting the reciprocal values of substrate concentration and velocity, giving a linear graph. The slope of the graph and its intercept with the axes are used to calculate the Michaelis-Menten constant (K_M) and maximal reaction rate (V_{max}) of an enzymatic reaction.

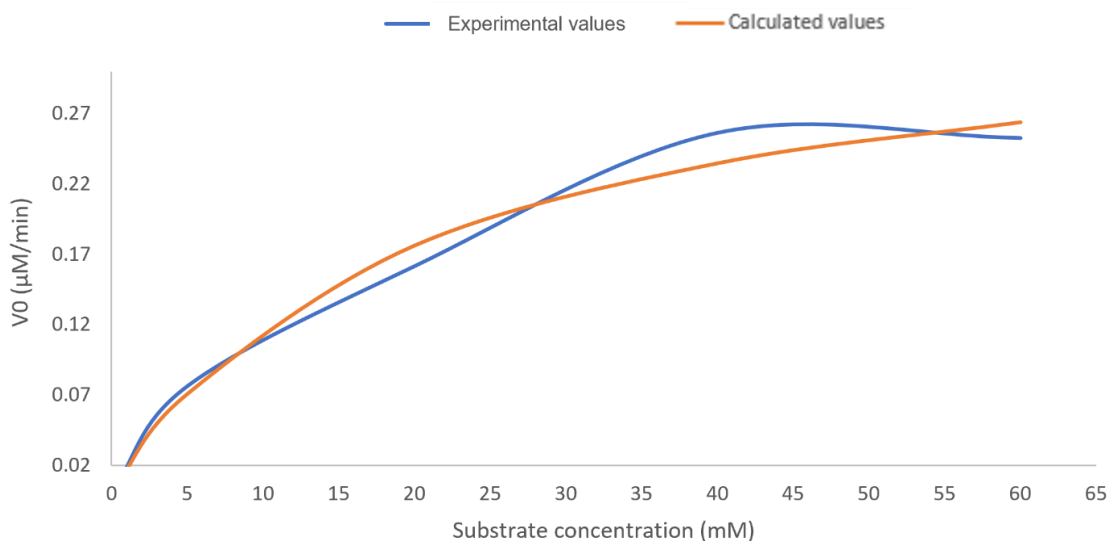


Figure 22: Michaelis-Menten plot generated from experimental values (blue) and calculated values (orange). Substrate concentration is plotted against initial velocities V_o calculated from raw data, and the calculated values were determined by the Michaelis-Menten equation (Appendix E). The raw data with standard deviations for the experimental values is included in Appendix F.

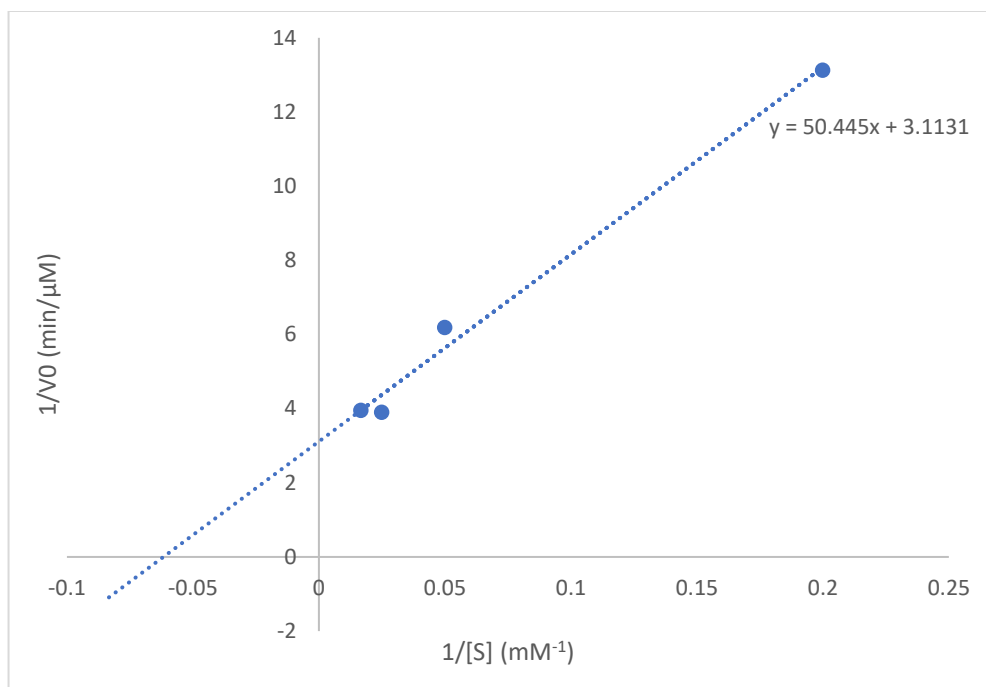


Figure 23: Lineweaver-Burk plot generated from experimental values. Inverted substrate concentrations are plotted against inverted initial velocities. The slope of the trendline and the graph's intercept with the y-axis were used to calculate the V_{\max} and K_M values (calculations shown in Appendix E).

The K_M and V_{\max} are important parameters for understanding the kinetics of the enzyme and they can be used in further research and for guiding future engineering design (Ghanbarzadeh et al., 2018). The K_M is defined as the substrate concentration at which the enzymatic reaction rate is half its maximal reaction rate, V_{\max} (Stryer, 1998), and indicates the substrate concentration where the enzyme has most influence in the rate of reaction.

When all the active sites in the added enzyme solution are saturated, the enzyme has reached its maximum reaction velocity. V_{\max} is affected by both the concentration of enzyme but also its flexibility. A highly specific enzyme will reach V_{\max} slower than a flexible enzyme, and a higher substrate concentration will also contribute to reaching V_{\max} faster, as more substrate will be available to the active sites.

In this study, interpretation of Lineweaver-Burk plot (Figure 23) gave a K_M value of 16.2 mM, and a V_{\max} value of 0.32 $\mu\text{M}/\text{min}$ (calculations shown in Appendix E). The V_{\max} for AMOR_S25 is generally lower than for other sulfatases. Kinetics analysis of a carrageenan sulfatase from *Pseudoalteromonas atlantica* showed a V_{\max} of 1.95 $\mu\text{M}/\text{s}$ (117 $\mu\text{M}/\text{min}$) (Préchoux et al., 2013),

while a sulfatase from *Pedobacter yulinensis* had a V_{\max} of 1.16 $\mu\text{M}/\text{min}$ (Schlachter et al., 2021).

The K_M , on the other hand, is generally higher for AMOR_S25 than for previously characterized sulfatases. Kinetics analyses of PsFucS1 on pNCS showed a K_M of 0.88 mM (Mikkelsen et al., 2021), while apparent K_M values for sulfatases from *Pseudoalteromonas carrageenovora* vary from approximately 13 to 68 μM (Genicot et al., 2014). As a smaller K_M value indicates a higher affinity between enzyme and substrate, and the K_M is high for AMOR_S25 in comparison to other sulfatases, it is apparent that AMOR_S25 does not have a very high affinity for pNPS. The low affinity is not unexpected as pNPS is not the enzyme's natural substrate, and although previously characterized enzyme with higher K_M values also have utilized artificial substrates, there will be variation in affinity to pNPS/pNCS between enzymes.

4.8.7 Time course

Activity on the fucoidan substrates might differ from the activity observed with artificial substrates, as the natural substrates are chemically and structurally more complex. Time courses of AMOR_S25 reacting with the fucoidan substrates *M. pyrifera* and enzymatically hydrolyzed *F. vesiculosus* were therefore performed. The enzymatic reactions were sampled for sulfate release at various time points from 0 to 30 hours, using a substrate concentration of 5 mg/ml and enzyme concentrations 0.1 μM or 1 μM . The time courses are depicted in Figure 24.

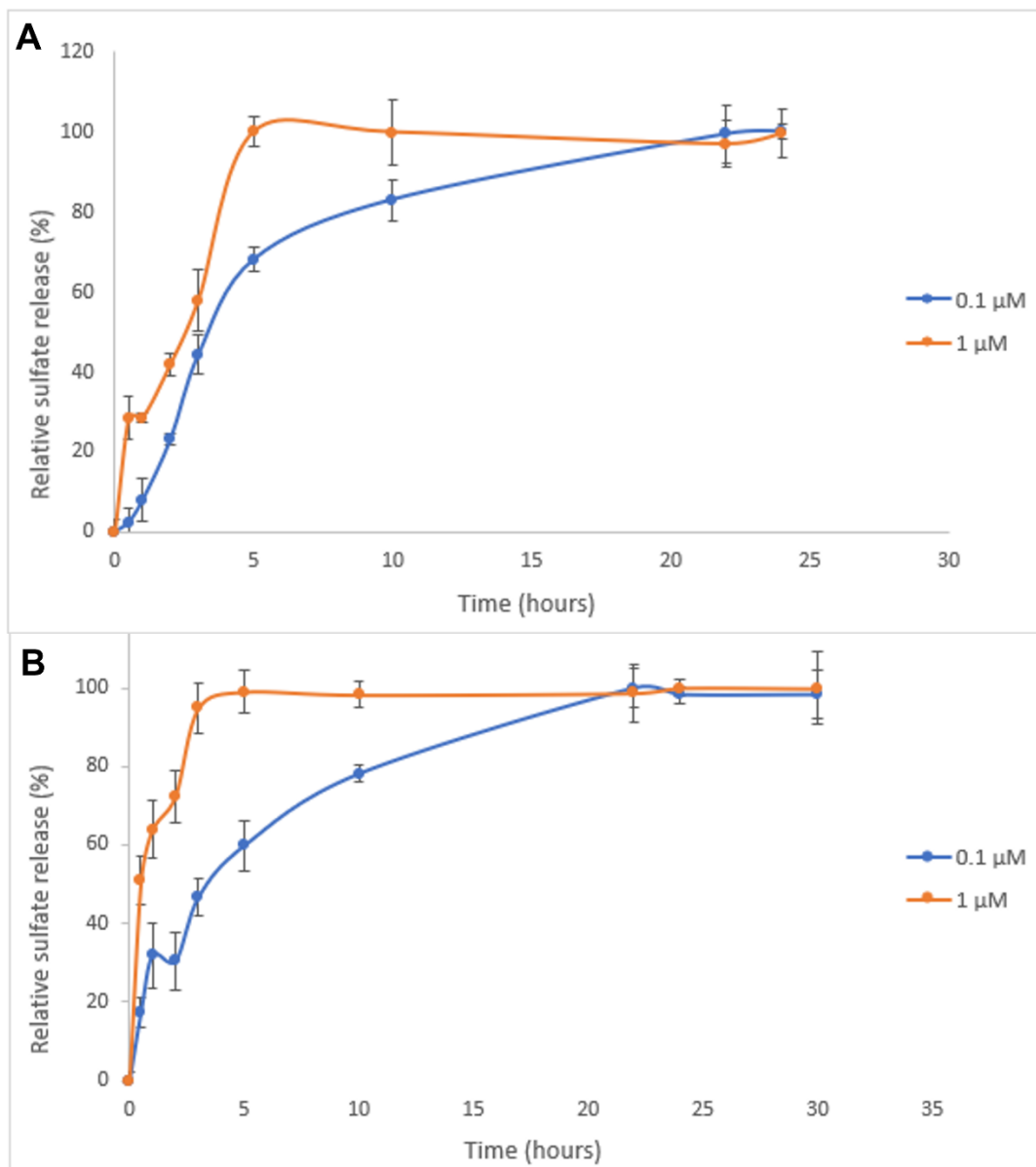


Figure 24: Time courses for AMOR_S25 reacting with fucoidan from *M. pyrifera* (A) and enzymatically hydrolyzed fucoidan from *F. vesiculosus* (B). The relative sulfate release (%) was measured after 0.1 μM (blue) or 1 μM (orange) FunA_50 reacted with 5 mg/ml of the respective substrate at optimal conditions for different durations 0-32 hours. Each data point represents the average value of three triplicates, with the control values subtracted.

The data illustrates that the reaction with the higher enzyme concentration of 1 μM reached completion faster than the reactions with 0.1 μM. At 5 mg/ml substrate, both reactions with 1 μM enzyme were complete after approximately 5 hours, but those with 0.1 μM took about 25 hours to complete. The maximum sulfate release achieved by reaction with AMOR_S25 was approximately 70 mg/g fucoidan substrate for *F. vesiculosus* and 40 mg/g fucoidan substrate for *M. pyrifera*. Based on the total sulfate contents on approximately 430 mg/g and 350 mg/g

fucoïdan for fucoïdan from *F. vesiculosus* and *M. pyrifera*, this accounted for a 12 % and 17 % sulfate release. In comparison, the sulfatase SWF5 released 7 % sulfate after reacting with *Fucus evanescens* and 9 % sulfate after reacting with a high-molecular weight hydrolysis product from the same fucoïdan (Silchenko et al., 2021). Although the sulfate release of AMOR_S25 is higher than that of SWF5, the percentage release is still low when considering the flexibility (in terms of specificity and selectivity) of the enzyme and indicates that AMOR_S25 only cleaves off a small portion of the sulfate substitutions on the fucoïdan polysaccharides.

The overarching obstacle with not knowing the composition of the substrates is also prevalent when analyzing the release of sulfate in the enzymatic reaction. It is unclear where the sulfate substitutions are positioned, but the low percentages of sulfate release suggest that there must be more than one sulfate substitution in both fucoïdan substrates. AMOR_S25's specificity in recognition could also be contributing to the low sulfate release, as it may be that the sulfatase only recognizes sulfate in a specific conformation, e.g. sulfates in a fucose next to a fucose or next to a sulfated/methylated fucose. However, these suggestions are simply speculations, and further studies are required to determine the exact specificity of the enzyme.

4.9 Characterization of FunA_50

FunA_50 did not show activity on the artificial substrate pNP-fucose, meaning a similar kinetic characterization method as used for AMOR_S25 could not be utilized for the *Lentimonas* enzyme. Characterization of endo-fucoïdanases has indeed proved a bit challenging, as the structure somehow can influence the measurements of the reducing ends. Several methods for measuring reducing ends have been tried both in this study and for previous projects, but PAHBAH seemed to be the assay that was best reproduced and had the lowest standard deviations. By employing the reducing sugar assay PAHBAH, the activity of FunA_50 was tested in various ranges of temperature, enzyme concentration, substrate concentration, and pH, to determine the enzyme's optimal conditions. Reducing ends release was quantified using fucose as a standard.

4.9.1 Effect of enzyme- and substrate concentrations on activity

The effect of enzyme- (Figure 25) and substrate concentration (Figure 26) for FunA_50 activity was tested for 45-minute reactions at pH 7.4 and 200 mM NaCl.

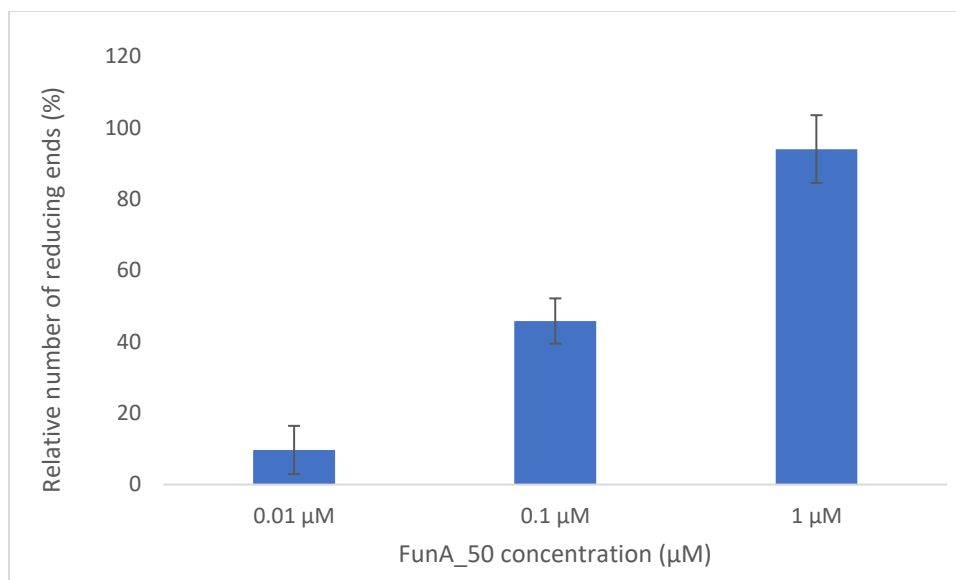


Figure 25: FunA_50 activity with increasing enzyme concentration. The relative number of reducing ends (%) was measured after 0.01, 0.1, or 1 µM enzyme reacted with 6 mg/ml hydrolyzed *F. vesiculosus* for 45 minutes in 20 mM Tris pH 7.4, 200 mM NaCl. Each data point represents the average value of three triplicates, with the control values subtracted

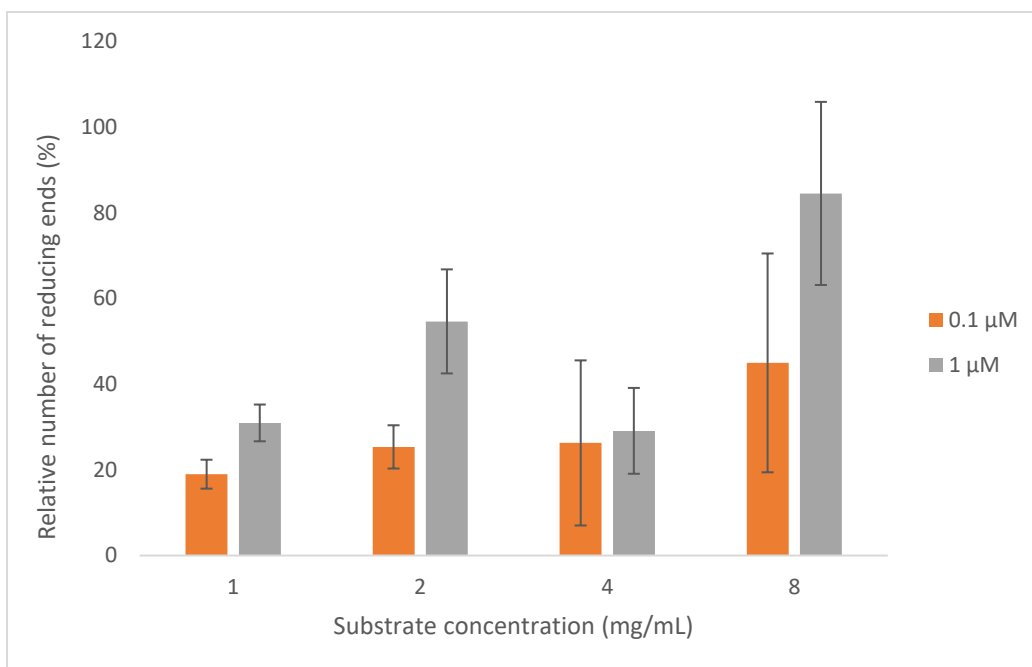


Figure 26: FunA_50 activity with increasing substrate concentration. The relative number of reducing ends (%) was measured after 0.1 or 1 µM enzyme reacted with 1-8 mg/ml hydrolyzed *F. vesiculosus* for 45 minutes in 20 mM Tris pH 7.4, 200 mM NaCl. Each data point represents the average value of three triplicates, with the control values and blanks subtracted.

The enzyme activity was highest at 1 µM FunA_50 (Figure 25) and 8 mg/ml substrate (Figure 26), which was expected as higher enzyme and/or substrate concentrations normally result in a higher yield of product, as discussed in 4.8.6. Furthermore, an increase in activity was observed for the lower enzyme concentration 0.1 µM once the substrate concentration was raised to 8

mg/mL (Figure 26). Such an increase in activity, even with a low enzyme concentration, indicates that a sufficient product yield can be obtained as long as there is an adequate amount of substrate available, which is in line with traditional enzyme kinetics. Still, high standard deviations for the samples with 0.1 μ M added enzyme suggest that 1 mM is the more appropriate enzyme concentration to use for this reaction.

4.9.2 Effect of temperature on activity

The effect of temperature on FunA_50 activity was tested for 45-minute reactions at pH 7.4 and 200 mM NaCl. The results are presented in Figure 27.

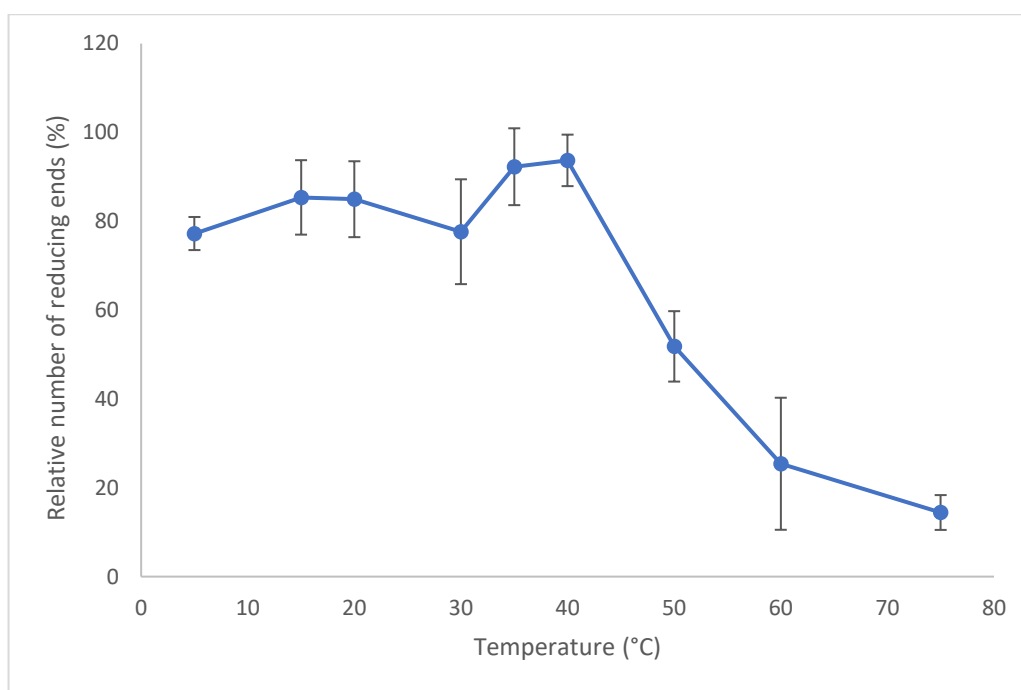


Figure 27: FunA_50 activity with increasing temperature 5-75 °C. The relative number of reducing ends (%) was measured after 1 μ M enzyme reacted with 6 mg/ml hydrolyzed *F. vesiculosus* for 45 minutes in 20 mM Tris pH 7.4, 200 mM NaCl. Each data point represents the average value of three triplicates, with the control values subtracted.

The data indicates that FunA_50 activity peaks at 40 °C, and the measurements at 40 °C also resulted in one of the lowest standard deviations of all the temperatures. The optimal temperature for activity being 40 °C was expected as a previously characterized FunA endo-fucoanase was also most active at that temperature (Shen et al., 2020). The most recently characterized FunA endo-fucoanase, a member of the novel GH174 family, had maximum activity at 30 °C (Liu et al., 2023). The endo-fucoanase Fhf1 Δ 470 displayed activity between 20 and 50°C with an optimum around 37-40 °C (Vuillemin et al., 2020), which is very similar to the observations of

FunA_50 and also considered typical for marine bacterial fucoidanases (Kusaykin et al., 2016). The highest enzyme activity was seen at temperatures 24-40 °C for endo-fucoidanases FWf1 and FWf2 as well (Zueva et al., 2020).

Obtaining and maintaining some of the temperatures in this experiment proved to be challenging, as the thermomixers that were utilized easily went up or down in temperature upon adding the samples for incubation. The high standard deviation observed for measurements at 60 °C, for example, could possibly be explained by this challenge with equipment. Pre-incubating the samples at the desired temperatures would be a potential solution to avoid inaccurate reaction temperatures.

4.9.3 Effect of pH on activity

The effect of pH on FunA_50 activity was tested for 45-minute reactions at 200 mM NaCl and 35 °C. The results are presented in Figure 28.

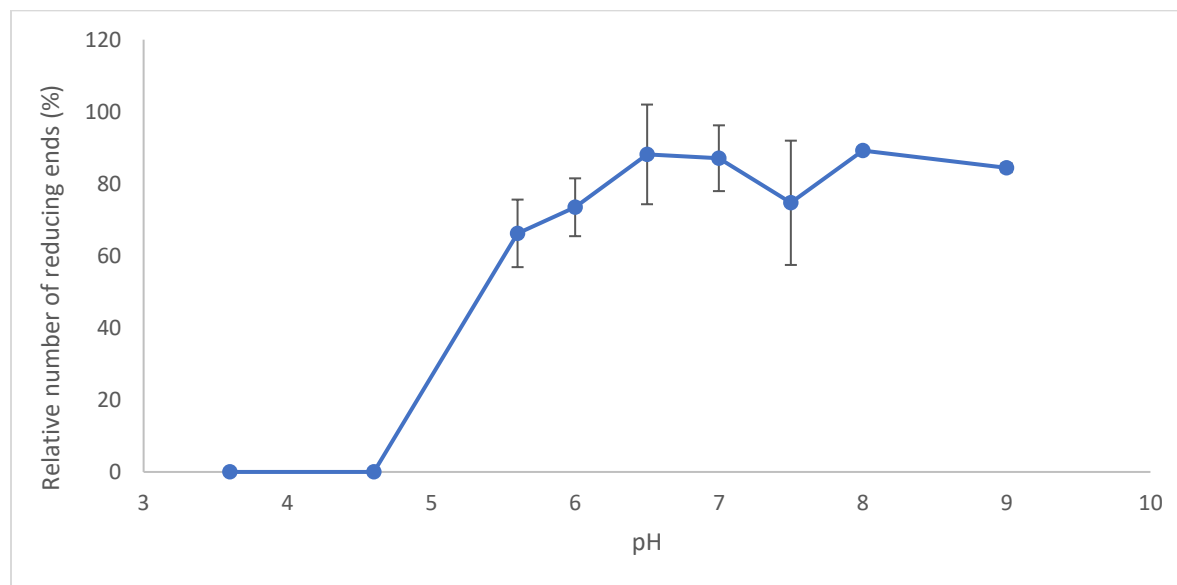


Figure 28: FunA_50 activity with increasing pH 3.6-9.0. The relative number of reducing ends (%) was measured after 1.5 μ M enzyme reacted with 6 mg/ml hydrolyzed *F. vesiculosus* for 45 minutes in buffers according to Table 10. Each data point represents the average value of three replicates, with the control values subtracted.

The optimal pH for FunA_50 ranged between 6.5 and 9.0, but the pH with the very highest number of reducing ends was pH 8. The values at pH 8 additionally gave a standard deviation of almost 0, indicating highly trustworthy data. The optimal temperature for activity being pH 8.0 was expected as a previously characterized FunA endo-fucoidanase was also most active at that pH (Shen et al., 2020). Despite a lower optimal pH of 5.5 for Fun174A, it has high activity in

almost the same pH range, 5.0 to 9.0, as with FunA_50 (Liu et al., 2023). The optimal pH is similar for Fhf1 Δ 470 as well, where fucoidanase activity is displayed between pH 5.0 and pH 9.0 and the apparent optimum is 8.0 (Vuillemin et al., 2020). Optimal pHs for additional characterized endo-fucoidanases are 6.0-6.8 for FWf1 and 6.4-7.2 for FWf2 (Zueva et al., 2020).

Using a fucose standard curve, the number of reducing ends formed under optimal conditions (40 °C, pH 8, 1 μ M, 6 mg/ml substrate) were calculated (Appendix E) to be 0.61 mg/ml.

The characterization of FunA_50 is still an ongoing project. Testing the effect of salinity and presence of ions on FunA_50 activity, as well as kinetics experiments, are the next steps in future work for this enzyme.

4.10 Conclusion and future perspectives

This study's aim of contributing to increased knowledge of the fucoidan molecule and fucoidan-acting enzymes was met by the discovery and characterization of two novel enzymes acting on fucoidan. A sulfatase from the AMOR metagenome and an endo-fucoidanase from the genome of *Lentimonas* sp. were produced and characterized to determine their optimal reaction conditions. For AMOR_S25 this also involved an enzyme time course as well as investigating enzyme kinetics and thermostability. Such experiments will also be conducted for further characterization of FunA_50. The discovery and characterization of a novel fucoidan sulfatase and a novel endo-fucoidanase will be contributions to on-going research on practical applications of fucoidan, like ingredients in salmon feed.

Further steps in researching both enzymes should include experiments to test possible applications. This may include applying the enzymes to produce oligosaccharides with specific biological properties. As more environmentally friendly biochemical routes are replacing the harsh chemical-dominant industrial processes (Elleuche et al., 2015), these enzymes may find a role in the processing of seaweeds. This would also need to include optimization and scale-up of enzyme production.

Uncovering the enzymes' structures would be important, and determining the structure can be obtained either with structure prediction or by producing enzyme crystals. Protein sequences can be submitted into AlphaFold, which is an artificial intelligence program capable of predicting the 3-dimensional protein structure based on amino acid sequences (<https://alphafold.ebi.ac.uk/>).

One disadvantage with AlphaFold is that only makes predictions based on training data, which potentially could result in some inaccuracy.

Crystal structures made by X-ray crystallography provide actual detailed structural information of enzymes, rather than predictions, and are common additions to databases for enzymes that have been characterized. The limitation with crystal structures, however, is that they only capture a limited number of conformations. As enzymes are dynamic molecules where several different conformations are involved in substrate binding, transition state, and product release, crystal structures do not provide a complete picture of the protein structure. Those X-ray crystal structures that are captured might not even be relevant for the function of the enzyme (Pochapsky & Pochapsky, 2019). An alternative approach to characterizing enzyme structure is using nuclear magnetic resonance (NMR), where the enzymes can be analyzed by characterizing the conformational dynamic processes over multiple time scales with atomic site resolution (Palmer, 2015). Structure information can be used to better understand the enzyme's mode of action and also be the basis for doing genetic engineering to improve enzyme properties like catalytic rate and stability. Information about the mode of action for both AMOR_S25 and FunA_50 can also be done by analyzing the end products of their reactions on NMR. The analysis would identify the cleavage points of the enzymes on the fucoidan molecule.

Another important topic for future studies would be enzyme synergy. This may include using enzymatic products from reactions with AMOR_S25 as substrates to test the AMOR endo- and exo-fucoidanases that did not show activity in this study. There could also be conducted synergy experiments including other novel or characterized enzymes.

All these suggested next experimental steps focus on the enzymes, but investigations of the produced oligomers will also be important work. Once the oligomeric products from the enzymatic reactions are better characterized, modifying them and/or testing their application can be done (Fernando et al., 2019). Already, some fucoidan substrates produced in the laboratory have been tested for cell viability and immune response in salmon spleen and head kidney cells and are showing promising results, but more experiments are needed to make exact conclusions.

References

- Ale, M. T., & Meyer, A. S. (2013). Fucoidans from brown seaweeds: an update on structures, extraction techniques and use of enzymes as tools for structural elucidation. *RSC Adv.*, 3(22), 8131-8141. <https://doi.org/10.1039/c3ra23373a>
- Altschul, S. F., Gish, W., Miller, W., Myers, E. W., & Lipman, D. J. (1990). Basic local alignment search tool. *J Mol Biol*, 215(3), 403-410. [https://doi.org/10.1016/s0022-2836\(05\)80360-2](https://doi.org/10.1016/s0022-2836(05)80360-2)
- Ani, F. N. (2016). Utilization of bioresources as fuels and energy generation. In M. H. Rashid (Ed.), *Electric Renewable Energy Systems* (pp. 140-155). Academic Press. <https://doi.org/https://doi.org/10.1016/B978-0-12-804448-3.00008-6>
- Antonopoulos, A., Hardouin, J., Favetta, P., Helbert, W., Delmas, A. F., & Lafosse, M. (2005). Matrix-assisted laser desorption/ionisation mass spectrometry for the direct analysis of enzymatically digested kappa- iota- and hybrid iota/nu-carrageenans. *Rapid Communications in Mass Spectrometry*, 19(16), 2217-2226. <https://doi.org/https://doi.org/10.1002/rcm.2051>
- Aquino, R. S., Landeira-Fernandez, A. M., Valente, A. P., Andrade, L. R., & Mourão, P. A. S. (2004). Occurrence of sulfated galactans in marine angiosperms: evolutionary implications. *Glycobiology*, 15(1), 11-20. <https://doi.org/10.1093/glycob/cwh138>
- Arntzen, M. Ø., Pedersen, B., Klau, L. J., Stokke, R., Oftebro, M., Antonsen, S. G., Fredriksen, L., Sletta, H., Aarstad, O. A., Aachmann, F. L., Horn, S. J., & Eijsink, V. G. H. (2021). Alginate Degradation: Insights Obtained through Characterization of a Thermophilic Exolytic Alginate Lyase. *Applied and Environmental Microbiology*, 87(6). <https://doi.org/doi:10.1128/AEM.02399-20>
- Balina, K., Romagnoli, F., & Blumberga, D. (2017). Seaweed biorefinery concept for sustainable use of marine resources. *Energy Procedia*, 128, 504-511. <https://doi.org/https://doi.org/10.1016/j.egypro.2017.09.067>
- Barbeyron, T., Brillet-Guéguen, L., Carré, W., Carrière, C., Caron, C., Czjzek, M., Hoebeke, M., & Michel, G. (2016). Matching the Diversity of Sulfated Biomolecules: Creation of a Classification Database for Sulfatases Reflecting Their Substrate Specificity. *PLoS One*, 11(10). <https://doi.org/10.1371/journal.pone.0164846>
- Berman, H. M., Westbrook, J., Feng, Z., Gilliland, G., Bhat, T. N., Weissig, H., Shindyalov, I. N., & Bourne, P. E. (2000). The Protein Data Bank. *Nucleic Acids Research*, 28(1), 235-242. <https://doi.org/10.1093/nar/28.1.235>
- Biosynth. (2023a). *L-fucose*. <https://www.biosynth.com/p/MF06710/2438-80-4-1-fucose>
- Biosynth. (2023b). *4-Nitrophenyl sulfate potassium salt*. <https://www.biosynth.com/p/EN27113/6217-68-1-4-nitrophenyl-sulfate-potassium-salt>
- Buck-Wiese, H., Andskog, M. A., Nguyen, N. P., Bligh, M., Asmala, E., Vidal-Melgosa, S., Liebeke, M., Gustafsson, C., & Hehemann, J.-H. (2023). Fucoid brown algae inject fucoidan carbon into the ocean. *Proceedings of the National Academy of Sciences*, 120(1). <https://doi.org/doi:10.1073/pnas.2210561119>
- Chao, G., Min, J., Zhiwei, Y., & Runying, Z. (2015). Characterization of a Recombinant Thermostable Arylsulfatase from Deep-Sea Bacterium *Flammeovirga pacifica*. *Journal of Microbiology and Biotechnology*, 25(11), 1894-1901. <https://doi.org/10.4014/jmb.1504.04028>

- Charoensiddhi, S., Conlon, M. A., Franco, C. M. M., & Zhang, W. (2017). The development of seaweed-derived bioactive compounds for use as prebiotics and nutraceuticals using enzyme technologies. *Trends in Food Science & Technology*, 70, 20-33. <https://doi.org/https://doi.org/10.1016/j.tifs.2017.10.002>
- Chen, A., Liu, Y., Zhang, T., Xiao, Y., Xu, X., Xu, Z., & Xu, H. (2023). Chain conformation, mucoadhesive properties of fucoidan in the gastrointestinal tract and its effects on the gut microbiota. *Carbohydrate Polymers*, 304. <https://doi.org/https://doi.org/10.1016/j.carbpol.2022.120460>
- Colin, S., Deniaud, E., Jam, M., Descamps, V., Chevolut, Y., Kervarec, N., Yvin, J.-C., Barbeyron, T., Michel, G., & Kloareg, B. (2006). Cloning and biochemical characterization of the fucanase FcnA: definition of a novel glycoside hydrolase family specific for sulfated fucans. *Glycobiology*, 16(11), 1021-1032. <https://doi.org/10.1093/glycob/cwl029>
- Colliec, S., Fischer, A. M., Tapon-Brethaudiere, J., Boisson, C., Durand, P., & Jozefonvicz, J. (1991). Anticoagulant properties of a fucoidan fraction. *Thrombosis Research*, 64(2), 143-154. [https://doi.org/https://doi.org/10.1016/0049-3848\(91\)90114-C](https://doi.org/https://doi.org/10.1016/0049-3848(91)90114-C)
- Cornish-Bowden, A. (1981). Robust Estimation in Enzyme Kinetics. In L. Endrenyi (Ed.), *Kinetic Data Analysis: Design and Analysis of Enzyme and Pharmacokinetic Experiments* (pp. 105-119). Springer US. https://doi.org/10.1007/978-1-4613-3255-8_8
- Deniaud-Bouët, E., Hardouin, K., Potin, P., Kloareg, B., & Hervé, C. (2017). A review about brown algal cell walls and fucose-containing sulfated polysaccharides: Cell wall context, biomedical properties and key research challenges. *Carbohydr Polym*, 175, 395-408. <https://doi.org/10.1016/j.carbpol.2017.07.082>
- Deniaud-Bouët, E., Kervarec, N., Michel, G., Tonon, T., Kloareg, B., & Hervé, C. (2014). Chemical and enzymatic fractionation of cell walls from Fucales: insights into the structure of the extracellular matrix of brown algae. *Annals of Botany*, 114(6), 1203-1216. <https://doi.org/10.1093/aob/mcu096>
- Dierks, T., Lecca, M. R., Schlotterhose, P., Schmidt, B., & von Figura, K. (1999). Sequence determinants directing conversion of cysteine to formylglycine in eukaryotic sulfatases. *The EMBO Journal*, 18(8), 2084-2091. <https://doi.org/https://doi.org/10.1093/emboj/18.8.2084>
- Dussan, K., Dijkstra, J. W., Luzzi, S., van Zandvoort, I., & van Hal, J. W. (2023). Seaweed versatility for biorefinery: Blessing or burden? *Current Opinion in Green and Sustainable Chemistry*, 39. <https://doi.org/https://doi.org/10.1016/j.cogsc.2022.100728>
- EIA. (2022). *Biomass explained. Biomass and the environment*. <https://www.eia.gov/energyexplained/biomass/biomass-and-the-environment.php>
- El-Said, G. F., & El-Sikaily, A. (2013). Chemical composition of some seaweed from Mediterranean Sea coast, Egypt. *Environ Monit Assess*, 185(7), 6089-6099. <https://doi.org/10.1007/s10661-012-3009-y>
- Elleuche, S., Schäfers, C., Blank, S., Schröder, C., & Antranikian, G. (2015). Exploration of extremophiles for high temperature biotechnological processes. *Current Opinion in Microbiology*, 25, 113-119. <https://doi.org/https://doi.org/10.1016/j.mib.2015.05.011>
- EMBL-EBI. (2022). *HMMER: biosequence analysis using profile hidden Markov models*. <http://hmmer.org/>

- Fernando, I. P. S., Kim, D., Nah, J.-W., & Jeon, Y.-J. (2019). Advances in functionalizing fucoidans and alginates (bio)polymers by structural modifications: A review. *Chemical Engineering Journal*, 355, 33-48. <https://doi.org/https://doi.org/10.1016/j.cej.2018.08.115>
- Fleurence, J. (1999). Seaweed proteins: biochemical, nutritional aspects and potential uses. *Trends in Food Science & Technology*, 10(1), 25-28. [https://doi.org/https://doi.org/10.1016/S0924-2244\(99\)00015-1](https://doi.org/https://doi.org/10.1016/S0924-2244(99)00015-1)
- Fonseca, R. J. C., & Mourão, P. A. S. (2021). Pharmacological Activities of Sulfated Fucose-Rich Polysaccharides after Oral Administration: Perspectives for the Development of New Carbohydrate-Based Drugs. *Mar Drugs*, 19(8). <https://doi.org/10.3390/md19080425>
- Furukawa, S.-i., Fujikawa, T., Koga, D., & Ide, A. (1992). Purification and Some Properties of Exo-type Fucoidanases from *Vibrio* sp. N-5. *Bioscience, Biotechnology, and Biochemistry*, 56(11), 1829-1834. <https://doi.org/10.1271/bbb.56.1829>
- Gasteiger, E., Hoogland, C., Gattiker, A., Duvaud, S. e., Wilkins, M. R., Appel, R. D., & Bairoch, A. (2005). Protein Identification and Analysis Tools on the ExPASy Server. In J. M. Walker (Ed.), *The Proteomics Protocols Handbook* (pp. 571-607). Humana Press. <https://doi.org/10.1385/1-59259-890-0:571>
- Genicot, S. M., Groisillier, A., Rogniaux, H., Meslet-Cladière, L., Barbeyron, T., & Helbert, W. (2014). Discovery of a novel iota carrageenan sulfatase isolated from the marine bacterium *Pseudoalteromonas carrageenovora*. *Frontiers in Chemistry*, 2. <https://doi.org/10.3389/fchem.2014.00067>
- Ghanbarzadeh, M., Golmoradzadeh, A., & Homaei, A. (2018). Carrageenans and carrageenases: versatile polysaccharides and promising marine enzymes. *Phytochemistry Reviews*, 17(3), 535-571. <https://doi.org/10.1007/s11101-018-9548-2>
- Green, E. (2023). *Contig*. National Human Genome Research Institute <https://www.genome.gov/genetics-glossary/Contig>
- Hanson, S. R., Best, M. D., & Wong, C.-H. (2004). Sulfatases: Structure, Mechanism, Biological Activity, Inhibition, and Synthetic Utility. *Angewandte Chemie International Edition*, 43(43), 5736-5763. <https://doi.org/https://doi.org/10.1002/anie.200300632>
- Helbert, W. (2017). Marine Polysaccharide Sulfatases. *Frontiers in Marine Science*, 4. <https://doi.org/10.3389/fmars.2017.00006>
- Hettle, A. G., Vickers, C., Robb, C. S., Liu, F., Withers, S. G., Hehemann, J.-H., & Boraston, A. B. (2018). The Molecular Basis of Polysaccharide Sulfatase Activity and a Nomenclature for Catalytic Subsites in this Class of Enzyme. *Structure*, 26(5), 747-758. <https://doi.org/https://doi.org/10.1016/j.str.2018.03.012>
- Holdt, S. L., & Kraan, S. (2011). Bioactive compounds in seaweed: functional food applications and legislation. *Journal of Applied Phycology*, 23(3), 543-597. <https://doi.org/10.1007/s10811-010-9632-5>
- Holtkamp, A. D., Kelly, S., Ulber, R., & Lang, S. (2009). Fucoidans and fucoidanases—focus on techniques for molecular structure elucidation and modification of marine polysaccharides. *Applied Microbiology and Biotechnology*, 82(1), 1-11. <https://doi.org/10.1007/s00253-008-1790-x>
- Horn, S. J. (2000). *Bioenergy from brown seaweeds* (Publication Number 609630) Norwegian University of Science and Technology]. Trondheim. https://ntnuopen.ntnu.no/ntnu-xmlui/bitstream/handle/11250/245590/125539_FULLTEXT01.pdf?sequence=1
- Invitrogen. (2010). *One Shot® BL21(DE3) Competent Cells*. https://assets.thermofisher.com/TFS-Assets/LSG/manuals/oneshotbl21_man.pdf

- Invitrogen. (2013). *One Shot® TOP10 Competent Cells*. https://assets.thermofisher.com/TFS-Assets/LSG/manuals/oneshottop10_man.pdf
- Ito, K., & Hori, K. (1989). Seaweed: Chemical composition and potential food uses. *Food Reviews International*, 5(1), 101-144. <https://doi.org/10.1080/87559128909540845>
- Jönsson, M., Allahgholi, L., Sardari, R. R. R., Hreggviðsson, G. O., & Nordberg Karlsson, E. (2020). Extraction and Modification of Macroalgal Polysaccharides for Current and Next-Generation Applications. *Molecules*, 25(4). <https://doi.org/10.3390/molecules25040930>
- Kılınc, B., Cirik, S., Turan, G., Tekogul, H., Koru, E. (2013). Seaweeds for Food and Industrial Applications. In M. Innocenzo (Ed.), *Food Industry* (pp. Ch. 31). IntechOpen. <https://doi.org/10.5772/53172>
- Kusaykin, M. I., Silchenko, A. S., Zakharenko, A. M., & Zvyagintseva, T. N. (2016). Fucoidanases. *Glycobiology*, 26(1), 3-12. <https://doi.org/10.1093/glycob/cwv072>
- Lenntech. (2023). *Calcium (Ca) and water*. <https://www.lenntech.com/periodic/water/calcium/calcium-and-water.htm>
- Lever, M. (1972). A new reaction for colorimetric determination of carbohydrates. *Analytical Biochemistry*, 47(1), 273-279. [https://doi.org/https://doi.org/10.1016/0003-2697\(72\)90301-6](https://doi.org/https://doi.org/10.1016/0003-2697(72)90301-6)
- Li, Q., Jiang, C., Tan, H., Zhao, X., Li, K., & Yin, H. (2021). Characterization of recombinant *E. coli* expressing a novel fucosidase from *Bacillus cereus* 2–8 belonging to GH95 family. *Protein Expression and Purification*, 186. <https://doi.org/https://doi.org/10.1016/j.pep.2021.105897>
- Liu, G., Shen, J., Chang, Y., Mei, X., Chen, G., Zhang, Y., & Xue, C. (2023). Characterization of an endo-1,3-fucanase from marine bacterium *Wenyngzhuangia aestuarii*: The first member of a novel glycoside hydrolase family GH174. *Carbohydrate Polymers*, 306. <https://doi.org/https://doi.org/10.1016/j.carbpol.2023.120591>
- Lombard, V., Golaconda Ramulu, H., Drula, E., Coutinho, P. M., & Henrissat, B. (2014). The carbohydrate-active enzymes database (CAZy) in 2013. *Nucleic Acids Res*, 42, D490-D495. <https://doi.org/10.1093/nar/gkt1178>
- Madhavan, A., Sindhu, R., Parameswaran, B., Sukumaran, R. K., & Pandey, A. (2017). Metagenome Analysis: a Powerful Tool for Enzyme Bioprospecting. *Applied Biochemistry and Biotechnology*, 183(2), 636-651. <https://doi.org/10.1007/s12010-017-2568-3>
- Manns, D., Deutschle, A. L., Saake, B., & Meyer, A. S. (2014). Methodology for quantitative determination of the carbohydrate composition of brown seaweeds (Laminariaceae). *RSC Adv.*, 4(49), 25736-25746. <https://doi.org/10.1039/c4ra03537b>
- Megazyme. (2023). *4-Nitrophenyl- α -L-fucopyranoside*. <https://www.megazyme.com/4-nitrophenyl-alpha-l-fucopyranoside>
- Mikkelsen, M. D., Cao, H. T. T., Roret, T., Rhein-Knudsen, N., Holck, J., Tran, V. T. T., Nguyen, T. T., Tran, V. H. N., Lezyk, M. J., Muschiol, J., Pham, T. D., Czjzek, M., & Meyer, A. S. (2021). A novel thermostable prokaryotic fucoidan active sulfatase PsFucS1 with an unusual quaternary hexameric structure. *Scientific Reports*, 11(1). <https://doi.org/10.1038/s41598-021-98588-3>
- Ministry of Climate and Environment. (2015). *Seas and coastlines - the need to safeguard species diversity*. Regjeringen. <https://www.regjeringen.no/en/topics/climate-and-environment/biodiversity/innsiktsartikler-naturmangfold/hav-og-kyst/id2076396/>

- Motone, K., Takagi, T., Sasaki, Y., Kuroda, K., & Ueda, M. (2016). Direct ethanol fermentation of the algal storage polysaccharide laminarin with an optimized combination of engineered yeasts. *Journal of Biotechnology*, 231, 129-135. <https://doi.org/https://doi.org/10.1016/j.jbiotec.2016.06.002>
- Ohmes, J., Mikkelsen, M. D., Nguyen, T. T., Tran, V. H. N., Meier, S., Nielsen, M. S., Ding, M., Seekamp, A., Meyer, A. S., & Fuchs, S. (2022). Depolymerization of fucoidan with endo-fucoidanase changes bioactivity in processes relevant for bone regeneration. *Carbohydrate Polymers*, 286. <https://doi.org/https://doi.org/10.1016/j.carbpol.2022.119286>
- Olsen, J. L., Rouz , P., Verhelst, B., Lin, Y.-C., Bayer, T., Collen, J., Dattolo, E., De Paoli, E., Dittami, S., Maumus, F., Michel, G., Kersting, A., Lauritano, C., Lohaus, R., T pel, M., Tonon, T., Vanneste, K., Amirebrahimi, M., Brakel, J., . . . Van de Peer, Y. (2016). The genome of the seagrass *Zostera marina* reveals angiosperm adaptation to the sea. *Nature*, 530(7590), 331-335. <https://doi.org/10.1038/nature16548>
- Palmer, A. G., III. (2015). Enzyme Dynamics from NMR Spectroscopy. *Accounts of Chemical Research*, 48(2), 457-465. <https://doi.org/10.1021/ar500340a>
- Peteiro, C. (2018). Alginate Production from Marine Macroalgae, with Emphasis on Kelp Farming. In B. H. A. Rehm & M. F. Moradali (Eds.), *Alginates and Their Biomedical Applications* (pp. 27-66). Springer Singapore. https://doi.org/10.1007/978-981-10-6910-9_2
- Pochapsky, T. C., & Pochapsky, S. S. (2019). What Your Crystal Structure Will Not Tell You about Enzyme Function. *Accounts of Chemical Research*, 52(5), 1409-1418. <https://doi.org/10.1021/acs.accounts.9b00066>
- Pr choux, A., Genicot, S., Rogniaux, H., & Helbert, W. (2013). Controlling Carrageenan Structure Using a Novel Formylglycine-Dependent Sulfatase, an Endo-4S-iota-Carrageenan Sulfatase. *Marine Biotechnology*, 15(3), 265-274. <https://doi.org/10.1007/s10126-012-9483-y>
- Raven, J. A., Johnston, A. M., K bler, J. E., Korb, R., Mcinroy, S. G., Handley, L. L., Scrimgeour, C. M., Walker, D. I., Beardall, J., Clayton, M. N., Vanderklift, M., Fredriksen, S., & Dunton, K. H. (2002). Seaweeds in Cold Seas: Evolution and Carbon Acquisition. *Annals of Botany*, 90(4), 525-536. <https://doi.org/10.1093/aob/mcf171>
- Reys, L. L., Vaithilingam, V., Sthijns, M. M. J. P. E., Soares, E., Rademakers, T., de Vries, R., Mohammed, S. G., de Bont, D., Jetten, M. J., Hermanns, C., Filho, O. P. d. S., Stell, A., Mourad, N. I., Gianello, P., LaPointe, V. L. S., Silva, S. S., Reis, R. L., Silva, T. H., & van Apeldoorn, A. A. (2021). Fucoidan Hydrogels Significantly Alleviate Oxidative Stress and Enhance the Endocrine Function of Encapsulated Beta Cells. *Advanced Functional Materials*, 31(35). <https://doi.org/https://doi.org/10.1002/adfm.202011205>
- Rhein-Knudsen, N., Guan, C., Mathiesen, G., & Horn, S. J. (2021). Expression and production of thermophilic alginate lyases in *Bacillus* and direct application of culture supernatant for seaweed saccharification. *Algal Research*, 60. <https://doi.org/10.1016/j.algal.2021.102512>
- Rhein-Knudsen, N., Reyes-Weiss, D., & Horn, S. J. (2023). Extraction of high purity fucoidans from brown seaweeds using cellulases and alginate lyases. *International Journal of Biological Macromolecules*, 229, 199-209. <https://doi.org/https://doi.org/10.1016/j.ijbiomac.2022.12.261>

- Riebesell, U., Körtzinger, A., & Oschlies, A. (2009). Sensitivities of marine carbon fluxes to ocean change. *Proceedings of the National Academy of Sciences*, 106(49), 20602-20609. <https://doi.org/doi:10.1073/pnas.0813291106>
- Schlachter, C. R., O'Malley, A., Grimes, L. L., Tomashek, J. J., Chruszcz, M., & Lee, L. A. (2021). Purification, Characterization, and Structural Studies of a Sulfatase from *Pedobacter yulinensis*. *Molecules*, 27(1). <https://doi.org/10.3390/molecules27010087>
- Schultz-Johansen, M., Stougaard, P., Svensson, B., & Teze, D. (2021). Two marine GH29 α -L-fucosidases from an uncultured *Paraglaciecola* sp. specifically hydrolyze fucosyl-N-acetylglucosamine regioisomers. *bioRxiv*. <https://doi.org/10.1101/2021.06.01.446583>
- Seghetta, M., Romeo, D., D'Este, M., Alvarado-Morales, M., Angelidaki, I., Bastianoni, S., & Thomsen, M. (2017). Seaweed as innovative feedstock for energy and feed – Evaluating the impacts through a Life Cycle Assessment. *Journal of Cleaner Production*, 150, 1-15. <https://doi.org/https://doi.org/10.1016/j.jclepro.2017.02.022>
- Shen, J., Chang, Y., Zhang, Y., Mei, X., & Xue, C. (2020). Discovery and Characterization of an Endo-1,3-Fucanase From Marine Bacterium *Wenyngzhuangia fucanilytica*: A Novel Glycoside Hydrolase Family. *Frontiers in Microbiology*, 11. <https://doi.org/10.3389/fmicb.2020.01674>
- Shi, Q., Wang, A., Lu, Z., Qin, C., Hu, J., & Yin, J. (2017). Overview on the antiviral activities and mechanisms of marine polysaccharides from seaweeds. *Carbohydrate Research*, 453-454, 1-9. <https://doi.org/https://doi.org/10.1016/j.carres.2017.10.020>
- Shiau, J.-P., Chuang, Y.-T., Yang, K.-H., Chang, F.-R., Sheu, J.-H., Hou, M.-F., Jeng, J.-H., Tang, J.-Y., & Chang, H.-W. (2022). Brown Algae-Derived Fucoidan Exerts Oxidative Stress-Dependent Antiproliferation on Oral Cancer Cells. *Antioxidants*, 11(5). <https://doi.org/10.3390/antiox11050841>
- Sichert, A., Corzett, C. H., Schechter, M. S., Unfried, F., Markert, S., Becher, D., Fernandez-Guerra, A., Liebeke, M., Schweder, T., Polz, M. F., & Hehemann, J. H. (2020). *Verrucomicrobia* use hundreds of enzymes to digest the algal polysaccharide fucoidan. *Nat Microbiol*, 5(8), 1026-1039. <https://doi.org/10.1038/s41564-020-0720-2>
- Sigma-Aldrich. (2023). *4-Nitrocatechol sulfate dipotassium salt*. <https://www.sigmaaldrich.com/NO/en/product/sigma/n7251>
- Silchenko, A. S., Rasin, A. B., Zueva, A. O., Kusaykin, M. I., Zvyagintseva, T. N., Kalinovsky, A. I., Kurilenko, V. V., & Ermakova, S. P. (2018). Fucoidan Sulfatases from Marine Bacterium *Wenyngzhuangia fucanilytica* CZ1127T. *Biomolecules*, 8(4). <https://doi.org/10.3390/biom8040098>
- Silchenko, A. S., Rasin, A. B., Zueva, A. O., Kusaykin, M. I., Zvyagintseva, T. N., Rubtsov, N. K., & Ermakova, S. P. (2021). Discovery of a fucoidan endo-4O-sulfatase: Regioselective 4O-desulfation of fucoidans and its effect on anticancer activity in vitro. *Carbohydrate Polymers*, 271. <https://doi.org/https://doi.org/10.1016/j.carbpol.2021.118449>
- Silchenko, A. S., Rubtsov, N. K., Zueva, A. O., Kusaykin, M. I., Rasin, A. B., & Ermakova, S. P. (2022). Fucoidan-active α -L-fucosidases of the GH29 and GH95 families from a fucoidan degrading cluster of the marine bacterium *Wenyngzhuangia fucanilytica*. *Archives of Biochemistry and Biophysics*, 728. <https://doi.org/https://doi.org/10.1016/j.abb.2022.109373>
- Silchenko, A. S., Ustyuzhanina, N. E., Kusaykin, M. I., Krylov, V. B., Shashkov, A. S., Dmitrenok, A. S., Usoltseva, R. V., Zueva, A. O., Nifantiev, N. E., & Zvyagintseva, T. N.

- (2017). Expression and biochemical characterization and substrate specificity of the fucoidanase from *Formosa algae*. *Glycobiology*, 27(3), 254-263. <https://doi.org/10.1093/glycob/cww138>
- Song, M., Pham, H. D., Seon, J., & Woo, H. C. (2015). Marine brown algae: A conundrum answer for sustainable biofuels production. *Renewable and Sustainable Energy Reviews*, 50, 782-792. <https://doi.org/10.1016/j.rser.2015.05.021>
- Stam, M., Lelièvre, P., Hoebeke, M., Corre, E., Barbeyron, T., & Michel, G. (2023). SulfAtlas, the sulfatase database: state of the art and new developments. *Nucleic Acids Res*, 51(D1), D647-D653. <https://doi.org/10.1093/nar/gkac977>
- Stryer, L. (1998). *Biochemistry* (4th ed.). W. H. Freeman and Company.
- Sudhakar, K., Mamat, R., Samykano, M., Azmi, W. H., Ishak, W. F. W., & Yusaf, T. (2018). An overview of marine macroalgae as bioresource. *Renewable and Sustainable Energy Reviews*, 91, 165-179. <https://doi.org/https://doi.org/10.1016/j.rser.2018.03.100>
- Suprunchuk, V. E. (2019). Low-molecular-weight fucoidan: Chemical modification, synthesis of its oligomeric fragments and mimetics. *Carbohydrate Research*, 485. <https://doi.org/https://doi.org/10.1016/j.carres.2019.107806>
- Synytsya, A., Bleha, R., Synytsya, A., Pohl, R., Hayashi, K., Yoshinaga, K., Nakano, T., & Hayashi, T. (2014). Mekabu fucoidan: Structural complexity and defensive effects against avian influenza A viruses. *Carbohydrate Polymers*, 111, 633-644. <https://doi.org/https://doi.org/10.1016/j.carbpol.2014.05.032>
- Tabarsa, M., Rezaei, M., Ramezanpour, Z., Robert Waaland, J., & Rabiei, R. (2012). Fatty acids, amino acids, mineral contents, and proximate composition of some brown seaweeds. *Journal of Phycology*, 48(2), 285-292. <https://doi.org/https://doi.org/10.1111/j.1529-8817.2012.01122.x>
- Takkellapati, S., Li, T., & Gonzalez, M. A. (2018). An overview of biorefinery-derived platform chemicals from a cellulose and hemicellulose biorefinery. *Clean Technologies and Environmental Policy*, 20(7), 1615-1630. <https://doi.org/10.1007/s10098-018-1568-5>
- Torres, M. D., Kraan, S., & Domínguez, H. (2019). Seaweed biorefinery. *Reviews in Environmental Science and Bio/Technology*, 18(2), 335-388. <https://doi.org/10.1007/s11157-019-09496-y>
- Tran, V. H. N., Nguyen, T. T., Meier, S., Holck, J., Cao, H. T. T., Van, T. T. T., Meyer, A. S., & Mikkelsen, M. D. (2022). The Endo- α -(1,3)-Fucoidanase Mef2 Releases Uniquely Branched Oligosaccharides from *Saccharina latissima* Fucoidans. *Marine Drugs*, 20(5). <https://doi.org/10.3390/md20050305>
- USGS. (2019). *How Much Water is There on Earth?* <https://www.usgs.gov/special-topics/water-science-school/science/how-much-water-there-earth>
- Usov, A. I., & Zelinsky, N. D. (2013). Chemical structures of algal polysaccharides. In H. Domínguez (Ed.), *Functional Ingredients from Algae for Foods and Nutraceuticals* (pp. 23-86). Woodhead Publishing. <https://doi.org/https://doi.org/10.1533/9780857098689.1.23>
- Vickers, C., Liu, F., Abe, K., Salama-Alber, O., Jenkins, M., Springate, C. M. K., Burke, J. E., Withers, S. G., & Boraston, A. B. (2018). Endo-fucoidan hydrolases from glycoside hydrolase family 107 (GH107) display structural and mechanistic similarities to α -L-fucosidases from GH29. *J Biol Chem*, 293(47), 18296-18308. <https://doi.org/10.1074/jbc.RA118.005134>

- Vuillemin, M., Silchenko, A. S., Cao, H. T. T., Kokoulin, M. S., Trang, V. T. D., Holck, J., Ermakova, S. P., Meyer, A. S., & Mikkelsen, M. D. (2020). Functional Characterization of a New GH107 Endo- α -(1,4)-Fucoidanase from the Marine Bacterium *Formosa haliotis*. *Marine Drugs*, 18(11). <https://doi.org/10.3390/md18110562>
- Vuoristo, K. S., Fredriksen, L., Oftebro, M., Arntzen, M. O., Aarstad, O. A., Stokke, R., Steen, I. H., Hansen, L. D., Schuller, R. B., Aachmann, F. L., Horn, S. J., & Eijsink, V. G. H. (2019). Production, Characterization, and Application of an Alginate Lyase, AMOR_PL7A, from Hot Vents in the Arctic Mid-Ocean Ridge. *J Agric Food Chem*, 67(10), 2936-2945. <https://doi.org/10.1021/acs.jafc.8b07190>
- Wang, M., Veeraperumal, S., Zhong, S., & Cheong, K.-L. (2023). Fucoidan-Derived Functional Oligosaccharides: Recent Developments, Preparation, and Potential Applications. *Foods*, 12(4). <https://doi.org/10.3390/foods12040878>
- Wang, S., Jiang, X. M., Han, X. X., & Wang, H. (2008). Fusion Characteristic Study on Seaweed Biomass Ash. *Energy & Fuels*, 22(4), 2229-2235. <https://doi.org/10.1021/ef800128k>
- Wang, Y., Xing, M., Cao, Q., Ji, A., Liang, H., & Song, S. (2019). Biological Activities of Fucoidan and the Factors Mediating Its Therapeutic Effects: A Review of Recent Studies. *Marine Drugs*, 17(3). <https://doi.org/10.3390/md17030183>
- Wi, S. G., Kim, H. J., Mahadevan, S. A., Yang, D.-J., & Bae, H.-J. (2009). The potential value of the seaweed Ceylon moss (*Gelidium amansii*) as an alternative bioenergy resource. *Bioresource Technology*, 100(24), 6658-6660. <https://doi.org/https://doi.org/10.1016/j.biortech.2009.07.017>
- Widin, S. L., Billings, K. M., McGowen, J., & Cardinale, B. J. (2022). Biodiversity and disease risk in an algal biofuel system: An experimental test in outdoor ponds using a before-after-control-impact (BACI) design. *PLoS One*, 17(4). <https://doi.org/10.1371/journal.pone.0267674>
- Wiencke, C., & Bischof, K. (2012). *Seaweed biology*. Springer Berlin, Heidelberg. <https://doi.org/https://doi.org/10.1007/978-3-642-28451-9>
- Xu, S. Y., Huang, X., & Cheong, K. L. (2017). Recent Advances in Marine Algae Polysaccharides: Isolation, Structure, and Activities. *Mar Drugs*, 15(12). <https://doi.org/10.3390/md15120388>
- Zayed, A., El-Aasr, M., Ibrahim, A.-R. S., & Ulber, R. (2020). Fucoidan Characterization: Determination of Purity and Physicochemical and Chemical Properties. *Marine Drugs*, 18(11). <https://doi.org/10.3390/md18110571>
- Zhao, D., Xu, J., & Xu, X. (2018). Bioactivity of fucoidan extracted from *Laminaria japonica* using a novel procedure with high yield. *Food Chemistry*, 245, 911-918. <https://doi.org/https://doi.org/10.1016/j.foodchem.2017.11.083>
- Zueva, A. O., Silchenko, A. S., Rasin, A. B., Kusaykin, M. I., Usoltseva, R. V., Kalinovskiy, A. I., Kurilenko, V. V., Zvyagintseva, T. N., Thinh, P. D., & Ermakova, S. P. (2020). Expression and biochemical characterization of two recombinant fucoidanases from the marine bacterium *Wenyinzhuangia fucanilytica* CZ1127T. *International Journal of Biological Macromolecules*, 164, 3025-3037. <https://doi.org/https://doi.org/10.1016/j.ijbiomac.2020.08.131>

Appendix

Appendix A: Expression vectors

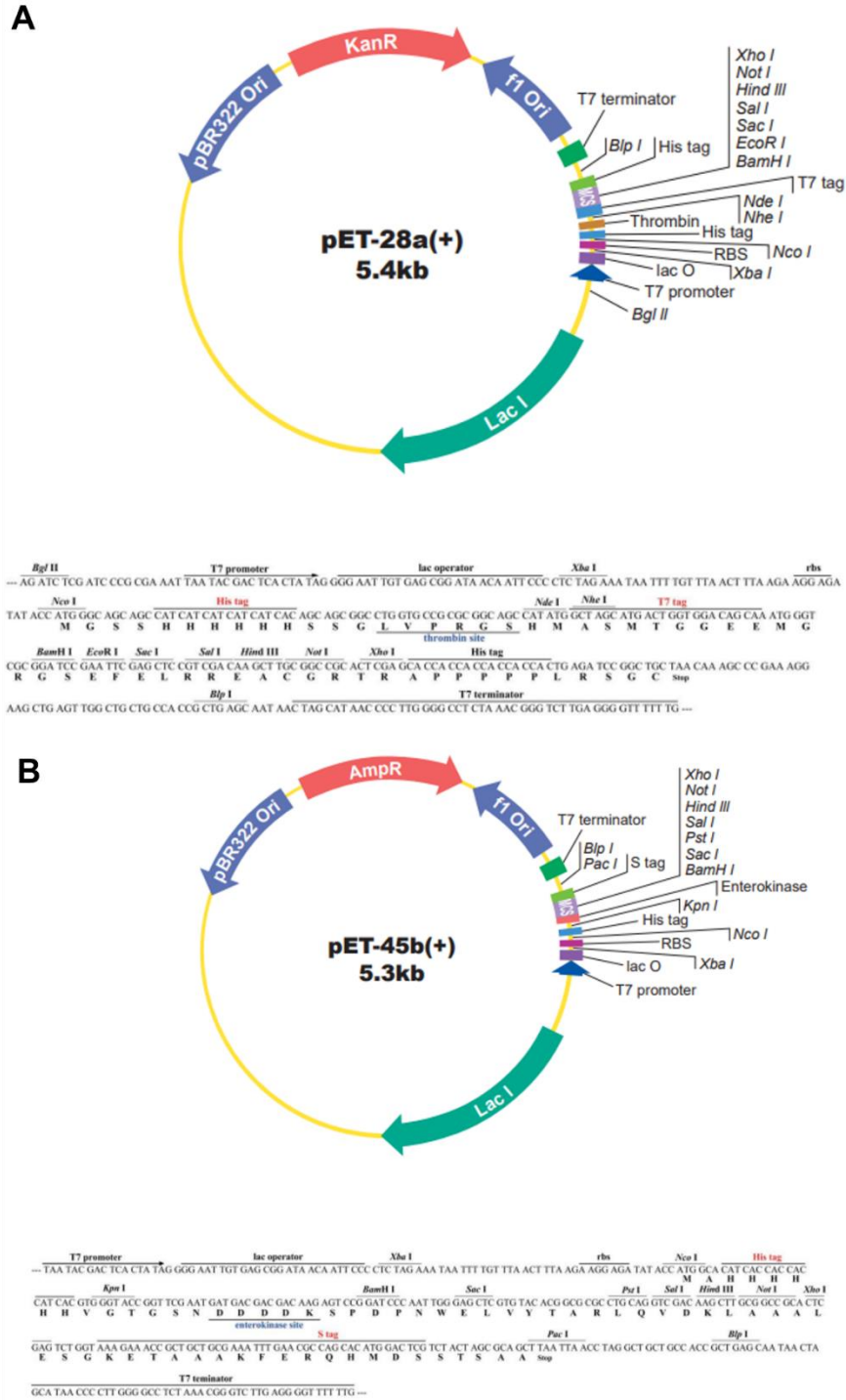
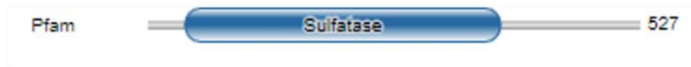


Figure 29: Expression vectors for expression in *E.coli*. The sequences for putative exo-fucoidanases and sulfatases were cloned into vector pET-28a(+) (A), while the putative endo-fucoidanases were cloned into plasmid vector pET-45b(+) (B).

Appendix B: Bioinformatics

A



B

Description	Scientific Name	Max Score	Total Score	Query Cover	E value	Per. Ident	Acc. Len	Accession
<input checked="" type="checkbox"/> sulfatase [Bacteroidetes bacterium]	Bacteroidetes bacterium	873	873	93%	0.0	82.96%	509	MCP3927611.1
<input checked="" type="checkbox"/> sulfatase [Flammeovirga pacifica]	Flammeovirga pacifica	758	758	90%	0.0	71.58%	523	WP_044228804.1
<input checked="" type="checkbox"/> Arylsulfatase A [Muricauda parva]	Muricauda parva	747	747	92%	0.0	69.53%	517	SNZ01160.1
<input checked="" type="checkbox"/> sulfatase [Muricauda parva]	Muricauda parva	747	747	92%	0.0	69.53%	488	WP_207763900.1
<input checked="" type="checkbox"/> sulfatase-like hydrolase/transferase [Gaetbulibacter sp. 2012CJ34-3]	Gaetbulibacter sp. 2012CJ34-3	739	739	90%	0.0	69.81%	501	WP_249973202.1
<input checked="" type="checkbox"/> sulfatase-like hydrolase/transferase [Gaetbulibacter sp. 4G1]	Gaetbulibacter sp. 4G1	736	736	90%	0.0	69.60%	501	WP_099563503.1

C

[3D View](#)

6HR5: Entity 1

Structure of the S1_25 family sulfatase module of the rhamnosidase FA22250 from *Formosa agariphila*

Roret, T., Prechoux, A., Czjzek, M., Michel, G.
(2019) Nat Chem Biol 15: 803-812

Released: 2019-06-26
Method: X-RAY DIFFRACTION 2.912 Å
Chain ID: A
Organism: *Formosa agariphila* KMM 3901
Macromolecule: Alpha-L-rhamnosidase/sulfatase (GH78)
Sequence Match: Sequence Identity: 34%, E-Value: 2.677e-62, Region: 19-456

[Download File](#) [View File](#) [Download Alignment](#)

QUERY: 6HR5_1

Figure 30: Examples of HMMER (A), BLAST (B) and RCSB PDB (C) outputs for AMOR_S25.

```

AMOR_S25  MNNNFLFKADKCKKVTLSLLILIV--I---IGHGYSQSVENVAPNIIFFFTDDQCYDTQ 55
AMOR_S15  -----MMKNL--KKQVAVLVVLVVLVYSCKTNHSENYNVEKHPNIVFILADDLGYGDL 52
AMOR_S16  -----MRYI--KFIQKSFIVFSSLLCLYTCSPKE----AKNPQPNIIIMFLVDDMGWQDT 47
          :: * : : : : : : : : : : : : : : : : : : : : : : : : : : : : : :
          : : * : : : : : : : : : : : : : : : : : : : : : : : : : : : : :

AMOR_S25  R-----DYGNPDVKTPNIDKLANSLVFMRYHTTAICMASRANVMIGQYKYKTCNFF 108
AMOR_S15  SCLN-----SESKIETPHLDKLTKDGIILFTDAHSGSAVCTPTRYGILTGRYCWRSQ LKS 106
AMOR_S16  SVPFWKETPINEKFHTPSMERLASEGMKFTQAY-ACSV CSPSRTSLMTGMNAARHRVTN 106
          : : : * * : : * : : * : * : : : : * : * : : * : : : : : : :
          : : * * : : * : : * : * : : : : * : * : : * : : : : : : :

AMOR_S25  EH-----GPMKTEKWS-----DAYPLK LKEAGYRVGFAGKF 139
AMOR_S15  SVL-----WPWDEPLIEPD-----QLTVGDLLKKNGYNTACIGKW 141
AMOR_S16  WTLRKNQTVDAKDDILEFPKWNLNGLQPESVDITINQSVSATTLPQLKSNGYFTIHC GKA 166
          * : : : : : : : : : : : : : : : : : : : : : : : : : : : : :
          : : * * : : * : : * : * : : : : * : * : : * : : : : : : :
    
```

Figure 31: Multiple Sequence Alignment of the selected putative AMOR sulfatases. Clustal Omega was used to carry out the alignments of AMOR_S15, AMOR_S16, and AMOR_S25. The amino acids are marked according to similarity, where the * sign indicates aligned amino acids that are identical, and the · sign indicates that the amino acids have similar properties. The conserved active site CXXXRXXXXXG for S1 sulfatases, as described by (Dierks et al., 1999) and (Mikkelsen et al., 2021), is marked by a black square.

Appendix C: His-tag purification chromatograms

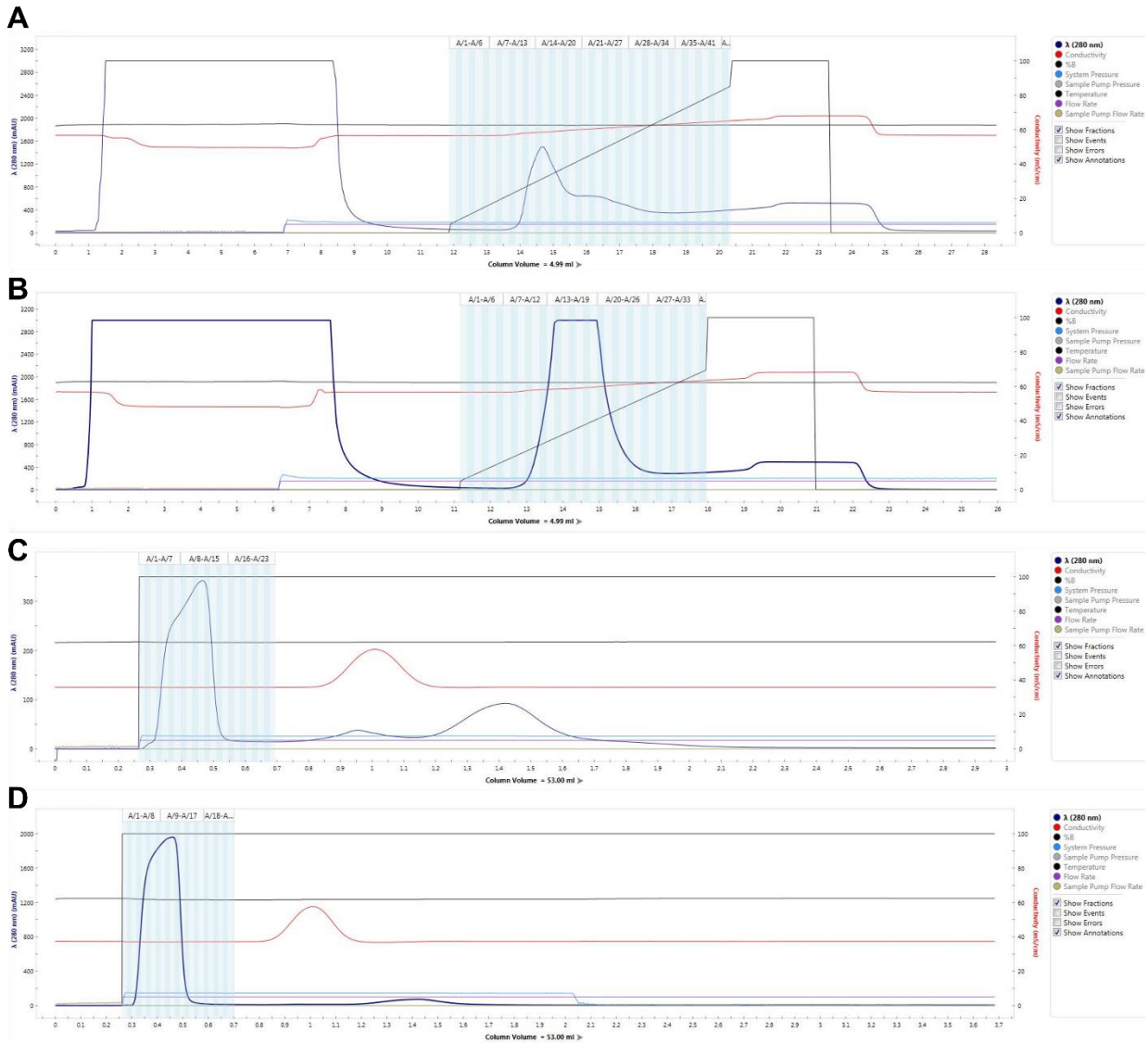


Figure 32: Examples of chromatograms from protein purification of putative AMOR enzymes. The proteins were first purified by affinity chromatography using a His-tag column, shown here with AMOR_29 (A) and AMOR_S25 (B), before undergoing buffer exchange and removal of Imidazole, also shown with AMOR_29 (C), and AMOR_S25 (D).

Appendix D: Chromatogram for monomer detection

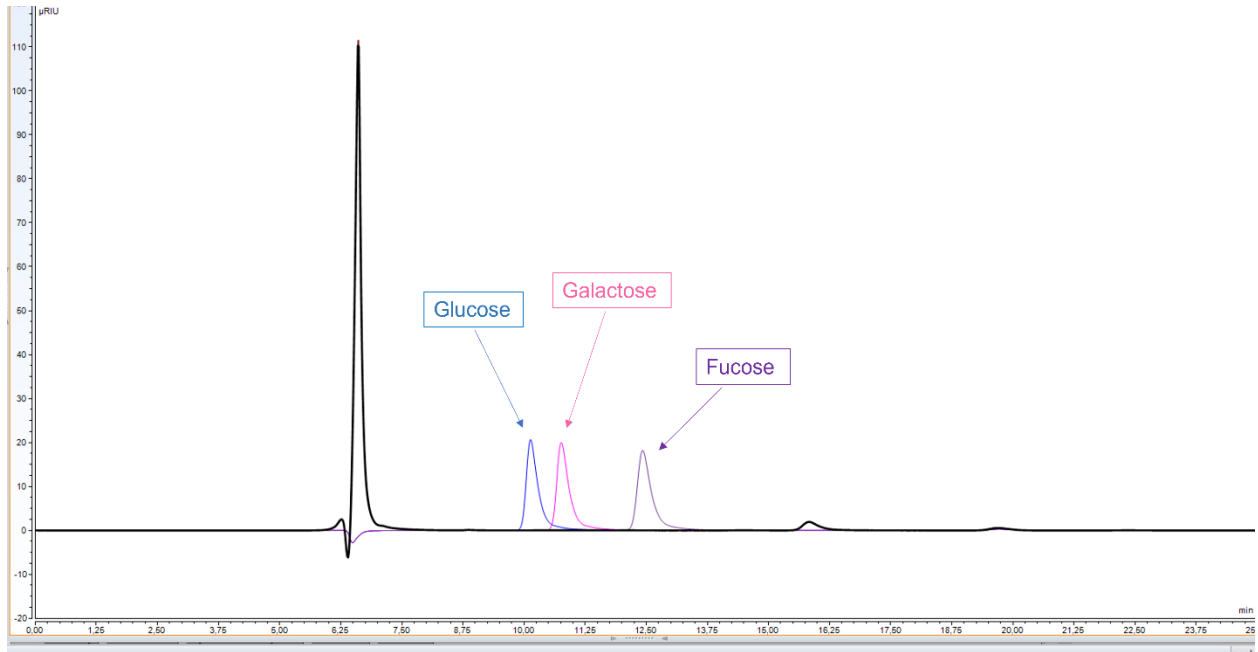


Figure 33: HPAEC-PAD chromatograms from samples of AMOR_141 reacting with fucoidan from *U. pinnatifida*. Standards of glucose (blue), galactose (pink), and fucose (purple) were used to evaluate peaks. The black line represents the substrate (fucoidan) control, while the light brown line represents the enzyme samples (triplicates). As there was no detected activity with AMOR_141, the line for the enzyme samples and the line for the substrate controls fall atop each other and are difficult to distinguish.

Appendix E: Calculations

Protein concentration

The final protein concentrations were calculated using Beer's law $[S] = A/L * \epsilon$, where $[S]$ is the final protein concentration, A is the measured absorbance (average), L is the optical path length, and ϵ is the molar absorption coefficient (extinction coefficient). Absorption was measured in 96-well plates with 100 μL volume, and the optical path length used for measuring protein concentrations was 0.28 cm., while the extinction coefficient varied between proteins. The extinction coefficient, as well as molecular weight, for each protein was determined using the ProtParam tool at www.expasy.org (Gasteiger et al., 2005). Here, calculation of the protein concentration of AMOR_S25 is shown as an example, and its molar absorption coefficient is $95035 \text{ M}^{-1}\text{cm}^{-1}$.

$$[S] = A/L * \epsilon$$

$$[S] = (0.873)/(0.28 \text{ cm} * 95035 \text{ M}^{-1}\text{cm}^{-1})$$

$$[S] = 3.28 * 10^{-5} \text{ M} = \underline{32.8 \mu\text{M}}.$$

Release of reducing ends during FunA_50 characterization

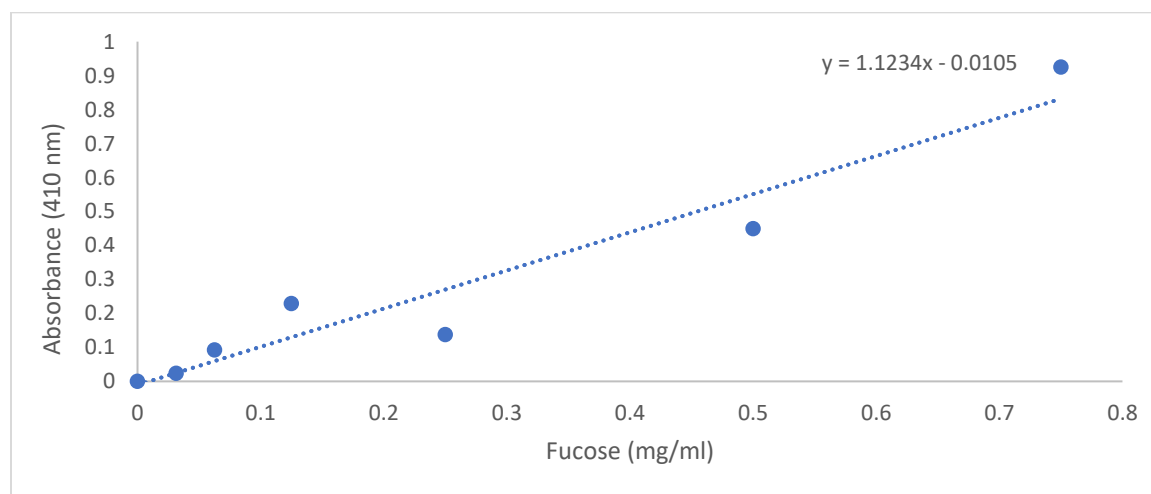


Figure 34: Standard curve for fucose. The equation for the regression line was used to calculate absorbance values to the number of reducing ends (equal to fucose units) produced during the reaction of FunA_50 with *F. vesiculosus* under optimal conditions.

The reducing ends formed with FunA_50 reacting with *F. vesiculosus* under optimal conditions were calculated by using the slope of a fucose standard curve (Figure 34), giving the equation $x = (A + 0.0105)/1.1234$ where A is the average absorbance value subtracted by controls.

$$x = (0.67+0.0105)/1.1234 = \underline{0.61\text{mg/ml}}.$$

Enzyme kinetics

The Michaelis-Menten equation used to calculate values for the graph extrapolated in Figure 22:

$$V_0 = \frac{V_{\max} \times [S]}{[S] + K_m}$$

In kinetics, Lineweaver-Burk plots are used to calculate K_M and V_{\max} , where the Slope = K_M/V_{\max} and the Y-intercept = $1/V_{\max}$. From Figure 23, these equations give

$$V_{\max} = 1/3.1131 = \underline{0.32 \mu\text{M/min}} \text{ and } K_M = 50.445 \times 0.32 = \underline{16.2 \text{ mM}}.$$

Appendix F: AMOR_S25 kinetics

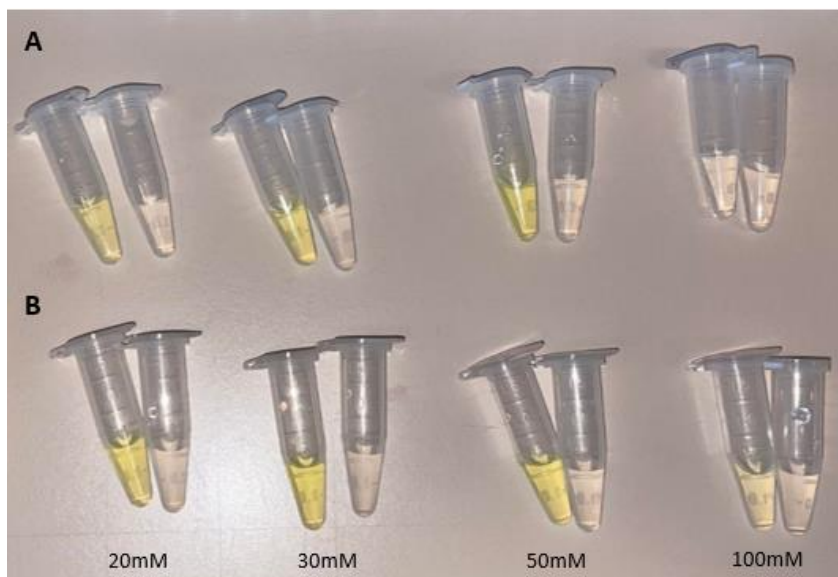


Figure 35: Initial testing of substrate and enzyme concentrations for characterization of AMOR_S25. Reactions of 1.5 μM (A) and 10 μM (B) AMOR_S25 were set up with increasing concentrations 20-100 mM of pNPS.

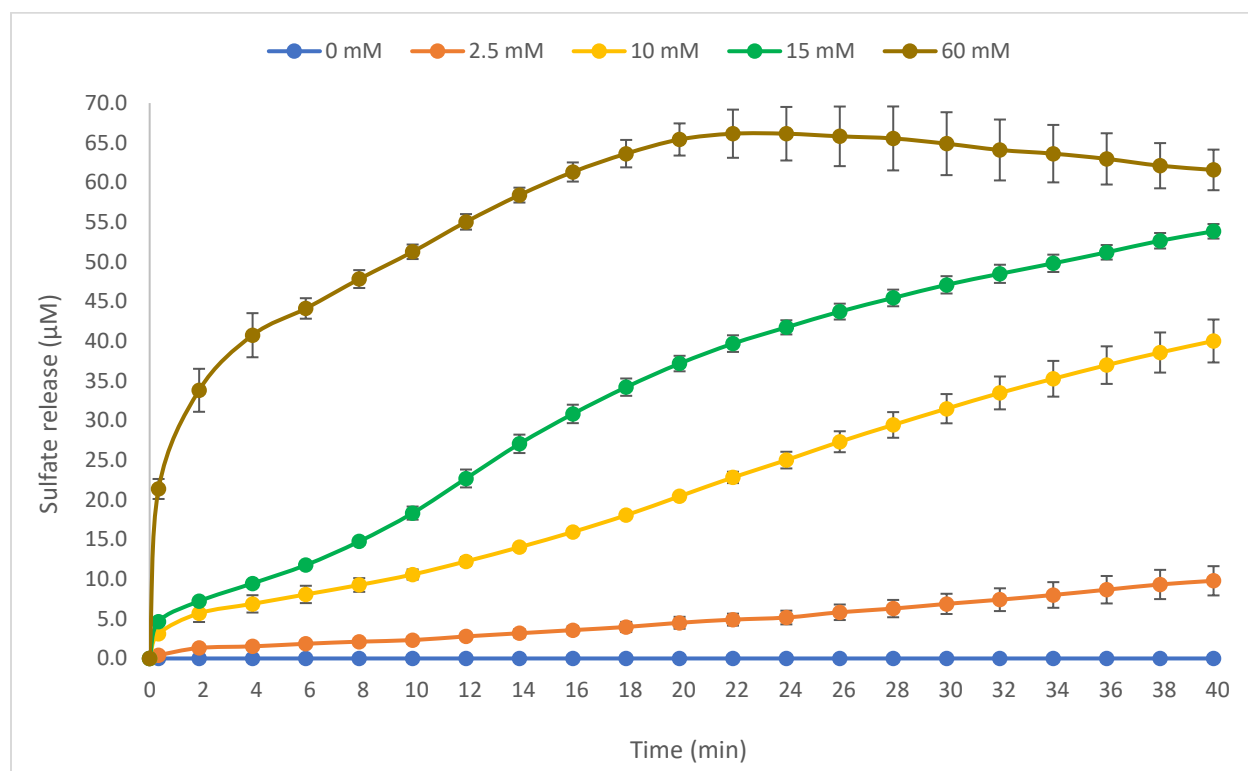


Figure 36: Sulfate release (μM) for 1 μM AMOR_25 incubated with 0-60 mM pNPS at optimal conditions. Absorbance measurements (280 nm) were taken every 2 minutes and the sulfate release was calculated using Beer's law. Each data point represents the average value of three replicates, with the control values subtracted.

Appendix G: MALDI data

Table 15: MALDI-data from substrate production where *M. pyrifera*, *L. digitata*, *Alaria sp.*, *F. serratus*, and *A. nodosum* were enzymatically cleaved by P5AFcnA to produce fucoidan oligosaccharides. The area (intensity) of the signals (m/z) with distances of 146 Da and 102 Da from each other confirmed successful hydrolysis.

Substrate	Commercial fucoidan polymer		Enzymatic hydrolysate	
	m/z	Intensity values	m/z	Intensity values
<i>M. pyrifera</i>	243.345	289	243.322	26571
	345.372	186	345.312	4549
	389.500	239	389.478	8492
	491.486	98.6	491.493	2128
	535.718	314	535.685	7684
	593.681	52.2	593.553	258
	637.745	101	637.727	1599
	681.948	227	681.934	11724
<i>Alaria sp.</i>	243.316	25.7	243.354	845
	345.399	115	345.349	177
	389.429	46.8	389.509	290
	491.508	22.3	491.512	106
			535.681	271
	593.609	16.7	593.534	30.8
			637.622	133
			681.957	2726
<i>F. serratus</i>			243.342	11420
	345.426	77.2	345.340	2810
	389.449	86.8	389.512	2371
	491.540	25.5	491.526	713
			535.714	1258
	593.634	16	593.592	132
			637.761	311
			681.974	8976
<i>L. digitata</i>	243.337	12	243.336	15416
	345.394	35.8	345.332	3449
	389.460	87.4	389.501	2927
	491.506	18.3	491.520	707
			535.713	1937
	593.626	13.2	593.578	105
	637.647	23.4	637.761	419
			681.972	10298
<i>A. nodosum</i>			243.343	4395
	345.421	79.2	345.339	798
	389.457	96.5	389.505	1661
	491.547	23.5	491.522	427
			535.716	764
	593.639	16.7	593.592	59.9
			637.761	171
			681.973	6418



Norges miljø- og biovitenskapelige universitet
Noregs miljø- og biovitenskapelige universitet
Norwegian University of Life Sciences

Postboks 5003
NO-1432 Ås
Norway